Remote sensing of forest health: The detection and mapping of *Thaumastocoris peregrinus* damage in plantation forests

ZAKARIYYAA OUMAR

Submitted in fulfilment of the academic requirements for the degree of

Doctor of Philosophy (PhD) in Environmental Science

School of Agricultural, Earth and Environmental Sciences

University of KwaZulu-Natal

South Africa

November 2012

Abstract

Thaumastocoris peregrinus (T. peregrinus) is a sap-sucking insect that feeds on *Eucalyptus* leaves. It poses a major threat to the forest sector by reducing the photosynthetic ability of the tree, resulting in stunted growth and even death of severely infested trees. The foliage of the tree infested with *T. peregrinus* turns into a deep red-brown colour starting at the northern side of the canopy but progressively spreads to the entire canopy. The monitoring of *T. peregrinus* and the effect it has on plantation health is essential to ensure productivity and future sustainability of forest yields. Insitu hyperspectral remote sensing combined with greater availability and lower cost of new generation multispectral satellite data, provides opportunities to detect and map *T. peregrinus* damage in plantation forests. This research advocates the development of remote sensing techniques to accurately detect and map *T. peregrinus* damage, an assessment that is critically needed to monitor plantation health in South Africa.

The study first provides an overview of how improvements in multispectral and hyperspectral technology can be used to detect and map *T. peregrinus* damage, based on the previous work done on the remote sensing of forest pests. Secondly, the utility of field hyperspectral remote sensing in predicting *T. peregrinus* damage was tested. High resolution field spectral data that was resampled to the Hyperion sensor successfully predicted *T. peregrinus* damage with high accuracies using narrowband normalized indices and vegetation indices. Field spectroscopy was further tested in predicting water stress induced by *T. peregrinus* infestation, in order to identify early physiological stages of damage. A neural network algorithm successfully predicted plant water content and equivalent water thickness in *T. peregrinus* infested plantations. The result is promising for forest health monitoring programmes in detecting previsual physiological stages of damage.

The analysis was then upscaled from field hyperspectral sensing to spaceborne sensing using the new generation WorldView-2 multispectral sensor, which contains key vegetation wavelengths. Partial least squares regression models were developed from the WorldView-2 bands and indices and significant predictors were identified by variable importance scores. The red edge and near-infrared bands of the WorldView-2 sensor, together with pigment specific indices predicted and mapped *T. peregrinus* damage with high accuracies. The study further combined environmental variables and vegetation indices calculated from the

WorldView-2 imagery to improve the prediction and mapping of *T. peregrinus* damage using a multiple stepwise regression approach. The regression model selected the near infrared band 8 of the WorldView-2 sensor and the temperature dataset to predict and map *T. peregrinus* damage with high accuracies on an independent test dataset. This research contributes to the field of knowledge by developing innovative remote sensing techniques that can accurately detect and map *T. peregrinus* damage using the new generation WorldView-2 sensor. The result is significant for forest health monitoring and highlights the importance of improved sensors which contain key vegetation wavelengths for plantation health assessments.

Preface

The research described in this thesis was carried out in the School of Agricultural, Earth and Environmental Sciences, University of KwaZulu-Natal, Pietermaritzburg, from March 2009 to November 2012, under the supervision of Professor Onisimo Mutanga.

I Zakariyyaa Oumar declare that:

1. The research reported in this thesis, except where otherwise indicated, is my original research.
2. This thesis has not been submitted for any degree or examination at any other university.
3. This thesis does not contain other persons' data, pictures, graphs, or other information, unless specifically acknowledged as being sourced from other persons.
4. This thesis does not contain other persons' writing, unless specifically acknowledged as being sourced from other researchers. Where other written sources have been quoted, then:
    a. Their words have been re-written, but the general information attributed to them has been referenced.
    b. Where their exact words have been used, then their writing has been placed in italics and inside quotation marks, and referenced.
5. This thesis does not contain text, graphics, or tables copied and pasted from the Internet, unless specifically acknowledged and the source being detailed in the thesis and in the References section.

…….

Zakariyyaa Oumar

As the candidate's supervisor, I certify the above statements and have approved this thesis for submission.

…….

Professor Onisimo Mutanga

Publications

Oumar, Z., & Mutanga, O. (2011). The potential of remote sensing technology for the detection and mapping of *Thaumastocoris peregrinus* in plantation forests. *Southern Forests: A Journal of Forest Science, 73* (1), 23-31.

Oumar, Z., Mutanga, O., & Ismail, R. (2013). Predicting *Thaumastocoris peregrinus* damage using narrow band normalized indices and hyperspectral indices using field spectra resampled to the Hyperion sensor. *International Journal of Applied Earth Observation and Geoinformation, 21*, 113-121.

Oumar, Z., & Mutanga, O. (In review). Predicting water stress induced by *Thaumastocoris peregrinus* infestations in plantation forests using field spectroscopy and neural networks. *Journal of Spatial Science*.

Oumar, Z., & Mutanga, O. (2013). Using WorldView-2 bands and indices to predict bronze bug (*Thaumastocoris peregrinus*) damage in plantation forests. *International Journal of Remote Sensing*, *34* (6), 2236-2249.

Oumar, Z., & Mutanga, O. (In review). Integrating environmental variables and WorldView-2 image data to improve the prediction of *Thaumastocoris peregrinus* damage in plantation forests. *ISPRS Journal of Photogrammetry and Remote Sensing*.

Signed…….

Dedication

For my dearly loved parents Essack and Fatima Sheik Oumar, my beloved wife Naadhirah and my precious daughter Yusayrah

Also for my much loved brother and sister, Muhammad and Somayya Sheik Oumar

Acknowledgements

First and foremost, all thanks go to Almighty ALLAH (SWT), who has guided me throughout my life and made it possible for me to complete my PhD. I also extend my gratitude to my parents who encouraged me to do a PhD and always provided me with love and support.

I thank my supervisor, Professor Onisimo Mutanga who groomed me from an undergraduate student and motivated me to do a PhD. Onnie; I thank you for all the support and guidance you have offered me throughout my tertiary studies. You taught me how to be a scientist and write scientifically, which resulted in our papers being readily accepted by international journals.

My gratitude extends to the National Research Foundation and the University of KwaZulu-Natal for providing me with the necessary funding to carry out my research. I also wish to thank Digital Globe Inc. for supplying me with satellite imagery to carry out this research.

I wish to thank my dear friend and colleague Clement Adjorlolo for his valuable advice and support. It was always a comfort for me when I called you Clems. You gave encouragement and motivation to me to complete my studies.

Special thanks go to Riyad Ismail, Elhadi Adam, Kabir Peerbhay and Romano Lottering for their valuable comments, advice and support. Thanks go to Brice Gijsbertsen for assisting me with the ASD field spectrometer. I must also thank my brother Muhammad Sheik Oumar and Romano Lottering for assisting in my data collection. The assistance that you guys provided is greatly appreciated. I also extend my gratitude to Shani Ramroop from geography for arranging transport and all the logistics related to my study.

Thanks go to Michael Chetty and the ICFR team for assisting in my water and chlorophyll analysis. I also wish to thank Ryan Nadel from the ICFR who provided me with valuable advice on *T. peregrinus* infestations. Thanks goes to Vivek from the CSIR who supplied me with the necessary equipment needed for my field data collection.

I extend my appreciation to the NCT team: Craig Norris, Jeremy Dixon, Lance Bartlett, Peter Odell, Ian Thompson and Thato, for all the assistance and support you gave me in identifying *T. peregrinus* infestations on our plantations.

With gratitude, I thank my family and friends for all their love and support. Finally, I wish to thank my beloved wife Naadhirah for been a dedicated wife who always gave me love and support.

Table of Contents

CHAPTER SEVEN

CHAPTER ONE

1. General Introduction

1.1 Introduction

Eucalyptus is one of the most extensive tree genera planted in the world due to its economic value and rapid growth in a variety of habitats (Nadel and Noack, 2012). Eucalypts are planted extensively in commercial forest plantations and are cultivated mainly for pulp and fibre production (Turnbull, 1999). The success of eucalypt plantations are dependent on accelerating forest productivity and tree growth by correct site species matching and isolation from natural pests and pathogens (Wingfield et al., 2008). Due to an increase in trade and travel there has been an increase in new pest and pathogens introduced into eucalypt plantations globally (Nadel and Noack, 2012; Wingfield et al., 2008). *T. peregrinus* is one of the new emerging pests found in eucalypt plantations. *T. peregrinus* originates from Australia and has recently spread to South Africa and Argentina (Carpintero and Dellape, 2006; Jacobs and Neser, 2005). *T. peregrinus* is a small (2-4 mm) sap sucking insect that feeds on eucalypt leaves. It poses a major threat to the forest sector by reducing the photosynthetic ability of the tree resulting in stunted growth and death of severely infested trees (FAO, 2007). Infested trees initially display a reddening of the leaves and as infestation progresses the entire canopy turns reddish yellow to reddish brown, shedding leaves and reducing tree growth (Jacobs and Neser, 2005; Nadel and Noack, 2012). A full description of the biology and impact of *T. peregrinus* on plantation forests is described in chapter two of this study. The monitoring of *T. peregrinus* and the effect it has on plantation health is essential for ensuring productivity and future sustainability of eucalypt plantations globally. Remote sensing technology has rapidly developed as a promising tool for the monitoring of forest health. Advances in remote sensing technology which include hyperspectral sensing together with new generation spaceborne multispectral scanners, provide opportunities to detect and map *T. peregrinus* damage in plantation forests. This study advocates the development of remote sensing techniques to accurately detect and map *T. peregrinus* damage in plantation forests. Once developed and tested, remote sensing can be applied operationally to detect and map the damage.

1.2 Remote sensing *T. peregrinus* damage

Remote sensing technology has been extensively used to detect and map insect damage in plantation forests due to advances in hyperspectral and multispectral scanners (Bentz and Endreson, 2003; Campbell et al., 2004; Coops et al., 2003; Coops et al., 2004; Coops et al., 2006; Dennison et al., 2010; Dye et al., 2008; Fraser and Lativofic, 2005; Ismail et al., 2007;

Ismail et al., 2008; Wulder et al., 2006a; Wulder et al., 2006b). Hyperspectral sensors which contain very narrow contiguous spectral bands throughout the visible, near-infrared, mid-infrared and thermal infrared portions of the electromagnetic spectrum make it possible to detect manifestations in vegetation health and reveal physiological changes in forest health as a result of insect infestation (Milton et al., 2009; Treitz and Howarth, 1999). New improvements in multispectral sensors which contain higher spatial and spectral information as compared to previous sensor developments make remote sensing a valuable tool in detecting and mapping insect damage in plantation forests.

Although numerous studies have assessed the capability of remote sensing applications in monitoring insect infestation in plantation forests, there are still challenges that need to be met. The unique physiological and structural effects that *T. peregrinus* infestation has on forest plantations differ vastly from other forest pest invasions. Therefore, previous remote sensing efforts that have been successful in mapping insect damage in plantation forest cannot be guaranteed to effectively map *T. peregrinus* damage. To the best of our knowledge, no studies have tested the applicability of remote sensing techniques in detecting and mapping *T. peregrinus* damage in plantation forests. Hence, the research advocates the development and testing of techniques that can accurately detect and map *T. peregrinus* damage.

Trees infested with *T. peregrinus* damage turn into a red brown colour, starting at the northern side of the canopy that progressively spreads throughout the canopy. Initial stages of infestation may show little or no sign of damage and trees that are heavily infested display a reddening of leaves (FAO, 2007; Jacobs and Neser, 2005). The physiological changes associated with *T. peregrinus* damage include a reduction in the photosynthetic ability of the tree (Carpintero and Dellape, 2006; Jacobs and Neser, 2005) due to the reduction in chlorophyll pigments and moisture deficit. Hence, there is a challenge to identify early physiological stages of infestation related to water and chlorophyll stress, therefore appropriate intervention methods can be implemented before trees reach a stage of severe infestation. Hyperspectral data which contain narrow contiguous bands offer the potential to detect these physiological changes associated with water and chlorophyll stress. Although numerous hyperspectral indices related to stress detection in vegetation health have been developed, little is known about their feasibility for mapping *T. peregrinus* damage. Therefore vegetation indices and band combinations calculated from hyperspectral data need to be developed and tested in order to predict the physiological stages of *T. peregrinus*

damage. However, hyperspectral data is often associated with the problem of multicollinearity, whereby there is a high degree of intercorrelation that exists between spectral bands. Robust stochastic models which reduce the large number of collinear variables and overcome the multicollinearity problem offer the potential to predict the physiological changes associated with *T. peregrinus* damage. Such an investigation provides an insight into spectral curves and key wavelength regions that are critical for detecting the impacts of insect damage on eucalypt forests from an early stage of infestation.

Due to large outbreaks of *T. peregrinus* infestation, the timely collection of information related to the spread and stage of infestation is essential for effective management of forest plantations. *Cleurchoides noackae* has been identified as a biological control agent for *T. peregrinus* (TPCP, 2008b), however the ability to spatially quantify *T. peregrinus* damage over large spatial areas is a crucial factor for the deployment of this agent. The new and improved WorldView-2 multispectral sensor which contains key vegetation wavelengths such as the red edge, coastal, yellow and an extra near-infrared band, offers the potential to detect and map *T. peregrinus* damage over large spatial scales. Due to WorldView-2 being a relatively new sensor, there is limited knowledge regarding its use in plantation health monitoring. Vegetation indices calculated from the WorldView-2 sensor bands, which are sensitive to plantation health, might further augment the mapping and monitoring of early to advanced stages of *T. peregrinus* damage. Furthermore, predictive statistical models that integrate environmental datasets with improved WorldView-2 sensor data allow us to model the spread of damage, and facilitate a better understanding of the factors that influence *T. peregrinus* damage. Hence, the development of remote sensing analytical techniques, which make use of these valuable bands are imperative for the mapping of *T. peregrinus* damage in plantation forests. A more detailed motivation of the study is provided in chapter two of this thesis.

1.3 Aim and Objectives

The aim of this research is to assess the utility of remote sensing techniques to successfully detect and map *T. peregrinus* damage in plantation forests. The main objectives of the thesis are:

1. To extensively review literature on the applicability of remote sensing technology in detecting and mapping *T. peregrinus* damage.
2. To assess the utility of hyperspectral narrow band data in predicting the physiological stages of *T. peregrinus* damage.
3. To predict and map *T. peregrinus* damage with the new generation WorldView-2 sensor using remote sensing methods.

1.4 The study area

The first study area (29^{o}37'S 30^{o}20'E) is located in Pietermaritzburg, KwaZulu-Natal, South Africa. The sampled compartment in the study area covers an area of 0.5 hectares. The study area is situated at an altitude of 819 m above mean sea level and receives an annual rainfall ranging from 800 mm to 1000 mm (Camp, 1997). The mean annual temperature of the study area is 18^{o}C. Forestry is ecologically suitable and *Eucalyptus*, *Pinus* and *Acacia* species are planted across the study area on deep well drained soils (Camp, 1997). The main climatic constraints are moisture deficit during the period of May to September which makes plantations in this area susceptible to stress.

The second study area (29^{o}48'S 30^{o}13'E) is situated in Richmond, KwaZulu-Natal, South Africa and covers an area of 875 hectares. Richmond has large areas of arable land with timber and sugar cane been the main resource planted on deep well drained soils. Richmond receives an annual rainfall ranging from 800-1280 mm with a mean annual temperature of 17^{o}C. Richmond is situated at an altitude of about 900-1400 m above mean sea level. Figure 1.1 shows a map outlining the study area in the South African context.

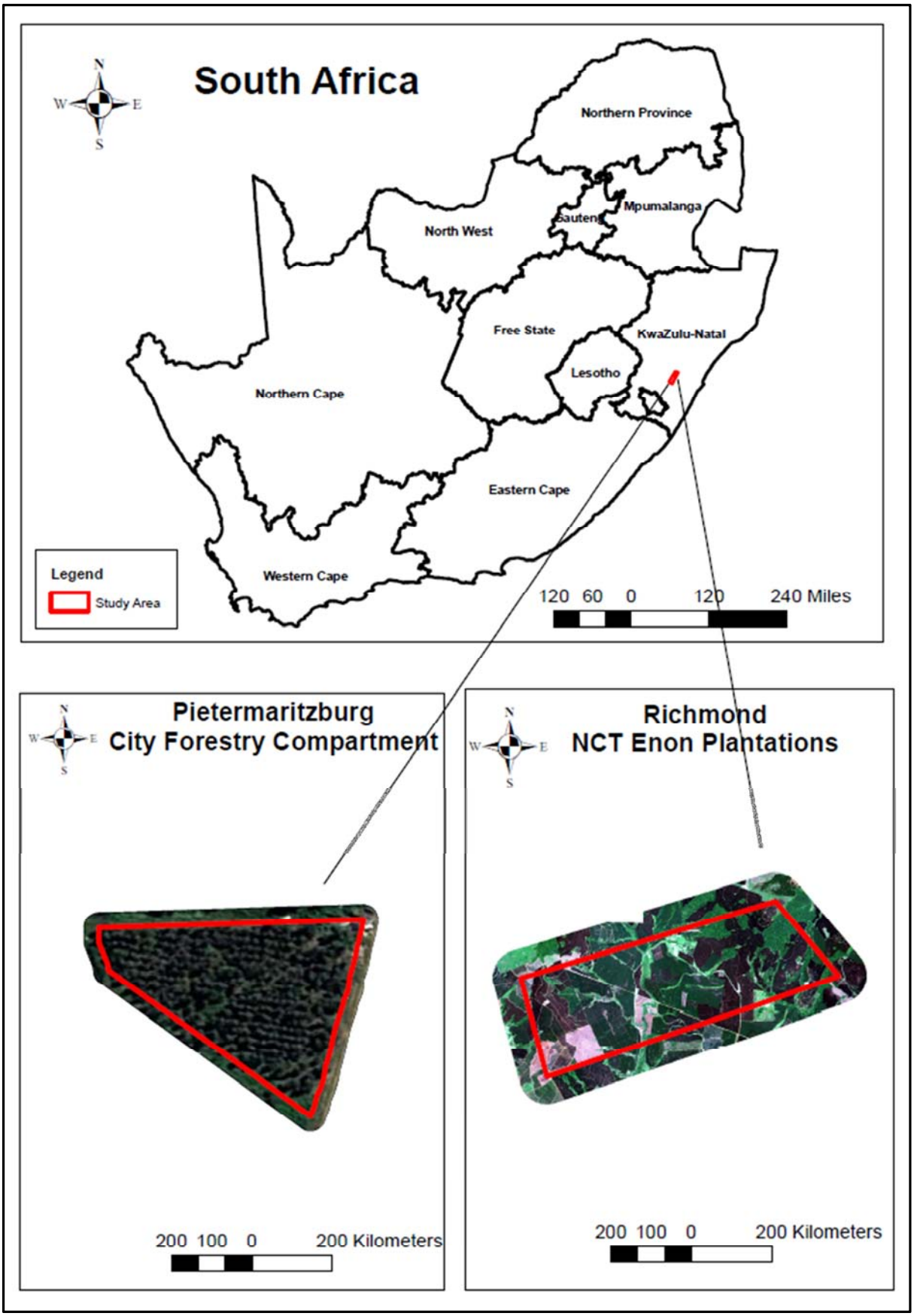

Figure 1.1 Map of the study area.

1.5 Outline of thesis

This thesis consists of seven chapters. The first chapter is the general introduction followed by five stand-alone papers. The last chapter is the conclusion which provides a synthesis of the overall research. Each chapter is written as a stand-alone paper that can be read separately from the rest but draws separate conclusions, which link the overall research aim and objectives. As a result, there are a number of overlaps and repetitions in the "Introduction" and "Methods" sections of the individual papers. This problem is deemed to be of little significance when one considers the strict peer review process and the fact that the different chapters are papers that can be read separately without losing the overall context.

Chapter two reviews the potential of remote sensing technology in detecting and mapping *T. peregrinus* damage in plantation forests, by drawing on the previous work done on the remote sensing of forest pests. The utility of multispectral and hyperspectral sensors in mapping the various stages of *T. peregrinus* damage are described. The challenges and future research regarding the mapping of *T. peregrinus* damage are outlined.

Chapter 3 assesses the capability of high resolution field spectral data resampled to the Hyperion sensor in predicting *T. peregrinus* damage. Normalized indices based on *NDVI* ratios were calculated from the visible and near-infrared bands of the Hyperion sensor, to assess its utility in predicting *T. peregrinus* damage using Partial Least Squares (PLS) regression. New indices directly linked to *T. peregrinus* damage estimation were proposed.

Chapter 4 assesses the potential of field spectroscopy and neural networks in predicting water stress induced by *T. peregrinus* infestations in plantation forests. Water absorption bands and indices were input into a neural network algorithm to predict plant water content and equivalent water thickness in order to assess early physiological stages of *T. peregrinus* infestation.

Chapter 5 assesses the potential of the new generation WorldView-2 multispectral sensor in predicting and mapping *T. peregrinus* damage. The WorldView-2 sensor bands and vegetation indices were input into PLS regression models to predict *T. peregrinus* damage. The PLS models developed from the WorldView-2 sensor bands and indices were inverted to map the severity of damage caused by *T. peregrinus.*

Chapter 6 focuses on integrating environmental variables together with high spectral resolution WorldView-2 imagery to improve on mapping *T. peregrinus* damage in plantation forests.

Chapter 7 provides a synthesis of all the research carried out and all the findings of the individual chapters are brought into perspective.

CHAPTER TWO

2. Literature Review

This chapter is based on: Oumar, Z., & Mutanga, O. (2011). The potential of remote sensing technology for the detection and mapping of *Thaumastocoris peregrinus* in plantation forests. *Southern Forests: A Journal of Forest Science, 73*, 23-31.

Abstract

T. peregrinus is a sap-sucking insect that feeds on *Eucalyptus* leaves. It poses a major threat to the forest sector by reducing the photosynthetic ability of the tree, resulting in stunted growth and even death of severely infested trees. The foliage of the tree infested with *T. peregrinus* is usually seen to turn a reddish brown colour starting at the northern side of the canopy but progressively spreading to the entire canopy. The monitoring of *T. peregrinus* and the effect it has on plantation forest health is essential to ensure productivity and future sustainability of forest yields. Internationally a number of studies have successfully used remote sensing technology to monitor forest damage. Remote sensing technology allows for instantaneous methods of assessments whereby ground assessments would be impossible on a regular basis. This paper provides an overview of how advances in remote sensing technology can be used to detect and map the different stages of *T. peregrinus* infestations using multispectral and hyperspectral scanners. The challenges and future research regarding the mapping and detection of *T. peregrinus* are also discussed. It is concluded that remote sensing techniques need to be tested, improved upon and applied for the successful detection and monitoring of *T. peregrinus* infestations.

Keywords: *T. peregrinus*, multispectral, hyperspectral.

2.1 Introduction

T. peregrinus is one of the new emerging invertebrate pests found in exotic *Eucalyptus* commercial plantations (Button, 2007). *T. peregrinus* originates from Queensland, Australia, and has recently taken on pest populations in *Eucalyptus* species in South Africa and Argentina (Jacobs and Neser, 2005; TPCP, 2007b). *T. peregrinus* is a small (2-4 mm) sap-sucking insect that feeds on *Eucalyptus* leaves. It poses a major threat to the forest sector by reducing the photosynthetic ability of the tree, resulting in stunted growth and even death of severely infested trees (FAO, 2007). The monitoring of *T. peregrinus* and the effect it has on plantation health is essential to ensure productivity and future sustainability of forest yields on a global scale.

Current methods used to identify *T. peregrinus* infestations involve field-based studies whereby foresters and taxonomists visually confirm their presence. The use of field based surveys to identify infested trees are costly, time consuming and spatially restrictive. Furthermore, the effectiveness of visual assessments are questionable because they are qualitative, subjective and depend on the skill of the surveyor (Ismail, 2009). A number of studies have used remote sensing technology to monitor forest damage (Ekstrand, 1994; Fraser and Lativofic, 2005; Ismail et al., 2007; Macomber and Woodcock, 1994; Radeloff et al., 1999). Remote sensing technology allows for instantaneous methods of assessments whereby ground assessments would be impossible on a regular basis (Ceccato et al., 2001; Datt, 1999). Advances in remote sensing technology such as hyperspectral imagery combined with greater availability and lower cost of high spatial resolution imagery provide opportunities to detect and map forest pests (Coops et al., 2003). Once developed and tested, remote sensing can be applied operationally and can improve the ability to detect and map insect infestations (Coops et al., 2003). However, for remote sensing technology to accurately detect and map *T. peregrinus* infestations, knowledge of the symptoms of *T. peregrinus* across leaf, canopy and landscape level is required in order to relate infestations to different spatial and spectral resolution data. Knowledge of these symptoms will allow for the development of algorithms to detect changes in foliar characteristics using remotely sensed data. This paper provides an overview of the potential of remote sensing technology in detecting and mapping *T. peregrinus* infestations. There has been no specific review on the use of remote sensing applications for the detection and mapping of *T. peregrinus*. Hence, this paper focuses specifically on the potential of remote sensing technology to detect and

map *T. peregrinus* infestations by drawing on the previous work undertaken on the remote sensing of forest pests in general.

2.2 The biology of *T. peregrinus* and its impact on forest plantations

T. peregrinus is a member of the Thaumastocoridae family which is a small family comprising of six genera and fifteen described species (Jacobs and Neser, 2005). The pest was originally identified as *T. australicus* by Jacob and Neser (2005) until Carpintero and Dellape (2006) described the species as *T. peregrinus* which is morphologically similar to *T. australicus*. The identification of the *Thaumastocoris* pest in South Africa has been confirmed as *T. peregrinus* through genetic testing and in consultation with taxonomic specialists (FAO, 2007).

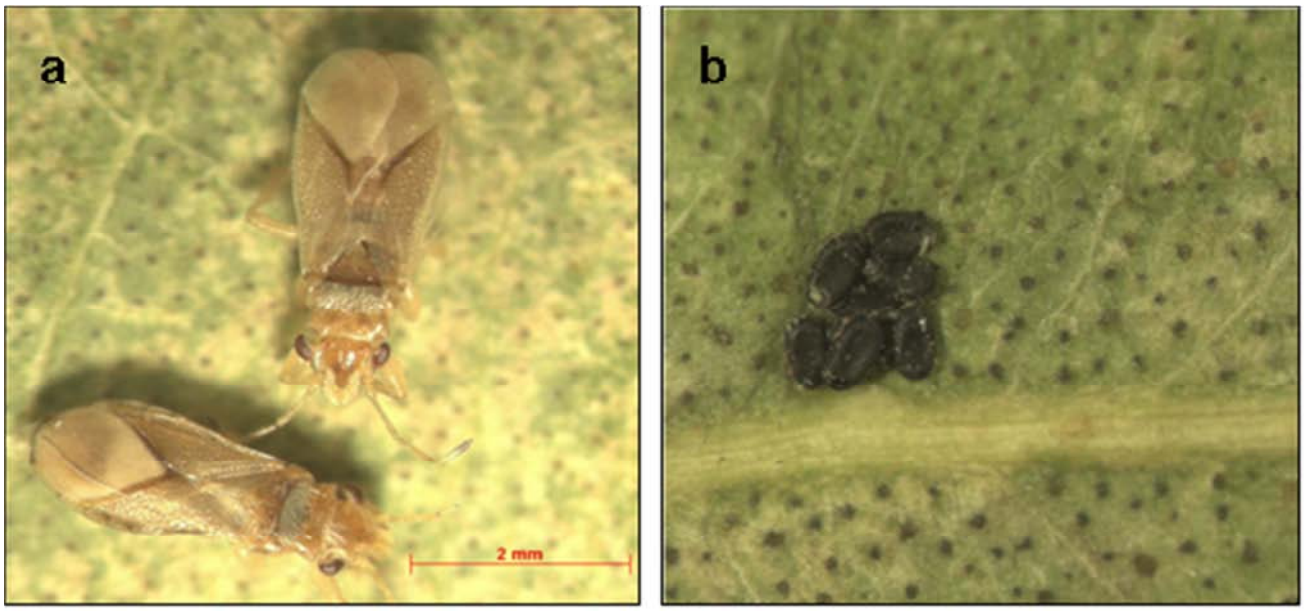

Figure 2.1 (a) *T. peregrinus* (b) Presence of eggs on *Eucalyptus* leaves (FABI, 2010).

T. peregrinus (Figure 2.1 a) also known as the 'bronze bug' is a gregarious, sap-sucking bug that has become an economically important pest in the *Eucalyptus* plantations of South Africa (FAO, 2007). The bug is now found in all *Eucalyptus* growing regions and is feeding on majority of the commercially available *Eucalyptus* species and clones in younger and older trees (TPCP, 2007b). The female bug lays eggs in clusters on *Eucalyptus* leaves where they are visible as black spots (Figure 2.1 b). The presence of such black spots is often the easiest way to identify infested trees (Jacobs and Neser, 2005). The female bug produces about sixty eggs in her life-cycle which lasts for about 35 days. The symptoms of infestation are referred

to as ‘winter bronzing’ or ‘winter dieback’. The symptoms of infestations are visible annually but they vary depending on location. Figure 2.2 shows a monitoring trial carried out by the Tree Protection Co-operative Programme (TPCP) throughout the *Eucalyptus* growing regions of South Africa revealing that *T. peregrinus* infestations vary according to site (TPCP, 2008a).

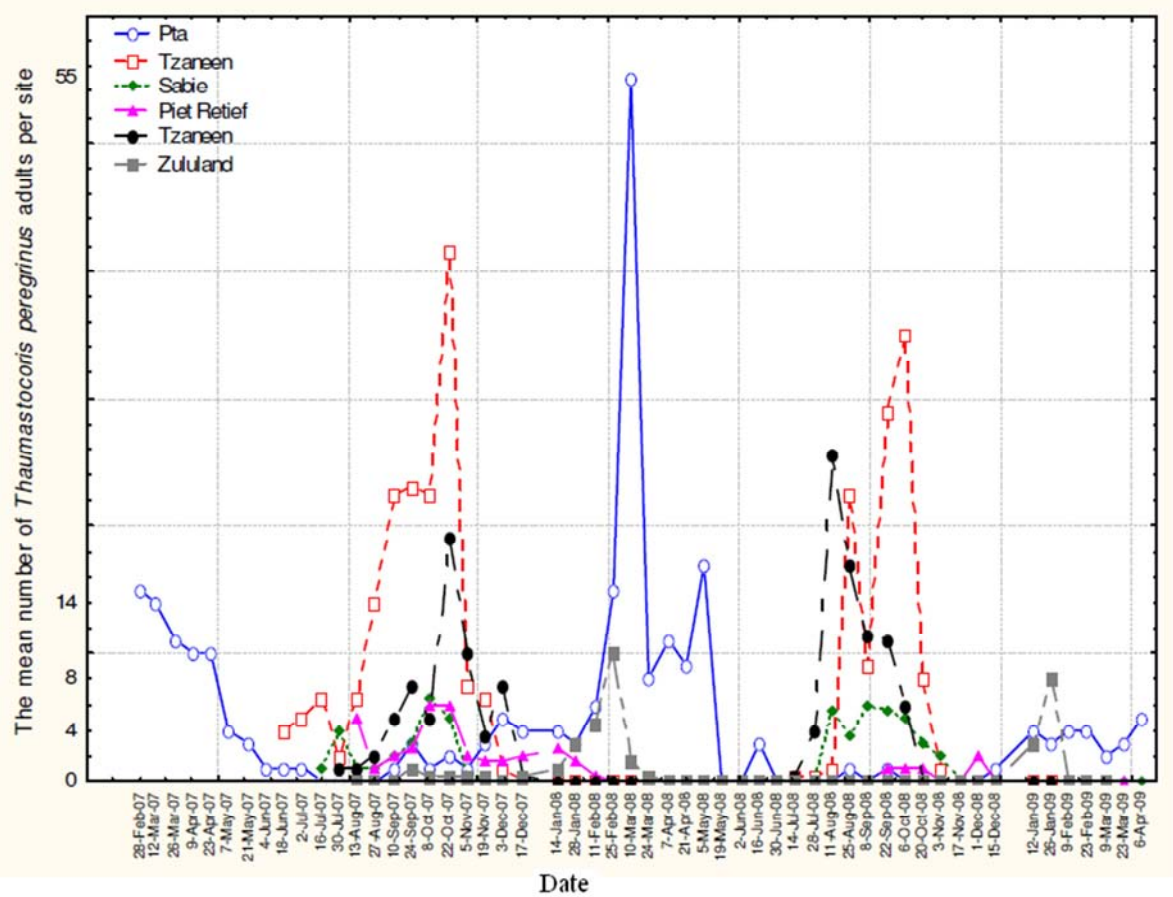

Figure 2.2 Monitoring trial carried out by the TPCP over a two year period showing fluctuations of *T. peregrinus* populations in the *Eucalyptus* growing regions of South Africa (TPCP, 2008a).

The *Eucalyptus* hybrids that are affected by the bug in South Africa are *E. grandis x camaldulensis* and *E. grandis x uropylla*, as well as *E. smithii* and *E. grandis* which are also found to be severely infested (Nadel et al., 2007). Trees and leaves that are lightly infested may show little or no sign of damage. Heavily infested trees display a reddening of the leaves and have a ‘washed out’ pale appearance when affected. According to Jacob and Neser (2005) heavily infested trees drop their leaves and branches may die back or the entire tree may die. The infested trees, however do appear to recover when *T. peregrinus* populations

are reduced and unfavourable conditions for their survival occur (Button, 2007). Table 2.1 shows the stages of *T. peregrinus* infestation.

Table 2.1 Symptoms of *T. peregrinus* infestation.

Stages of infestation	**Symptoms**
Light Infestation 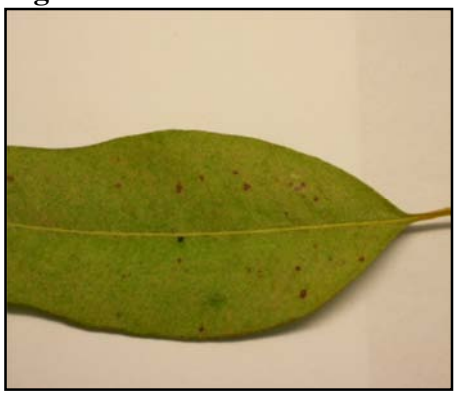 Source: FABI, (2010)	Trees and leaves that are lightly infested may show little or no sign of damage.
Heavy Infestation  Source: (Jacobs and Neser, 2005)	Trees that are heavily infested turn a deep red-brown colour starting at the northern side of the canopy sometimes referred to as 'winter bronzing'. The canopy has a 'washed out' pale appearance when heavily infested (Jacobs and Neser, 2005).
Very Severe Infestation  Source: FABI, (2010)	Trees that are severely infested result in defoliation and die back of branches, and in some cases the trees die (Jacobs and Neser, 2005).

There are currently no effective control measures in operation and no insecticides have been registered for use against infestations of this insect (Jacobs and Neser, 2005). Biological

control is currently deemed to be the only viable possibility to control *T. peregrinus* populations (TPCP, 2008b). This is the chosen route taken to deal with most forest pests because it offers a safe and effective means to reduce insect population (Nadel, 2007). Research on biological control of *T. peregrinus* is being currently carried out by the TPCP with the recent discovery of the egg parasitoid *Cleurchoides noackae*. Due to scarcity of information about the parasitoid more research regarding the biology and host preference is still to be undertaken (TPCP, 2008b). However, successful implementation and testing of these control measures depends on the ability to spatially quantify trees affected by *T. peregrinus*. Additionally, there is a need to spatially quantify *T. peregrinus* infestations so that forest managers can take appropriate intervention before the death of severely infested trees. The mapping of *T. peregrinus* in plantation forests is therefore essential to detect trees that are infested and to ensure forest sustainability.

2.3 Mapping *T. peregrinus* using remote sensing

Remote sensing technology has been explored as a cost effective and instantaneous method of assessing insect infestation (Fraser and Lativofic, 2005). The ability to detect *T. peregrinus* infestations in plantation forest using remote sensing would be beneficial to several aspects of plantation forest management including timber harvest and salvage operations. The early detection of *T. peregrinus* infestations would provide forest managers with rapid assessments of current damage so that stands of high mortality can be salvaged. Furthermore, remote sensing technology provides the opportunity to study *T. peregrinus* damage over large areas so that outbreaks can be related to other environmental parameters using spatial modeling techniques in a GIS environment. Environmental variables such as rainfall, altitude and host species will give insight on the buildup and decline of *T. peregrinus* populations, thus enabling future outbreaks to be modeled.

Forest damage usually appears as a change of colour on the forest canopy. The foliage of trees that are infested by insects changes colour from green to yellowish red and these trees are referred to as faders (Ciesla, 2000). In advanced stages of insect infestation whereby defoliation begins, the forest canopy takes on a red-brown or grey hue. The ability to detect subtle changes in the colour of the forest canopy is a key requirement when using remote sensing methods to detect and map forest damage (Ciesla, 2000). When light interacts with leaves it may be reflected, absorbed and/or transmitted. Leaves that depict changes in colour, reflect a different spectral response in the electromagnetic spectrum as compared to healthy

leaves (Carter and Knapp, 2001). Figure 2.3 shows the reflectance between a healthy and a discoloured leaf caused by *T. peregrinus* infestation indicating lower reflectance throughout the spectrum due to the effects of chlorosis. Leaves that undergo stress and discoloration due to the loss of chlorophyll show an increase in reflectance in the visible portion of the electromagnetic spectrum (400-700 nm) (Carter, 1993).

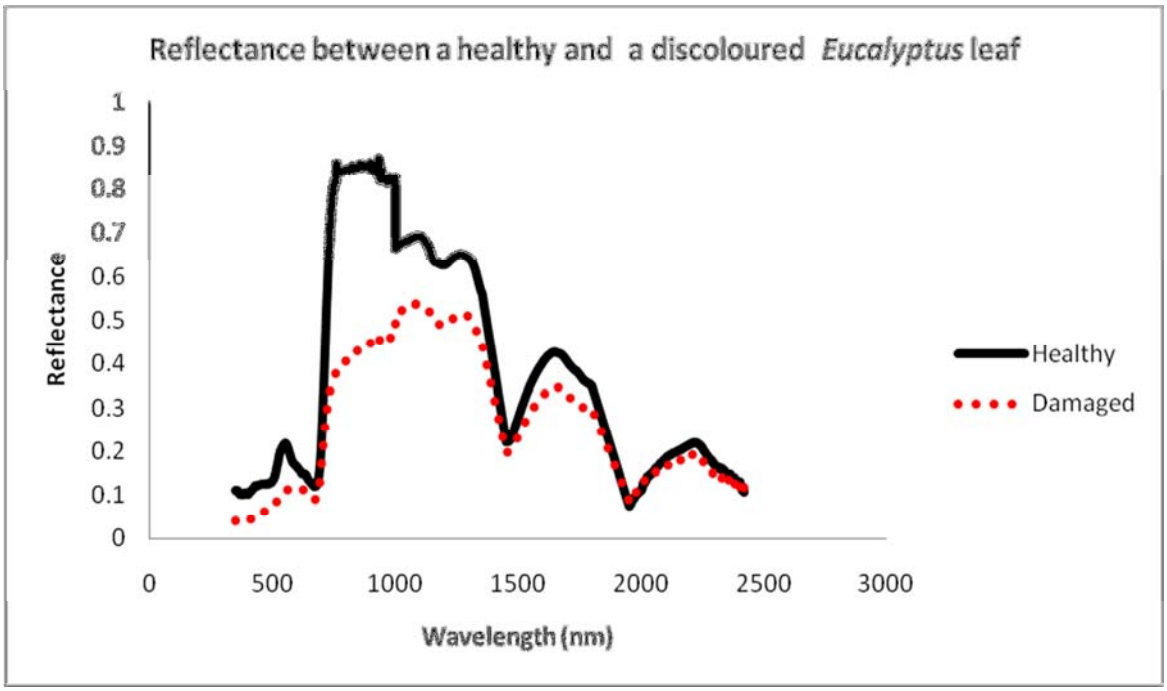

Figure 2.3 Reflectance between a healthy and a discoloured *Eucalyptus* leaf caused by *T. peregrinus* infestation.

Trees that undergo defoliation show a decrease in reflectance across the electromagnetic spectrum due to an increase of shadow and background within the field of view (Schmidt, 2003). Barry et al., (2008) used a series of spectral indices to evaluate discolouration and defoliation on eucalypt species under controlled conditions. When defoliation treatments in *E. globulus* or stress in *E. pilularis* resulted in large differences in leaf cover, indices such as the red edge, normalized difference vegetation indices (*NDVI*s) and the modified chlorophyll absorption ratio index 2 (*MCARI2*) were strongly correlated with leaf cover. Red leaves resulting from stress were strongly correlated with anthocyanin reflectance index (*ARI*) and the red-green index (*RGI*) in *E. grandis* and *E. pilularis* leaves (Barry et al., 2008). Crown discolouration (chlorosis) and defoliation along with a reduction in leaf area index (LAI) are therefore two important indicators of stress in eucalypts (Barry et al., 2008). Spectral indices such as the red edge, normalized difference indices and LAI need to be tested at leaf, branch

and tree level in *T. peregrinus* infested plantations to assess the importance in upscaling to airborne and spaceborne platforms.

Various remote sensing airborne and space borne scanners have been developed to map forest damage based on the reflectance properties of the electromagnetic spectrum (Coops et al., 2003; Coops et al., 2004; Coops et al., 2006; Dye et al., 2008; Ismail, 2009; Radeloff et al., 1999; White et al., 2005). Table 2.2 shows the different scanners that are commercially available and their respective spatial, spectral and temporal resolutions. The temporal coverage of a specific image allows for the monitoring and spread of forest damage over time. Sensors such as Landsat Thematic Mapper (TM) which has a repeat coverage of 16 days have been used to create transition maps that indicate the extent of forest damage over time (Bonneau et al., 1999). Other sensors which have shorter revisit times as indicated in Table 2.2 have the potential to assess the spread or seasonal variation in *T. peregrinus* infestations. This will serve as a spatial guide in monitoring *T. peregrinus* outbreaks. The next section will discuss how various remote sensing scanners which differ in spatial and spectral resolution can be applied to detect and map the different stages of *T. peregrinus* infestation.

Table 2.2 Commercially available scanners and their resolutions.

Satellite /Sensor	Spatial Resolution (m)	Spectral Resolution	Temporal Resolution (Repeat Coverage)
Landsat 7 + ETM	30	Blue, Green, Red, Near-infrared and Mid-infrared	16 days
ASTER	15	Visible near-infrared, Shortwave-infrared, Thermal-infrared	16 days
QuickBird 2	2.44	Blue, Green, Red, Near-infrared	1-3.5 days
IKONOS	4	Blue, Green, Red, Near-infrared	3 days
World View2	2	Blue, Green, Red, Near-infrared, Red-edge, Coastal, Yellow, Near-infrared 2	1.1 days
SPOT 5	10	Green, Red, Near-infrared, Shortwave-infrared	2-3 days
GeoEyE 2	1.65	Blue, Green, Red, Near-infrared	2-3 days

2.4 The detection and mapping of *T. peregrinus* using multispectral scanners

Multispectral remote sensing has been used to collect data of the earth's surface from airborne or spaceborne platforms since the 1960's (Landgrebe, 1999). Earth observation technologies such as satellites provide local to global coverage of remote areas where ground assessments are impossible on a regular basis. Different sensors are onboard earth observation satellites and may be used to monitor vegetation, forestry, water and other natural resources. According to Coops et al., (2006) satellite remote sensing has the ability to detect advanced stages of insect infestation over large spatial areas due to physiological changes present in the infested forest stands.

During the heavy and severe stages of *T. peregrinus* infestation the canopy turns a reddish colour and the foliage changes to a yellow-brown colour coupled with the loss of leaves. This yellowing effect whereby the leaves change colour is known as chlorosis as the green chlorophyll pigments are lost and the canopy exhibits a reddish colour (Ekstrand, 1994). Stone et al., (2001) states that leaves that undergo insect damage succumb to a variety of

processes which include damage or removal of the waxy cuticle, destruction of cell walls, reduction of moisture and a decline in chlorophyll content. The decline in the chlorophyll content reduces the photosynthetic ability of the tree and in severe infestation rates, large areas of forest lands are lost. The change in canopy colour of the infested trees will exhibit a different spectral response in the visible and near-infrared regions of the electromagnetic spectrum. Multispectral systems commonly collect data in three to six spectral bands within the visible and mid-infrared regions of the electromagnetic spectrum and have been applied to detect and map advanced stages of insect infestation (Coops et al., 2006; White et al., 2005). Table 2.3 summarizes selected studies that have used multispectral satellite imagery to map insect damage.

Table 2.3 Selected studies using multispectral satellite imagery for disease detection.

Study/Reference	Satellite	Method	Results
Identifying changes in hemlock forest health infested with the woolly adelgid (Bonneau et al., 1999).	Landsat TM	Classification and temporal analysis	A series of transition maps that indicate how forest damage changed over time.
Detecting defoliation levels of jack pine budworm (Radeloff et al., 1999).	Landsat TM	Spectral mixture analysis	Increase in near-infrared reflectance in defoliated stands, strong negative correlation between images and budworm population (r = -0.94).
Mapping insect induced defoliation caused by eastern hemlock looper (Fraser and Lativofic, 2005).	SPOT Vegetation	Change detection using logistic regression model	Mapped insect induced tree mortality in forest patches larger than 5-10 km^2.
Estimating mountain pine beetle attack (Bentz and Endreson, 2003).	Landsat, ETM, IKONOS	Classification based on linear discriminant analyses, quadratic discriminant analysis, regression trees and k's Nearest Neighbour	IKONOS image achieved lowest misclassification rate and over 95% red trees were correctly classified.
Detecting red attack stage of mountain pine beetle (White et al., 2005).	IKONOS	Unsupervised classification	70.1 % accuracy for low attack and 92.5 % for medium attack.
Assessing red attack damage due to mountain pine beetle (Coops et al., 2006).	QuickBird	Classification and Vegetation indices	Relationship between red attack pixels and red crowns based on an independent validation set resulted in an R^2 = 0.48, error =2.8 crowns.

Several authors have used medium spatial resolution imagery which collects data between 4 and 30 meters to accurately detect and map insect damage with accuracies ranging from 70% to 85% (Ekstrand, 1994; Franklin et al., 1995). Ekstrand (1994) used Landsat TM data to assess forest defoliation in stands composed of Norway spruce. The results showed that the best estimate of forest defoliation was acquired with an algorithm based on Landsat TM band 4. Fraser and Latifovic (2005) used SPOT Vegetation (VGT) imagery to map tree defoliation

and mortality caused by insect infestation in Canada. A logistic regression model based on satellite change metrics was developed to map defoliation and mortality. The results indicated that coarse spatial resolution imagery can be effective in mapping large scale forest mortality caused by insect infestation and can also be used for real-time monitoring of severe defoliation but with 2-3 times greater error of commission (Fraser and Lativofic, 2005). Bentz and Endreson (2003) used Landsat TM, Enhanced Thematic Mapper (ETM) and IKONOS imagery to predict pine mortality caused by mountain pine beetle. Bentz and Endreson (2003) argue that medium spatial resolution imagery such as Landsat (30 m) is not suitable for the detection of endemic level populations of insect damage and is more suited for detection at the building or epidemic phases of infestation. Medium spatial resolution imagery therefore has drawbacks due to the limited bandwidth, errors of commission and its inability to detect individual or small groups of infested trees (Bentz and Endreson, 2003; Fraser and Lativofic, 2005). In terms of *T. peregrinus*, medium spatial resolution imagery can be used to detect large outbreaks of infestations in the heavy stage as *T. peregrinus* is usually found across the whole compartment. The commercial availability of high spatial resolution satellite data offers the potential to detect and map individual or small groups of insect infestation compared to medium resolution imagery (Coops et al., 2006).

Coops et al., (2006) has shown that high spatial resolution satellite imagery has the ability to detect and map advanced stages of insect infestation with relatively high accuracies as data is collected between 0.5 and 4 meters. Coops et al., (2006) used QuickBird high spatial resolution satellite imagery (2.4 m) to detect and map mountain pine beetle red attack. QuickBird pixels that were classified as red attack were significantly correlated with the number of tree crowns identified as red attack damage. Bentz and Endreson (2003) used IKONOS high spatial resolution satellite imagery (4 m) to detect individual or small groups of pine mortality with relatively high accuracy as compared to Landsat imagery. The results suggest that high spatial resolution satellite imagery offers an alternative to medium resolution imagery for the location and estimation of advanced stages of insect damage. Ismail et al., (2007) also used high spatial resolution multispectral airborne imagery to detect and map *Sirex noctilio* (Eurasian woodwasp) infested plantations. The study demonstrated the potential of using high spatial resolution airborne imagery coupled with vegetation indices to discriminate between healthy and infested trees. Airborne imagery is advantageous in that it offers the potential to mobilize quickly at user specified locations as compared to satellite imagery which often has shorter times available for detection (Ismail et al., 2007). This is

essential for forest health monitoring as insect outbreaks are often linked to disturbance in compartments or climatic events making the date of image acquisition important (Ismail et al., 2007; Stone and Coops, 2004).

High spatial resolution satellite imagery offers the potential to accurately detect and map advanced stages of insect infestation with greater accuracies and reduced errors of commission. This is promising for the detection of the heavy and severe stages of *T. peregrinus* infestation using classification and statistical techniques combined with spectral indices so stands can be salvaged before they reach a point of no recovery (Coops et al., 2004; Coops et al., 2006; Ismail et al., 2007). However, even though medium and high spatial resolution satellite imagery have been successful in detecting and mapping moderate to severe stages of infestation, the early detection of insect infestation using these technologies have been difficult (Coops et al., 2003; Pontius et al., 2008). The strength of any forest health monitoring programme would be greatly improved if it were possible to detect the initial, often pre-visual strain that is caused by insect infestation (Coops et al., 2004). Remote sensing developments in hyperspectral technology have overcome the limitation of multispectral scanners and have made it possible to assess the initial stages of insect infestation. The next section will discuss the use of hyperspectral remote sensing in the detection and mapping of the initial stages of *T. peregrinus* infestations.

2.5 The detection and mapping of *T. peregrinus* using hyperspectral remote sensing

Hyperspectral refers to spectra consisting of a large number of very narrow contiguous bands in the electromagnetic spectrum and is also referred to as spectroscopy or spectrometry (Mutanga, 2004). Spectroscopy is the branch of physics concerned with the production, transmission and interpretation of electromagnetic energy. Spectrometers are used in laboratory, field, aircraft or satellite studies to measure the reflectance spectra of natural surfaces (Mutanga, 2004). Due to hyperspectral data having a variety of narrow spectral band features of less than 10 nanometers, phenological changes in forest health can be detected. In the initial or light phases of *T. peregrinus* infestation, trees may show little or no sign of infestation (Carpintero and Dellape, 2006). The ability to detect light or pre-visual stages of infestation depends on using high spectral resolution data to assess subtle changes in leaf reflectance which would be otherwise masked by broadband scanners (Hoque et al., 1992; Pu et al., 2008). Remote sensing developments in hyperspectral technology provide the potential to detect subtle changes in leaf reflectance. These narrow wavebands (visible, near-infrared,

red edge) within the electromagnetic spectrum regions have been recommended for the early detection of forest damage (Hoque et al., 1992).

According to Carter and Miller (1994) the early detection of vegetation stress depends on identifying the spectral regions in which vegetation reflectance is most responsive to unfavourable growth conditions. Recent research has established relationships between leaf reflectance and foliar biochemicals, especially the photosynthetic pigments which provide information on the physiological status of vegetation (Coops et al., 2003; Pontius et al., 2008; Zarco-Tejada et al., 2002). The availability of narrow, contiguous wavebands present in hyperspectral data make it possible to reveal physiological changes that characterize early stress responses and provides an early indication of decline in stand vigour and productive capacity (Zarco-Tejada et al., 2002). This is due to the tendency of stressed leaves to undergo a reduction in chlorophyll content and thereby alter the reflectance at chlorophyll sensitive wavelengths (Zarco-Tejada et al., 2002). Leaf reflectance in the visible and near-infrared portions of the electromagnetic spectrum can provide early indication of plant stress or the onset of disease (Coops et al., 2003). In the visible part of the spectrum (400-700 nm) an increase in leaf reflectance generally indicates stress in vegetation (Carter and Miller, 1994) and narrow waveband reflectance within the 690-700 nm range is sensitive to stress induced decreases in leaf chlorophyll content (Carter, 1993).

A number of studies have used hyperspectral data to detect and monitor early stages of insect infestation and forest damage (Entcheva Campbell et al., 2004; Ismail et al., 2008; Pontius et al., 2008). Table 2.4 summarizes selected studies that have used hyperspectral remote sensing for insect infestation and forest damage.

Table 2.4 Selected studies using hyperspectral sensing for disease detection and forest damage.

Study/Reference	Hyperspectral Sensor	Method	Results
Assessing Dothistroma needle blight in *Pinus radiata*, (Coops et al., 2003).	Compact Airborne Spectrographic Imager (CASI-2)	Spectral Indices based on severity classes	Independent accuracy assessment allowed for the detection of three levels of Dothistroma needle blight with an accuracy of over 70%.
Mapping previsual decline of hemlock stands due to hemlock woody adelgid (Pontius et al., 2008).	AISA Eagle	Spectral wavelengths and stress indices used in a stepwise linear regression model	AISA Eagle classified hemlock health at tree level with a one class tolerance accuracy of 88 %. The model predicted decline with an R^2 = 0.75 and *RMSE* = 0.81.
Detecting initial damage in Norway spruce (Campbell et al., 2004).	Airborne Solid-State Array Spectroradiometer (ASAS)	Reflectance indices and derivative analysis	Spectral indices were strongly correlated to damage. The 673-724 nm spectrum provided the highest potential for identifying forests with initial levels of damage.
Discriminating *Sirex noctilio* infestations (Ismail et al., 2008).	ASD Spectrometer	ANOVA and Jeffries-Matusita (J-M) distance analysis	Spectral bands located in the visible portion (350-700nm) and the red edge (670-737nm) could discriminate different levels of attack. (J-M) indicated 99,22% separability between classes.
Discriminating early stages of *Sirex noctilio* infestations (Ismail, 2009).	ASD Spectrometer	Random Forest Algorithm	Wavelengths located at 1990nm, 2009nm, 2028nm, 2047nm, 2065nm have the potential for discriminating green stage of attack.
Early detection of Douglas-Fir Beetle infestation (Lawrence and Labus, 2003).	Probe 1 sensor	Stepwise discriminant analysis (DISCRIM) and classification and regression tree analysis (CART)	Predictive accuracy of CART using cross-validation resulted in a classification accuracy of 69%. Classification among healthy, attacked and living trees gave an accuracy of 50-70%.

Detecting forest mortality caused by *Phytophthora ramorum* (Pu et al., 2008).	Compact Airborne Spectrographic Imager (CASI-2)	Classification Algorithms, Principal Components	Principal Components derived from the visible and near-infrared bands successfully classified stressed from non-stressed trees with a classification accuracy of 75.55%.

Ismail et al., (2008) used high spectral resolution data to discriminate different levels of *Sirex noctilio* infestation in pine plantations. The results showed that bands in the visible (350-700 nm) and the red edge (670-737 nm) portion of the electromagnetic spectrum could discriminate the different levels of attack. Ismail (2009) also used reflectance measurements in the shortwave infrared to discriminate between healthy and early stages of *Sirex noctilio* infestation. The results show that there is a link between the shortwave infrared wavelengths and the existing physiological conditions thereby making it possible to detect early stages of *Sirex* infestation. Bands located at 1990 nm, 2009 nm, 2028 nm, 2047 nm and 2065 nm were able to discriminate between healthy and early stages of *Sirex* infestation (Ismail, 2009). Campbell et al., (2004) used canopy hyperspectral imagery to separate healthy from initially damaged canopies using spectral indices. The region between 673-724 nm showed maximum sensitivity to initial damage and the results demonstrate the potential of hyperspectral canopy data in separating healthy from the initial stages of forest damage. Hyperspectral data collected at branch or canopy level takes into account variation in leaf area, leaf angle distribution and percentage ground coverage (Blackburn, 2007). This data is useful in estimating defoliation levels in forest stands as compared to leaf hyperspectral data which is used to assess stress in leaves based on pigment concentration. Pontius et al., (2008) used hyperspectral imagery (AISA Eagle) to map pre-visual decline of hemlock stands caused by hemlock wooly adelgid infestation. The AISA Eagle imagery was able to predict decline based on pre-visual changes in chlorophyll content and early stress.

Hyperspectral instruments (AISA Eagle, ASAS, CASI-2, Probe1 sensor) have the capability to identify the early signs of stress in forest plantations and in some cases before visual symptoms are apparent (Pontius et al., 2008). This is promising for the detection of the light and early stages of *T. peregrinus* infestation. Using hyperspectral data, key vegetation wavelengths could be identified to detect the onset of light stages of *T. peregrinus* infestation. Once techniques have been developed and tested, hyperspectral airborne imagery could be used to accurately detect and map areas of high infestation.

2.6 Challenges in mapping *T. peregrinus* and future research

Although considerable progress has been made in sensor development and the application of remote sensing technology for insect infestation, there are still challenges to be met. Firstly, to the best of our knowledge there has been no work done on applying remote sensing applications for the detection and mapping of *T. peregrinus* infestation in plantation forests. Despite the lack of research, there is a challenge to develop accurate operational techniques (airborne and spaceborne) to detect and map the stages of *T. peregrinus*; taking an advantage of improvements in sensor characteristics and processing techniques such as atmospheric correction algorithms, spectral resampling, spectral sharpening and classification algorithms.

Secondly, with the advancements in hyperspectral technology, there is a challenge to identify key vegetation wavelengths which can discriminate between healthy and infested trees. Vegetation indices which use information in the visible and near-infrared portions of the electromagnetic spectrum need to be tested to assess their strength in classifying *T. peregrinus* infestations. Robust spectral indices need to be developed to assess *T. peregrinus* infestations. Spectral regions such as the 'red edge' which characterizes stress in vegetation (Dawson and Curran, 1998; Filella and Penuelas, 1994) have not been tested to assess its relationship with *T. peregrinus* infestations. It is crucial to test these techniques at leaf, branch and tree level to develop sensitive bands which can be used in the scaling up process for the detection of *T. peregrinus* infestations using airborne and spaceborne platforms.

A third research challenge would be to test the utility of the South African satellite, SumbandilaSat to detect and monitor *T. peregrinus* infestations in plantation forests. The SumbandilaSat which was launched in February 2010 has 6 wavebands with a swath width of approximately 40 km and a ground sampling resolution of 6.5 meters (Oumar and Mutanga, 2010; Scholes and Annamalai, 2006). It is imperative to test the utility of data acquired using this satellite in monitoring plantation health and forest diseases in South Africa, as the sensor comprises key vegetation wavelengths such as the red edge (690-730 nm) and the xanthophylls (520-540 nm), which are not presently available on current operational multispectral satellite sensors but on hyperspectral sensors which are expensive to acquire (Oumar and Mutanga, 2010). In this regard, the development of techniques that can make use of the SumbandilaSat bands to detect and map *T. peregrinus* infestations in plantation forests are critical.

A fourth research challenge would be to develop models that predict plantations that are susceptible to potential infestation. Statistical techniques and machine learning algorithms are used as important tools to help us model and predict the spread of insect infestation (Ismail, 2009). By incorporating various factors (environmental, climatic, species preference) within a GIS model, the prediction of the onset and possible spread of *T. peregrinus* in plantation forests could be better understood. Environmental factors have a direct impact on the distribution of pest populations in forest plantations. The ability to model areas that are vulnerable to threat using environmental factors and remote sensing data will empower forest managers to focus their detection methods and make cost effective decisions related to the management of forest plantations (Coops et al., 2004; Radeloff et al., 1999). Forest managers will have the ability to adopt the most appropriate remediation measures (such as *Cleurchoides noackae*) before *T. peregrinus* can colonize uninfected forests.

Given all these challenges, it is essential to apply remote sensing techniques (identifying key vegetation wavelengths, potential of vegetation indices and the red edge in estimating insect infestation, texture measures and LAI to assess defoliation, multispectral and hyperspectral sensing at leaf, branch and tree level) to accurately detect and map *T. peregrinus* infestations in forest plantations. There is no doubt that remote sensing technology will play a pivotal role in the detection and mapping of *T. peregrinus*. Once these techniques have been tested and developed they can be used operationally as an effective method to quantify, detect and monitor *T. peregrinus* infestations in plantation forests.

2.7 Acknowledgements

We would like to thank the Forestry and Agricultural Biotechnology Institutes (FABI), for the photos. Funding for this research was provided by the National Research Foundation (NRF) of South Africa.

2.8 Link to next chapter

The above chapter provided a literature review on the current capabilities of hyperspectral and multispectral sensors in detecting and mapping the various stages of *T. peregrinus* infestations. The next chapter now tests the potential of narrowband hyperspectral field data in predicting *T. peregrinus* damage in plantation forests.

CHAPTER THREE

3. Predicting *T. peregrinus* damage using hyperspectral narrowband reflectance

This chapter is based on: Oumar, Z., Mutanga, O. and Ismail, R., 2013. Predicting *Thaumastocoris peregrinus* damage using narrow band normalized indices and hyperspectral indices using field spectra resampled to the Hyperion sensor. *International Journal of Applied Earth Observation and Geoinformation*, 21: 113-121.

.

Abstract

T. peregrinus is a sap sucking insect that feeds on *Eucalyptus* leaves. It poses a threat to the forest industry by reducing the photosynthetic ability of the tree, resulting in stunted growth and even death of severely infested trees. Remote sensing techniques offer the potential to detect and map *T. peregrinus* infestations in plantation forests using current operational hyperspectral scanners. This study resampled field spectral data measured from a field spectrometer to the band settings of the Hyperion sensor in order to assess its potential in predicting *T. peregrinus* damage. Normalized indices based on *NDVI* ratios were calculated using the resampled visible and near-infrared bands of the Hyperion sensor to assess its utility in predicting *T. peregrinus* damage using PLS regression. The top 20 normalized indices were based on specific biochemical absorption features and predicted *T. peregrinus* damage with a mean bootstrapped R^2 value of 0.63 on an independent test dataset. The top 20 indices were located in the near-infrared region between 803.3 nm and 894.9 nm. Twenty three previously published hyperspectral indices which have been used to assess stress in vegetation were also used to predict *T. peregrinus* damage and resulted in a mean bootstrapped R^2 value of 0.59 on an independent test dataset. The datasets were combined to assess its collective strength in predicting *T. peregrinus* damage and significant indices were chosen based on variable importance scores (VIP) and were then entered into a PLS model. The indices chosen by VIP predicted *T. peregrinus* damage with a mean bootstrapped R^2 value of 0.71 on an independent test dataset. A greedy backward variable selection model was further tested on the VIP selected indices in order to find the best subset of indices with the best predictive accuracy. The greedy backward variable selection model identified 3 indices and performed the best by predicting damage with an R^2 value of 0.74 with the lowest *RMSE* of 1.30% on an independent test dataset. The best three indices identified include the anthocyanin reflectance index, carotenoid reflectance index and the normalized index calculated at 864.4 and 884.7 nm. Individual relationships between these indices and *T. peregrinus* damage indicate that high correlations are obtained with the inclusion of a few severely infested trees in the sample size. When the severely infested trees were removed from the study, the normalized index (864.4 and 884.7 nm) and the anthocyanin reflectance index still yielded significant correlations at the 99% confidence interval. This study indicates the significance of normalized indices and spectral indices calculated from the visible and near-infrared bands in hyperspectral data for the prediction of *T. peregrinus* damage.

Keywords: *T. peregrinus*, PLS regression, normalized indices, hyperspectral indices.

3.1 Introduction

T. peregrinus is a small sap sucking insect that feeds on *Eucalyptus* leaves (Oumar and Mutanga, 2011). It poses a major threat to the forest sector by reducing the photosynthetic ability of the tree, resulting in stunted growth and even death of severely infested trees (FAO, 2007). The bug has become an economically important pest in the *Eucalyptus* plantations of South Africa and is feeding on the majority of commercially available eucalypt species and clones (TPCP, 2007a). The symptoms of infestation include, reddening of the leaves, dropping of leaves and branch dieback and in severe cases the entire tree may die (Jacobs and Neser, 2005). The monitoring of *T. peregrinus* and the effect it has on plantation health is essential to ensure forest productivity. Current methods used to identify infested trees involve field based studies whereby foresters and taxonomists confirm their presence visually. The use of field based studies to identify infested trees are costly, time consuming and spatially restrictive. Remote sensing techniques offer the alternative of a non-destructive and instantaneous method of identifying infested trees over large spatial scales (Datt, 1999).

A number of studies have used remote sensing technology to monitor forest damage (Bentz and Endreson, 2003; Bonneau et al., 1999; Coops et al., 2006; Franklin et al., 1995; Ismail et al., 2007; White et al., 2005). Earth observation technologies such as satellites provide local to global coverage on remote areas where ground assessments are impossible on a regular basis (Oumar and Mutanga, 2010). However even with airborne multispectral scanners; remote sensing data collection is limited to a specified and finite number of spectral bands, making it difficult to identify the early signs of insect infestation. The ability to detect early stages of infestation depends on using high spectral resolution data to assess subtle changes in leaf reflectance that would be otherwise masked by broadband scanners (Hoque et al., 1992; Ismail et al., 2008; Pu et al., 2008). The availability of narrow, contiguous wavebands present in hyperspectral data make it possible to reveal physiological changes that characterise early stress responses and provides an early indication of decline in stand vigour and productive capacity (Zarco-Tejada et al., 2002). This is because of the tendency of stressed leaves to undergo a reduction in chlorophyll content and thereby alter the reflectance at chlorophyll sensitive wavelengths (Zarco-Tejada et al., 2002). Recent advances in airborne imaging sensors, in particular high spectral resolution imaging platforms such as Hyperion, offer the potential to identify subtle changes in leaf reflectance due to the availability of narrow spectral channels of about 10 nm (Somers et al., 2010). These narrow spectral channels permit an in-depth understanding of insect infestation which is otherwise masked by the

broad wavebands acquired using multispectral data. Leaves that undergo insect damage succumb to a variety of processes which include damage or removal of the waxy cuticle, destruction of cell walls, reduction in moisture and loss in chlorophyll content (Stone et al., 2001). These physiological changes result in different spectral responses in the visible and near-infrared portions of the electromagnetic spectrum making narrow waveband reflectance crucial for the monitoring of forest damage (Hoque et al., 1992). Leaf reflectance in the visible and near-infrared portions of the electromagnetic spectrum provides an early indication of plant stress or the onset of disease (Coops et al., 2003). In the visible part of the spectrum (400–700 nm) an increase in leaf reflectance generally indicates stress in vegetation (Carter and Miller, 1994) and narrow waveband reflectance within the 690–700 nm range is sensitive to stress-induced decreases in leaf chlorophyll content (Carter, 1993).

The normalized difference reflectance index (*NDVI*) is used as a measure to assess plant growth and vigour and is calculated from the red and near-infrared bands of the electromagnetic spectrum (Tucker, 1979). Healthy vegetation absorbs most of the visible light and reflects a large portion of the near-infrared light, whereas unhealthy vegetation reflects more visible light and less near-infrared light thus yielding lower *NDVI*s (Rouse et al., 1973; Tucker, 1979). *NDVI* values have been widely used in remote sensing to assess vegetation properties at field, airborne and satellite levels (Penuelas and Filella, 1998). Several studies have used *NDVI* based indices for the detection of pests as it is sensitive to plant damage and defoliation (Genc et al., 2008; Luedeling et al., 2009) and is characterized by contrasting chlorophyll pigments in the red region against plant materials in the near-infrared. Authors such as Cho et al., (2007) argue that the computation of *NDVI* indices which are based on only the red and near-infrared region of the electromagnetic spectrum limits the usage of the rich spectral information contained in hyperspectral data. So in this study we calculate normalized indices using all the bands in the visible and near-infrared region of the electromagnetic spectrum. Normalized indices based on *NDVI* ratios have been computed using regression techniques to predict foliar nutrients and biomass (Cho et al., 2007; Mutanga et al., 2004; Mutanga and Skidmore, 2004b) but have not been exploited to the best of our knowledge for the prediction of insect damage in hyperspectral data. It is envisaged that normalized indices based on *NDVI* ratios could improve the prediction of *T. peregrinus* damage.

Several hyperspectral indices have also been used for the prediction of forest damage (Barry et al., 2008; Coops et al., 2004; Coops et al., 2006; Genc et al., 2008; Penuelas and Filella,

1998). Hyperspectral indices which are developed from the red and near infrared regions have been shown to be significantly correlated with plant physiological variables and leaf phenology (Penuelas and Filella, 1998). Spectral indices developed in these regions respond to changes in plant phenology and therefore could be important contributors in the prediction of *T. peregrinus* damage. Several authors (Barry et al., 2008; Campbell et al., 2004; Coops et al., 2003; Genc et al., 2008) have successfully used hyperspectral indices (pigment specific and red edge indices) to assess forest and vegetation stress. The utility of these indices in the prediction of *T. peregrinus* damage is yet to be tested. Due to the high collinearity present in hyperspectral narrow band data, a powerful method for the identification of the most useful narrow band indices is essential for the prediction of *T. peregrinus* damage.

PLS regression is a data compression technique which reduces a large number of collinear variables to a few non-correlated latent variables or factors (Frank and Friedman, 1993; Geladi and Kowlski, 1986; Tobias, 1995). In the field of hyperspectral remote sensing, there is often high collinearity between reflectances at different spectral wavelengths and ordinary regression methods tend to overfit prediction models. A number of researchers have shown that PLS regression is a powerful tool in identifying significant signals in such datasets (Feilhauer et al., 2010; Luedeling et al., 2009; Ye et al., 2008). The PLS algorithm iteratively produces a series of models, to find a few PLS factors (also known as components or latent variables) which explain most of the variation in both the predictor and response variable (Tobias, 1995). The PLS algorithm produces VIP scores which are used to select the relevant predictors in the model according to the magnitude of their values (Chong and Jun, 2005; Palermo et al., 2009). The utility of the PLS algorithm in predicting *T. peregrinus* damage using normalized indices and hyperspectral indices is yet to be established.

It is against this background that the study resamples fine spectral resolution data measured from a field spectrometer to the band settings of the Hyperion sensor. The objectives of the research are: (i) to assess the utility of narrow band normalized indices generated from resampled Hyperion data in predicting *T. peregrinus* damage and (ii) to assess if hyperspectral indices together with narrow band normalized indices could further improve the prediction of *T. peregrinus* damage.

3.2 Methods

3.2.1 Study area

The study area (29°37'S 30°20'E) is located in Pietermaritzburg, KwaZulu-Natal, South Africa. The study area is situated at an altitude of 819 m above mean sea level and receives an annual rainfall ranging from 800 to 1000 mm (Camp, 1997). Forestry is ecologically suitable and *Eucalyptus, Pinus* and *Acacia* species are planted across the study area on deep well drained soils (Camp, 1997). The main climatic constraints are moisture deficit during the period of May to September which makes plantations in this area susceptible to stress. A three year old *Eucalyptus macarthurii* compartment which was characterized by varied rates of *T. peregrinus* infestation was chosen for sampling.

3.2.2 Leaf sampling and visual damage assessment

Eight transects were arranged across the *Eucalyptus macarthurii* compartment. The distance between transects was one planted row of trees (3 meters apart). Every third tree (3 meters apart) in each transect was sampled. This was done in order to cover a wide variation of *T. peregrinus* infestation rates across the compartment. Thirty four trees were sampled and branches were cut down using a pruning saw. Fifty leaves were picked from each branch for visual damage assessments and reflectance measurements. Two to three samples were collected from each tree representing a range of decline symptoms across the tree. A total of 80 samples were collected.

Approximately ten mature leaves from each sample were used for visual damage assessment and *T. peregrinus* bugs were present on all samples. Each leaf was divided into quadrants and the percentage of necrotic tissue was visually estimated on ten mature leaves and then averaged for each sample by a plant pathologist. A visual assessment was preferred over a computer based approach as it allowed for a larger number of samples to be analyzed (Luedeling et al., 2009; Skaloudova et al., 2006). Reflectance measurements of the infested leaves were then taken with an analytical spectral device (ASD) spectrometer.

3.2.3 Leaf reflectance measurements

In situ spectral measurements were taken using an ASD field spectrometer (Fieldspec3 Pro FR) fitted with a 25° field of view bare fibre optic. The ASD field spectrometer senses in the spectral range of 350–2500 nm at a sampling interval of 1.4–2.0 nm and has a resampled bandwidth of 1 nm (Analytical Spectral Devices, 2002). This spectral range incorporates the

visible (400–700 nm), near infrared (700–1200 nm) and the short wave infrared (1200–2500 nm). The ASD spectroradiometer was mounted on a tripod and positioned 0.3 m above the leaf samples at nadir position to cover a field of view of 133 mm. Reflectance spectra were obtained by calibrating the radiance of the target leaf samples with the radiance of a standard white reference panel (spectralon) of known spectral characteristics. The leaf samples were stacked five leaf layers together and reflectance measurements were taken. This was done in order to get the infinite reflectance which is the maximum reflectance obtained from an optically thick medium (Datt, 1999). A test run was conducted before measurements and five successive leaves were shown to reach the infinite reflectance as there was no further increase in reflectance (Oumar and Mutanga, 2010). Reflectance measurements were taken by averaging ten scans with a dark current correction at every spectral measurement. No canopy reflectance was taken due to time constraints and the short life cycle of the *T. peregrinus* bug, therefore the scaling up from leaf to canopy studies would require canopy reflectance measurements to be taken.

3.3. Data analysis

3.3.1 Resampling the field spectra to the Hyperion sensor

The resampling of the field spectra was done using the ENVI software (ENVI, 2006). The method uses a Gaussian model with a full width at half maximum (FWHM) equal to the band spacings provided. The Gaussian model was chosen for resampling as it results in a normally distributed spectral dataset. The field spectral data was resampled to the calibrated band settings of the Hyperion sensor using the FWHM method. The resampled spectral data resulted in 198 calibrated bands located between 426.82 nm and 2395.50 nm. Figure 3.1 (a) and (b) shows the mean original reflectance and the mean resampled Hyperion reflectance for all the healthy and damaged leaves in the visible and near-infrared portion of the electromagnetic spectrum. The visible and near-infrared regions are zoomed in for both the original and resampled Hyperion data to show the selected regions that are used for the analysis.

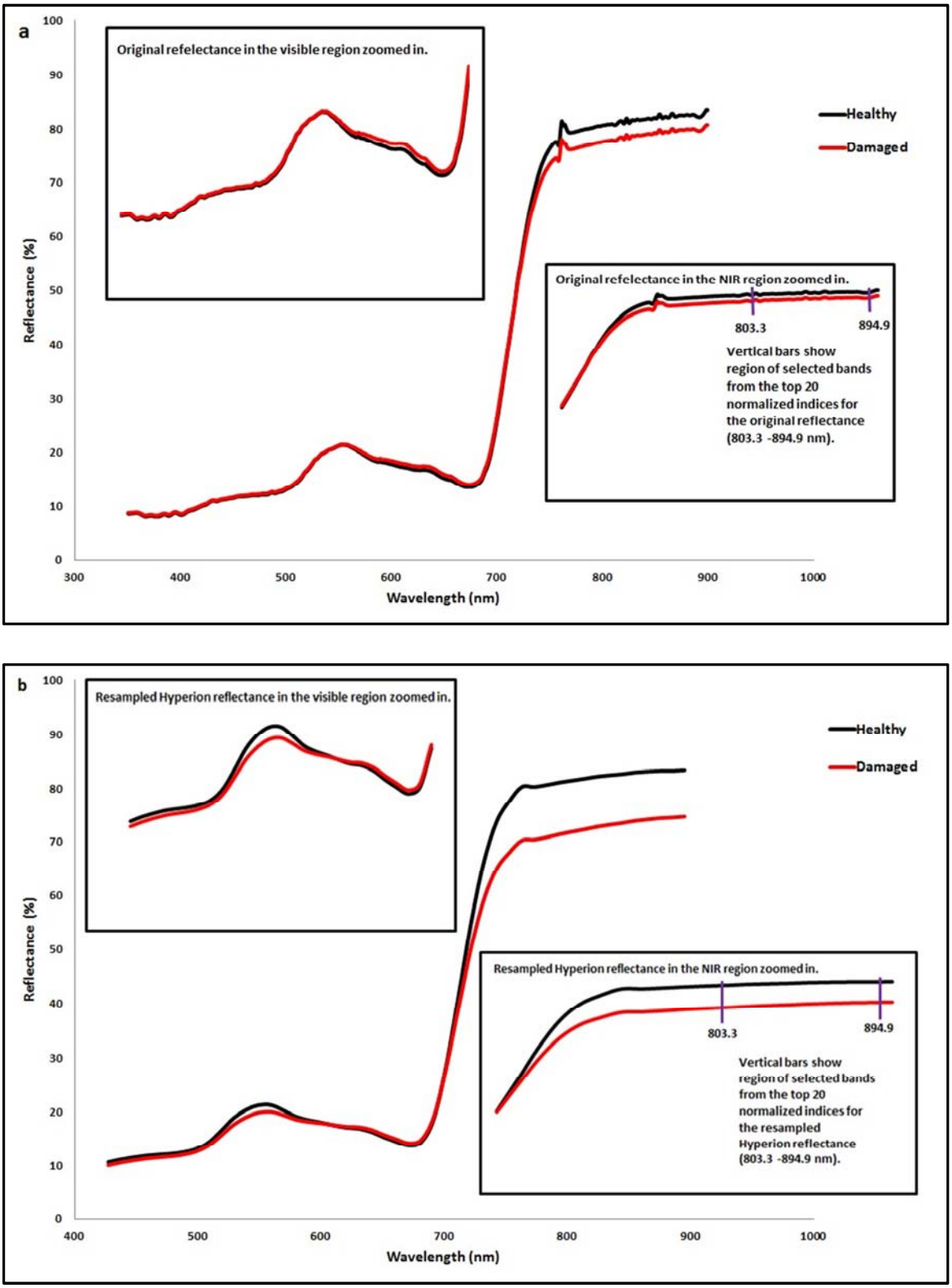

Figure 3.1 (a) The mean original reflectance **(b)** The resampled Hyperion reflectance for all the healthy and damaged leaves in the visible and near-infrared portion of the electromagnetic spectrum.

3.3.2 Narrowband normalized NDVI relationship with T. peregrinus damage

Using the resampled Hyperion data, narrow band normalized indices was computed from all possible two band combination between 426.82 nm and 894.9 nm. The discrete 47 narrow bands in the visible and near-infrared region allowed for a computation of 1081 narrow band indices. Linear regression coefficients (R^2) between all two possible normalized indices and visual damage were determined. The R^2 values were ranked and the top 20 of the two band combinations that yielded the highest R^2 values were grouped based on specific biochemical sensitivity and then selected for further analysis (Mutanga and Skidmore, 2004b).

3.3.3 Predicting T. peregrinus damage using the top 20 normalized indices and hyperspectral indices using PLS Regression

PLS regression is a technique that generalizes and combines the features of principal components and multiple regression (Ye et al., 2008). The PLS model finds a few PLS factors that explain most of the variation in both the predictors and response variables (Cho et al., 2007; Tobias, 1995; Ye et al., 2008). The PLS algorithm first projects both the predictor (X) and response (Y) variables onto one or more new axes with factors yielding scores that contain most of the information in the observed variables (Tobias, 1995; Ye et al., 2008). The PLS model is described in the form:

$$X = TP' + \mathrm{E}$$

$$Y = UQ' + F \qquad (3.1)$$

Where X = the predictors matrix; Y = the response matrix; T = X-scores; U = Y-scores; P = X-loadings; Q = Y-loadings; E = X-residuals; and F = Y-residuals (Ye et al., 2008). The PLS algorithm chooses successive factors that maximize the covariance between each X-score and the corresponding Y-score. The first few factors normally explain most of the correlation in the dataset. In any empirical modeling, it is essential to determine the correct complexity of the model since highly correlated X variables are at a risk of 'over fitting' (Wold et al., 2001). Hence, a strict test of predictive significance for each PLS component is necessary, and stopping when components start to be non-significant (Wold et al., 2001).

Cross validation is a practical and reliable way to test predictive significance and is incorporated in most PLSR software (Wold et al., 2001). Cross validation is performed by dividing the data into a number of groups and then developing a number of models from the reduced data with one of the groups deleted. V-fold cross validation is an example of this

whereby the data is randomly divided into v-subsamples, where a single subsample is used as the test dataset for testing the model and the remaining v-1 subsamples is used for training the model. After developing the models, the differences between the actual and predicted Y-values are calculated for the test dataset. The sum of squares of the differences are computed and collected from all the models to form the predicted residual sum of squares (*PRESS*), which estimates the predictive ability of the model. The cross validation method is performed in a sequential manner, on one component after the other and a component is judged significant if the *PRESS* ratio is smaller than 0.9 for at least one of the Y-variables (Wold et al., 2001). The calculations continue until a component is non-significant. The *PRESS* is calculated for the final model with the estimated number of significant components and is often re-expressed as Q^2 (the cross validated R^2) (Wold et al., 2001). Q^2 is defined as:

$$Q^2 = 1 - \text{PRESS (Predicted residual sum of squares)} / \text{SS (Sum of squares of Y corrected for the mean)} \quad (3.2)$$

The Q^2 parameter is used as a measure to identify significant components (Hoskuldsson, 2003; Hoskuldsson, 2008; Wold et al., 2001).

PLS regression was performed on the top 20 normalized indices that yielded the highest R^2. The data was randomly divided into 70% training (n=56) and 30% test (n=24) data samples. PLS regression was performed using the training dataset and v-fold cross validation was used to select the optimal number of components and was repeated 10 folds (Hoskuldsson, 2003). This was repeated for all possible permutations of the training and testing segments and the overall Q^2 was calculated in order to minimize the total prediction error and identify the significant components (Hoskuldsson, 2003; Hoskuldsson, 2008; Wold et al., 2001). Twenty three existing hyperspectral indices (Table 3.1) which have been previously used to assess stress in vegetation such as pigment specific indices and red edge indices were also analysed using PLS regression. The same training (n=56) and test (n=24) datasets were used to determine the importance of the indices in predicting *T. peregrinus* damage using the same methods described above. If the required wavebands were not available to compute the indices, the bands closest to that waveband were selected. The top 20 normalized indices and the twenty three existing hyperspectral indices were then combined into one dataset to assess its collective strength in predicting *T. peregrinus* damage. VIP scores were used to select the relevant predictors in the models and are calculated by summing the variables of influence over all the model dimensions (Chong and Jun, 2005; Palermo et al., 2009). The

recommendation by Wold (1995) was used to select relevant predictors whereby an absolute threshold value of 0.8 was used. The indices chosen by VIP were then put into a PLS model in order to assess an improvement in the prediction performance. The authors also further tested a greedy backward variable selection procedure on the VIP selected indices in order to find the best subset of indices with the best predictive accuracy. This process involved ranking the VIP indices based on their VIP scores and then iteratively dropping the lowest ranked index in a new PLS model. For example, the first iteration included all the VIP selected indices, the second iteration included all the indices without the lowest ranked VIP index and so on. For each stage of the backward selection procedure, the Q^2 cross validated error was calculated and the optimal number of VIP indices and components were then selected based on the lowest Q^2 calculated from the different PLS models. The analysis was carried out using STATISTICA 7 software (StatSoft, 2002).

Additionally, the performance of the PLS models was estimated with an independent test dataset using the coefficient of determination (R^2) and the root mean square error (*RMSE*) (equation 3.3) (Cho et al., 2007). In order to test the robustness of the model in predicting damage, bootstrapping correlations were performed on the independent test dataset. The *RMSE* was calculated according to Siska and Hung (2001):

$$RMSE = \sqrt{\frac{SSE^2}{n}} \tag{3.3}$$

Where *SSE* is the sum of errors (observed – predicted values) and *n* is the number of samples.

Table 3.1 Hyperspectral indices used in this study.

Number	Index Name	Abbreviation	Formula	Bands used in this study	Reference
1	Carter Stress Index	*CSI*	*R*695/*R*760	*R*691.4/*R*762.6	(Carter, 1994)
2	Carotenoid Reflectance Index 2	*CRI 2*	(1/*R*510)-(1/*R*700)	(1/*R*508.2)-(1/*R*701.5)	(Gitelson et al., 2002)
3	Anthocyanin Reflectance Index 1	*ARI 1*	(1/*R*550)-(1/*R*700)	(1/*R*548.9)-(1/*R*701.5)	(Gitelson et al., 2001)
4	Anthocyanin Reflectance Index 2	*ARI 2*	*R*800[(1/*R*550)-(1/*R*700)]	*R*803.3[(1/*R*548.9)-(1/*R*701.5)]	(Gitelson et al., 2001)
5	Plant Senescence Reflectance Index	*PSRI*	(*R*680-*R*500)/*R*750	(*R*681.2-*R*498)/*R*752.4	(Merzlyak et al., 1999)
6	Structure Insensitive Pigment Index	*SIPI*	(*R*800-*R*445) /(*R*800-*R*680)	(*R*803.3-*R*447.2) /(*R*803.3-*R*681.2)	(Penuelas et al., 1995)
7	Photochemical reflectance index	*PRI*	(*R*531-*R*570)/ (*R*531+*R*570)	(*R*528.6-*R*569.3)/ (*R*528.6+*R*569.3)	(Penuelas et al., 1995)
8	Simple Ratio	*SR*	*R*750/*R*710	*R*752.4/*R*711.7	(Gitelson and Merzlyak, 1994)
9	Modified Simple Ratio	*MSR*	(*R*750-*R*445)/ (*R*705-*R*445)	(*R*752.4-*R*447.2)/ (*R*701.5-*R*447.2)	(Sims and Gamon, 2002)
10	Modified Normalized Difference	*MND*	(*R*750-*R*445)/ (*R*750+*R*705-2 *R*445)	(*R*752.4-*R*447.2)/(*R*750+*R*701.5-2 *R*447.2)	(Sims and Gamon, 2002)
11	Red Green Ratio Index	*RGI*	(*R*600:700)/(*R*500:600)	(*R*599.8:701.5) /(*R*498:599.8)	(Gamon and Surfus, 1999)
12	Vogelmann Red Edge 1	*VOG1*	*R*740/*R*720	*R*742.3/*R*721.9	(Vogelmann et al., 1993)
13	Vogelmann Red Edge 2	*VOG2*	(*R*734-*R*747)/ (*R*715+*R*726)	(*R*732.1/*R*742.3)/(*R*711.7+*R*721.9)	(Vogelmann et al., 1993)
14	Red Edge First Derivative	*REFD*	Refer to reference.	Refer to reference.	(Dawson and Curran, 1998)

15	Red Edge Linear Four Point Interpolation	*REGB*	Refer to reference.	Refer to reference.	(Guyot and Barett, 1988)
16	Red Edge Linear Extrapolation	*RELE*	Refer to reference.	Refer to reference.	(Cho and Skidmore, 2006)
17	Modified Chlorophyll Absorption Reflectance Index	*MCARI*	[(*R*700-*R*670)-0.2(*R*700-*R*550)](*R*700/ *R*670)	[(*R*701.5-*R*671)-0.2(*R*701.5-*R*548.9)](*R*701.5/ *R*671)	(Daughtry et al., 2000)
18	Transformed Chlorophyll Absorption Reflectance Index	*TCARI*	3[(*R*700-*R*670)-0.2(*R*700-*R*550)(*R*700/ *R*670)]	3[(*R*701.5-*R*671)-0.2(*R*701.5-*R*548.9)(*R*701.5/ *R*671)]	(Daughtry et al., 2000)
19	Datt/Maccioni index	*DMI*	(*R*780-*R*710)/ (*R*780-*R*680)	(*R*783-*R*711.7)/ (*R*783-*R*681.2)	(Maccioni et al., 2001)
20	Far red to red index	*FFRI*	*R*750/*R*700	*R*752.4/*R*701.5	(Barry et al., 2008)
21	Lower red edge slope	*LRES*	(*R*710-*R*690)/(710-690)	(*R*711.7-*R*691.4)/(710-690)	(Barry et al., 2008)
22	Total red edge slope	*TRES*	(*R*740-*R*690)/(740-690)	(*R*742.3-*R*691.4)/(740-690)	(Barry et al., 2008)
23	Carotenoid Reflectance Index 1	*CRI 1*	(1/*R*510)-(1/*R*550)	(1/*R*508.2)-(1/*R*548.9)	(Gitelson et al., 2002)

3.4 Results

3.4.1 Visual damage

Table 3.2 shows the descriptive statistics for *T. peregrinus* visual damage assessments. The samples showed a range of decline symptoms, the majority of which were early infestation.

Table 3.2 Descriptive statistics for *T. peregrinus* visual damage assessments

Samples	Unit	Mean	Minimum	Maximum	Range	Standard deviation
80	%	11.7	1.2	72.5	71.3	11.8

3.4.2 Narrowband normalized indices and visual damage

The R^2 values for the normalized indices and visual damage ranged from 0.0 to 0.58. The top 20 normalized indices that yielded the highest R^2 were located in the region between 803.3 and 894.9 nm. These indices were then selected for further analysis (Mutanga and Skidmore, 2004b).

3.4.3 Predicting T. peregrinus damage using the top 20 normalized indices and hyperspectral indices

Table 3.3 shows the accumulated variation explained by the PLS models and the number of significant factors on the training data. The top 20 normalized indices predicted damage with an R^2 value of 0.55. The existing spectral indices predicted damage with an R^2 value of 0.39. The combined dataset yielded an R^2 value of 0.56 and the indices chosen by VIP importance (0.8 and above) yielded an R^2 value of 0.57. The backward variable selection model implemented, reduced the number of VIP selected indices from 23 to 3 and predicted *T. peregrinus* damage with an R^2 value of 0.54. The VIP indicates the importance of each variable in the contribution to the model. The following PLS models were then tested on an independent test dataset to assess its strength in predicting *T. peregrinus* damage.

Table 3.3 Percentage variation accounted for by the PLS models on the training data

Variable	**Number of Significant Factors**	**Predictor (R^2X) Cumulative**	**Response (R^2 Y) Cumulative**	**Q^2(Cumulative)**
Top 20 normalized indices (n=20)	3	0.99	0.55	0.37
Twenty three spectral indices (n = 23)	2	0.75	0.39	-0.44
Combined dataset (n = 43)	2	0.82	0.56	0.35
Indices based on VIP scores (n = 23)	2	0.96	0.57	0.40
Indices based on backward variable selection model (n = 3)	1	0.72	0.54	0.24

3.4.4 Testing the performance of the PLS models on an independent test dataset

The PLS models were tested on an independent hold out sample to assess its strength in predicting *T. peregrinus damage*. The top 20 normalized indices yielded an R^2 value of 0.63 with a *RMSE* value of 1.57%. The existing spectral indices predicted damage with an R^2 value of 0.59 and a *RMSE* value of 1.67%. The combined dataset yielded an R^2 value of 0.65 and a *RMSE* value of 1.49%. The indices chosen by VIP scores predicted damage with an R^2 value of 0.71 and a *RMSE* of 1.35%. The backward variable selection model performed the best and predicted damage with an R^2 value of 0.74 and a *RMSE* value of 1.30%. Table 3.4 shows the mean R^2 and the confidence limits on the independent test datasets. The small 95% confidence limits in Table 3.4 suggest that the bootstrapped mean R^2 approach the population estimate with a high precision (Mutanga and Skidmore, 2004b; Oumar and Mutanga, 2010).

Table 3.4 Bootstrapped R^2 values for the PLS models on the independent test data

PLS Models	**Mean R^2**	***RMSE* (%)**	**Standard error**	**95% Confidence limit**
Top 20 normalized indices (n=20)	0.63	1.57	0.07	0.01
Twenty three spectral indices (n = 23)	0.59	1.67	0.07	0.01
Combined dataset (n = 43)	0.65	1.49	0.06	0.01
Indices based on VIP scores (n = 23)	0.71	1.35	0.07	0.01
Indices based on backward variable selection model (n = 3)	0.74	1.30	0.06	0.01

3.5 Discussion

3.5.1 Relationship between normalized indices and T. peregrinus damage using Hyperion wavebands

The resampling of the field spectra to the Hyperion sensor was done in order to assess the utility of operational hyperspectral sensors such as Hyperion in predicting and ultimately mapping *T. peregrinus* infestation. Sensors such as Hyperion contain narrow wavebands of 10 nm which make it possible to reveal physiological changes that characterize stress in vegetation and provide early indication of stand vigour (Zarco-Tejada et al., 2002). This study utilized all the wavebands in the hyperspectral sensor to generate normalized indices

for the prediction of *T. peregrinus* damage. The narrow band normalized indices generated from all the wavelengths resulted in R^2 values ranging from 0.0 to 0.58. The high correlations obtained between *T. peregrinus* damage and the normalized indices were calculated from wavelengths in the near-infrared region from 803.3 nm to 894.9 nm. The strong correlations in these regions can be attributed to leaf phenological changes experienced due to stress on physiological variables as a result of *T. peregrinus* damage. The combined top 20 normalized indices resulted in a mean bootstrapped R^2 value of 0.63 on an independent test dataset with a *RMSE* of 1.57%. The result from this study indicates the potential of narrow band normalized indices calculated from *NDVI* ratios in predicting insect infestation using current operational hyperspectral sensors.

3.5.2 Relationship between T. peregrinus damage using hyperspectral indices and the top 20 normalized indices

Twenty three existing hyperspectral indices (Table 1) were evaluated to assess if they further improve the prediction of *T. peregrinus* infestation. The hyperspectral indices predicted *T. peregrinus* damage with a mean bootstrapped R^2 value of 0.59 on an independent test dataset with a *RMSE* of 1.67%. In PLS regression, a good indicator of a predictor's modeling power is VIP. The VIP gives insights into the usefulness of each variable in fitting both the indices and visual damage. The indices chosen based on VIP scores resulted in a mean bootstrapped R^2 value of 0.71 with a *RMSE* of 1.35%. The greedy backward variable selection model performed the best using only 3 indices and predicted damage with an R^2 value of 0.74 and the lowest *RMSE* of 1.30% on an independent test dataset. The *AR1* index was ranked number one with a VIP score of 1.20 followed by *CRI* (VIP = 1.04) and the 864.4 and 884.7 nm index (VIP = 1.03). The results signify the importance of spectral indices and near-infrared reflectance for monitoring insect infestation from hyperspectral data (Carter and Miller, 1994; Genc et al., 2008; Hoque et al., 1992). Figure 3.2 shows the relationship between the individual indices (anthocyanin reflectance index, carotenoid reflectance index and the 864.4 and 884.7 index) with *T. peregrinus* damage. The high correlations obtained by these indices are a result of a few highly infested trees in the sample size. This is due to the fact that we sampled trees that showed a range of *T. peregrinus* damage across the compartment and from this sample, only a few trees were severely infested. Figure 3.3 shows the correlation coefficients for the indices with the severely infested trees removed from the analysis. The normalized index using bands located at 864.4 and 884.7 nm and the *AR1* index are still significant at the 99 % confidence interval with the outliers removed. However, the

CRI yielded low and insignificant correlations. The inclusion of the severely infested trees in the study increased the range of variability, thereby strengthening the relationship with several indices. Care must therefore be taken to capture all ranges of samples (from no infestation to very high infestation) when collecting field data. The results indicate the potential of PLS regression and VIP in identifying important variables for the prediction of *T. peregrinus* damage. Ultimately, this study permits the extension of field experiments to operational hyperspectral sensors for mapping *T. peregrinus* infestation in plantation forests.

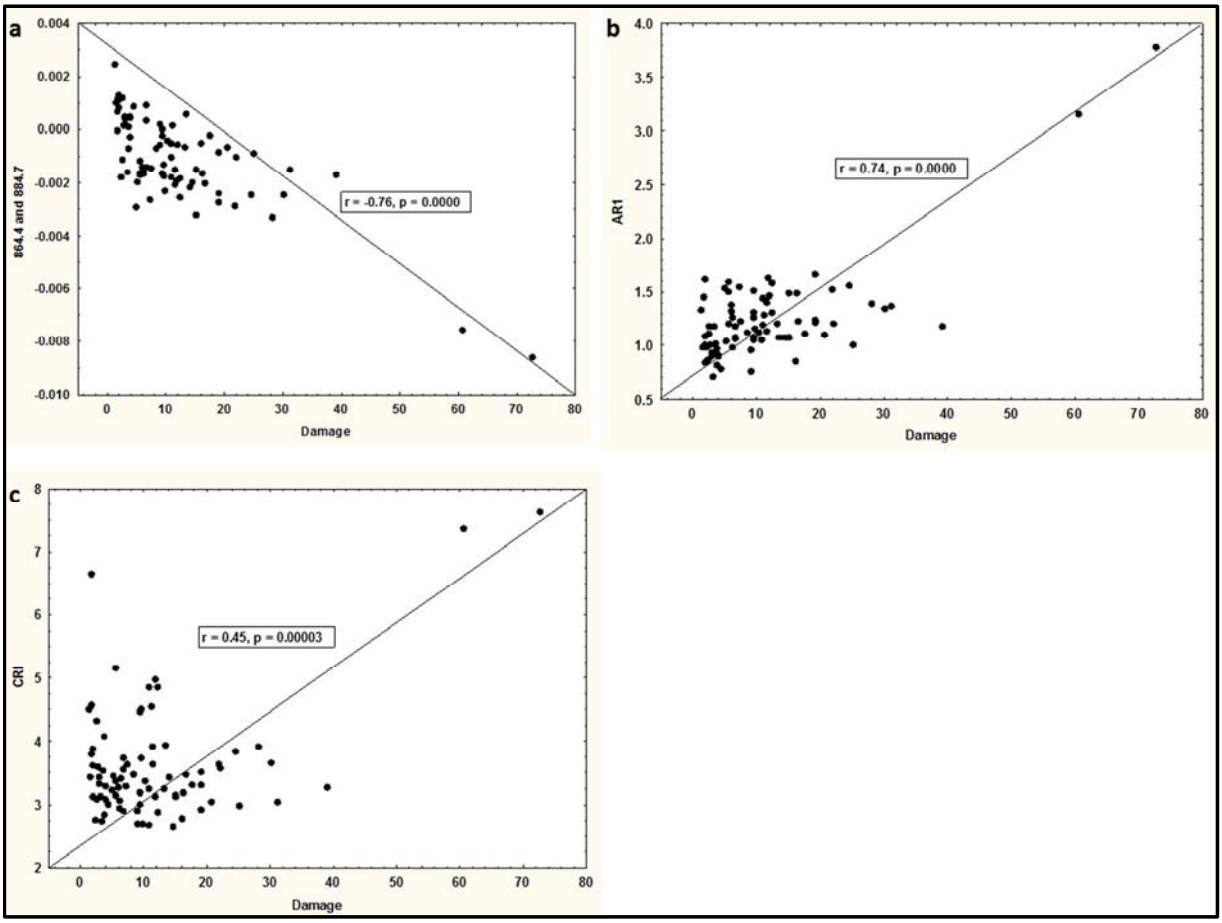

Figure 3.2 Linear relationship between selected indices and *T. peregrinus* damage. Indices shown are based on the greedy backward variable selection model. (a) 864.4 and 884.7 nm index, (b) anthocyanin reflectance index, and (c) carotenoid reflectance index. All the indices are significant at the 99% confidence level.

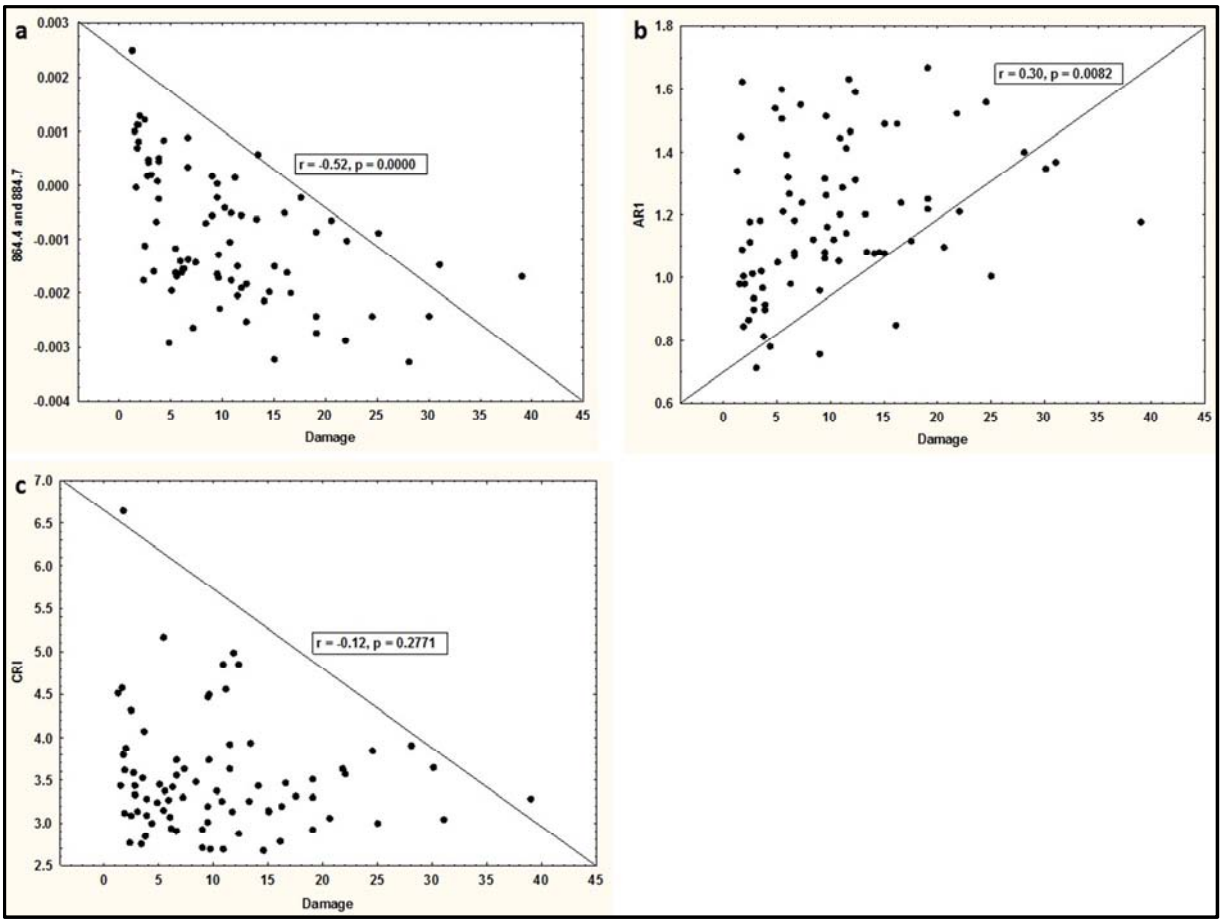

Figure 3.3 Linear relationship between selected indices and *T. peregrinus* damage with severely infested trees removed. (a) 864.4 and 884.7 nm index, (b) anthocyanin reflectance index, and (c) carotenoid reflectance index. All the indices except the *CRI* are significant at the 99% confidence level.

3.6 Conclusion

The aim of this research was to assess the utility of narrow band normalized indices generated from resampled Hyperion data in predicting *T. peregrinus* damage. The second objective was to assess if hyperspectral indices together with narrow band normalized indices could further improve the prediction of *T. peregrinus* damage. We conclude that:

1) Normalized indices that are generated from resampled Hyperion data and are based on specific biochemical absorption features could predict *T. peregrinus* damage with a mean bootstrapped R^2 value of 0.63 on an independent test dataset with a *RMSE* of 1.57%.
2) VIP indices chosen by the greedy backward selection model yielded the best results and predicted damage with an R^2 value of 0.74 and a *RMSE* of 1.30%.

3) PLS regression is a robust technique for spectral data reduction thereby identifying significant wavebands for the prediction of *T. peregrinus* damage.

Overall, this study offers the foundation for possible upscaling of the results to operational sensors such as Hyperion for the detection and mapping of *T. peregrinus* infested plantations. It must be noted that the results from this study are based on the resampled spectrometer data and does not take into account the effect of atmospheric influence. The sensitivity of the Hyperion sensor to atmospheric effects should be tested when upscaling the results.

3.7 Acknowledgements

We thank Muhammad Sheik Oumar and Romano Lottering for helping with the field work. Funding for this research was provided by the National Research Foundation of South Africa and the University of KwaZulu-Natal.

3.8 Link to next chapter

The above chapter showed the potential of normalized indices and vegetation indices generated from resampled field hyperspectral data in predicting *T. peregrinus* damage. However, the strength of any forest health monitoring programme depends on the ability to predict early, previsual stages of physiological stress associated with *T. peregrinus* damage. Hence, the next chapter focuses on the ability of field spectroscopy and neural networks to predict water stress induced by *T. peregrinus* infestations.

CHAPTER FOUR

4. Predicting plant water content in *T. peregrinus* infested plantations with field spectroscopy and neural networks

This chapter is based on: Oumar, Z. and Mutanga, O., (In review). Predicting water stress induced by *Thaumastocoris peregrinus* infestations in plantation forests using field spectroscopy and neural networks. *Journal of Spatial Science*.

Abstract

T. peregrinus is a sap sucking insect that is causing significant damage to *Eucalyptus* plantations internationally. It poses a severe threat to the forest sector by reducing the photosynthetic ability of the tree, resulting in inhibited growth and even death of severely infested trees. The monitoring of *T. peregrinus* and the effect it has on plantation health is essential to ensure future productivity and sustainability of forest yields on a global scale. Remote sensing techniques have been applied extensively to monitor advanced stages of insect infestation. However, the strength of any forest health monitoring programme would be greatly improved if it were possible to detect the initial, often previsual strain that is caused by insect damage. This study assessed the potential of high resolution field spectral data in predicting and ultimately mapping water stress induced by *T. peregrinus* infestations. Water indices and known water absorption bands were input into a neural network algorithm due to its ability to model non-linearity in a dataset and its inherent ability to perform better than linear models. The integrated approach involving field spectral data and neural networks predicted plant water content and equivalent water thickness with correlation coefficients of 0.88 and 0.71, and with *RMSE* of 0.32 % and 0.03 g cm^{-2} on an independent test dataset. The result indicates the potential of high resolution field spectral data in detecting the early stages of insect infestation due to physiological changes that alter water content. Ultimately, the results obtained from this study offer the foundation for the detection and monitoring of previsual stages of *T. peregrinus* infestations from airborne and spaceborne hyperspectral sensors.

Keywords: *T. peregrinus*, plant water content, equivalent water thickness, field spectroscopy, neural networks.

4.1 Introduction

T. peregrinus is a sap sucking insect that is causing extensive damage to eucalypt plantations internationally. It poses a threat to the forest sector by reducing the photosynthetic ability of the tree resulting in stunted growth and death of severely infested trees (FAO, 2007). Trees that are lightly infested may show little or no sign of damage and trees that are heavily infested display a reddening of leaves and have a washed out appearance (Jacobs and Neser, 2005). The monitoring of *T. peregrinus* and the effect it has on plantation health is essential to ensure productivity and future sustainability of forest yields on a global scale.

Remote sensing methods have been applied extensively to monitor advanced stages of insect damage due to colour changes associated with infestation. However, the strength of any forest health monitoring programme depends on identifying early stages of damage, often previsual colour changes that are associated with plant damage so that appropriate remediation methods can be carried out before trees reach a point of no recovery. Trees that succumb to insect infestation undergo a variety of physiological processes which include damage or removal of the waxy cuticle, destruction of cell walls and loss in water content (Stone et al., 2001). Water availability is a critical factor for plant survival and development and the monitoring of water status has important ramifications for understanding plants under stress and plantation health (Ripple, 1986; Toomey and Vierling, 2005).

In an effort to monitor vegetation health, a number of studies have used hyperspectral laboratory and field spectral data to estimate plant water content (Datt, 1999; Liu et al., 2004; Ripple, 1986). Hyperspectral data consists of many, very narrow contiguous spectral bands throughout the visible, near-infrared, mid-infrared and thermal infrared portions of the electromagnetic spectrum and has the ability to assess changes in plant water content. Water strongly absorbs radiant energy throughout the mid-infrared region (1300-2500 nm) of the electromagnetic spectrum with strong absorption bands centred on 1450, 1940 and 2500 nm; and weak absorption bands located in the near-infrared region (750-1300 nm) (Carter, 1991; Datt, 1999). The ability to predict plant water stress induced by *T. peregrinus* infestations using these water absorption bands allows for the early detection, often previsual strain that is associated with insect damage. This gives weight to many forest health monitoring programmes by quantifying the severity of water stress associated with *T. peregrinus* damage.

In order to identify water stress in plantation forests using hyperspectral data, there needs to be an understanding of how water influences the spectral reflectance of leaves. According to Carter (1991) water has several primary and secondary effects which influence the spectral reflectance of leaves. The absorption of radiation by water within the 400-2500 nm causes leaf reflectance to decrease making it an important primary effect that water has on reflectance. Other primary effects include multiple scattering by water molecules in leaves referred to as ray-leigh scattering or scattering of small particles (Carter, 1991; Gates et al., 1965). Ray-leigh scattering of water molecules however does not have a significant effect on the spectral reflectance of leaves due to the short path-length within leaves (Carter, 1991). Secondary effects of water content on the spectral reflectance of leaves are influenced by the transmissive properties of water. This occurs when water is absorbed by other substances such as pigments and depends on leaf internal structure, cell size and cell shape. Together with this, wavelength independent processes such as multiple reflections occur within leaves and hence influence the spectral reflectance of leaves (Carter, 1991). As water is lost from leaves the intercellular air spaces begin to increase thereby increasing the intensity of multiple reflections within leaves. These wave-optical processes partially explain how water loss in leaves increases reflectance in the water absorption bands and throughout the 400-2500 nm spectrum (Carter, 1991). Using these water absorption bands and the reflectance properties of leaves, various techniques and indices have been developed to estimate plant water content (Hunt and Rock, 1989; Stimson et al., 2005).

Numerous correlations between spectral bands and water indices have been developed to estimate plant water content and vegetation health (Ceccato et al., 2001; Datt, 1999; Liu et al., 2004; Penuelas et al., 1993; Toomey and Vierling, 2005). Penuelas et al., (1993) developed the water band index *(WBI)* which is based on the ratio between the water band 970 nm and reflectance at 900 nm. The *WBI* is used as an important indicator of plant water status and has been significantly correlated with water content measurements (Eitel et al., 2006; Penuelas et al., 1993). Hunt and Rock (1989) developed the moisture stress index *(MSI)* which is the ratio of the Landsat Thematic Mapper satellite bands 5 to 4 (1550-1750 and 760-900 nm). As leaf water increases the absorption around 1599 nm increases and this is sensitive to changes in moisture stress (Hunt and Rock, 1989). The normalized difference water index *(NDWI)* was developed by Gao (1996). The *NDWI* is an index that is sensitive to changes in canopy water content and uses reflectance at 857 and 1241 nm. Due to the scattering of light, the water absorption band at 1241 nm is enhanced and thus becomes

useful in predicting water stress. Stimson et al., (2005) showed that the *NDWI* is significantly correlated with water content (R^2 = 0.93) in trees that are undergoing mortality. Although numerous spectral indices and bands have been developed to measure water variations in plants, little is known about the suitability of these spectral indices to identify water stress in *T. peregrinus* infested plantations.

This study therefore aims to assess the utility of field spectral data in predicting water stress induced by *T. peregrinus* damage using water absorption bands and indices. Water absorption bands and indices were entered into a neural network algorithm to predict plant water content *(PWC)* and equivalent water thickness *(EWT)* (Ceccato et al., 2001; Eitel et al., 2006), measurements which are associated with quantifying vegetation water content in plants (Ceccato et al., 2001). A neural network algorithm was selected for water prediction due to its inherent ability to model non-linearity in a dataset and perform better than traditional linear models (Mutanga and Kumar, 2007; Sunar Erbek et al., 2004; Trombetti et al., 2008). Furthermore, neural networks are robust stochastic models that deal with the multicollinearity problem which is often associated with hyperspectral data and perform optimally in both linear and non-linear datasets (Chittineni and Bhogapathi, 2012).

4.2 Methods

4.2.1 Study area

The study area (29°37'S 30°20'E) is located in Pietermaritzburg, KwaZulu-Natal, South Africa. The study area is situated at an altitude of 819 m above mean sea level and receives an annual rainfall ranging from 800 to 1000 mm (Camp, 1997). Forestry is the main landuse and *Eucalyptus, Pinus* and *Acacia* species are planted across the study area on deep well drained soils (Camp, 1997). The main climatic constraints are moisture deficit during the period of May to September which makes plantations in this area susceptible to stress. A three year old *Eucalyptus macarthurii* compartment which was characterized by varied rates of *T. peregrinus* infestation was chosen for sampling.

4.2.2 Leaf sampling and spectral measurements

Systematic sampling was carried out whereby eight transects where arranged across the compartment. The distance between each transect was 3 meters apart and every third tree in each transect was sampled. This was done in order to cover a wide variation in plant water measurements and *T. peregrinus* damage levels across the compartment. A total of thirty four

trees were sampled and branches were cut down using a pruning saw. Fifty leaves were picked from each branch for reflectance and water measurements. Two to three samples were collected from each tree representing a range of decline symptoms across the tree. A total of eighty samples were collected.

In situ spectral measurements were taken using an ASD field spectrometer (Fieldspec3 Pro FR) fitted with a 25^{o} field of view bare fibre optic. The ASD field spectrometer senses in the spectral range of 350–2500 nm at a sampling interval of 1.4–2.0 nm and has a resampled bandwidth of 1 nm. This spectral range incorporates the visible (400–700 nm), near infrared (700–1200 nm) and the short wave infrared (1200–2500 nm). The ASD spectroradiometer was mounted on a tripod and positioned 0.3 m above the leaf samples at nadir position. Reflectance spectra were obtained by calibrating the radiance of the target leaf samples with the radiance of a standard white reference panel (spectralon) of known spectral characteristics. The leaf samples were stacked five leaf layers together and reflectance measurements were taken (Figure 4.1). This was done in order to get the infinite reflectance which is the maximum reflectance obtained from an optically thick medium (Datt, 1999). A test run was conducted before measurements and five successive leaves were shown to reach the infinite reflectance as there was no further increase in reflectance (Oumar and Mutanga, 2010). Reflectance measurements were taken by averaging ten scans with a dark current correction at every spectral measurement. After field reflectance measurements were taken the leaf samples were kept in ziplock plastic bags. The samples were stored over ice in a portable refrigeration unit to keep them fresh and were immediately taken to the laboratory for water content measurements.

Figure 4.1 Leaf spectral measurements taken using an ASD field spectrometer.

4.2.3 Plant water measurements

Various methods have been developed to estimate plant water content in vegetation (Ceccato et al., 2001; Eitel et al., 2006; Hunt and Rock, 1989; Liu et al., 2004; Stimson et al., 2005). This study used two of the most common techniques for estimating water content in vegetation, *PWC* and *EWT* (Ceccato et al., 2001). The eighty leaf samples were weighed fresh (fresh weigh: *FW*) and then dried in an oven for approximately 60^{o} C. The leaf samples were then weighed again after drying (dry weight: *DW*) and *PWC* was calculated after Liu et al., (2004):

$$PWC = FW - DW/ FW * 100\% \quad (4.1)$$

Leaf area measurements were also taken for each sample using the leaf area meter. *EWT* was then calculated and is defined as the ratio between the quantity of water and leaf area (Ceccato et al., 2001).

$$EWT = FW\text{-}DW/ leaf\ area \quad (4.2)$$

The reflectance measurements and water content measurements were used in the subsequent analysis.

4.3 Data analysis

4.3.1 Water absorption bands and indices

Known water absorption bands situated at 970, 1200, 1400, 1450 and 1940 nm (Carter, 1991; Curran, 1989; Datt, 1999) were selected for the prediction of *PWC* and *EWT*. In addition to known water absorption bands, spectral indices used for monitoring water stress were calculated from the reflectance data. The *MSI* is a reflectance measurement that is sensitive to changes in leaf water content. The *MSI* was calculated after Hunt and Rock (1989) using single wavelength reflectances in these two regions:

$$MSI = R1599/R819 \quad (4.3)$$

Where, *R* represents the reflectance at the indicated wavelengths.

The *WBI* which is sensitive to changes in canopy water status was calculated after Penuelas et al., (1993):

$$WBI = R900/R970 \quad (4.4)$$

The *NDWI* which is used to predict water stress in canopies and assess plant productivity was calculated after Gao (1996):

$$NDWI = (R860 - R1240) / (R860+R1240) \quad (4.5)$$

The normalized difference infrared index *(NDII)* is a reflectance measurement that is sensitive to changes in water content and is used for vegetation stress detection. The *NDII* was calculated after Hardisky et al., (1983):

$$NDII = (R819-R1649) / (R819+R1649) \quad (4.6)$$

The spectral indices and water absorption bands were then entered into a neural network algorithm for the prediction of *PWC* and *EWT*.

4.3.2 The neural network algorithm

An artificial neural network algorithm was used to predict *PWC* and *EWT*. A neural network algorithm consist of a large number of highly interconnected processing elements working in union to solve a problem through a learning process (Sunar Erbek et al., 2004). A multiple layer perceptron neural network was used as it has the ability to learn to give importance to significant variables and ignore less important ones.

Figure 4.2 shows the neural network structure that was used to predict *PWC* and *EWT*. A back propagation algorithm was used which consist of a three layer network and contains an input, hidden and output layer. The back propagation algorithm is designed to minimize the *RMSE* between the actual output of a multiple layer perceptron and the desired output (Mutanga and Skidmore, 2004a; Oumar and Mutanga, 2010).

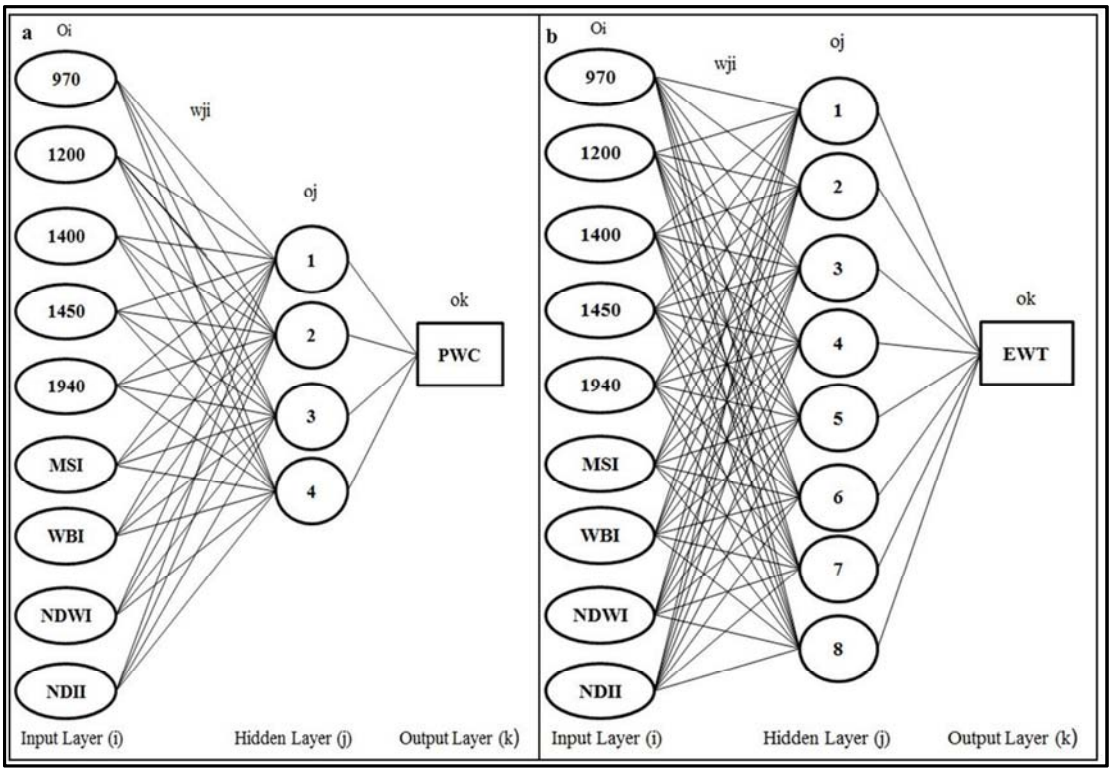

Figure 4.2 Neural network structure used to predict a) *PWC* and b) *EWT*.

The back-propagation algorithm comprises a forward and a backward phase through the neural network. The forward phase occurs when the input values which are the water absorption bands and spectral indices (o_i) are presented to a node and are multiplied by a weight factor (w_{ji}) (Skidmore et al., 1997). The products are then summed at the hidden nodes (o_j) to create a value z_j for the jth layer. The following description is after Skidmore et al., (1997):

$$Zj = \sum_{j} Wji * Oi \tag{4.7}$$

For a three layer network with the layers i, j, k with k being the output layer z_k may be calculated as equation (4.7). Non-linearity is added to the network when the value z_j is passed through a sigmoidal activation function for each node. The output of this function is defined as:

$$O_j = \frac{1}{1 + e^{-(Zj+\theta)\theta_0}} \tag{4.8}$$

Where z_j is defined from equation (4.7), θ is a threshold or bias and θ_0 is a constant (Skidmore et al., 1997).

The forward phase stops once the output values *PWC* and *EWT* (ok) are calculated for each output node. The second phase involves the back-propagation whereby the output node values are compared with the target values (measured *PWC* and *EWT*) and involves training of the network. The difference between the target (measured *PWC* and *EWT*) and calculated output values is referred to as error. This whole process whereby error is calculated represents one epoch of the back-propagation algorithm. Back-propagation of the error is achieved by changing the weights of each node during training. The whole process is repeated and the weights are recalculated at every iteration until the error is minimal.

The dataset was randomly divided into two parts. 70% (n=56) was used for training and the remaining 30% (n=24) was used for testing. The training process was run five times with random weights (Zhang et al., 2002). The neural network that yielded the highest correlation coefficient as well as the lowest *RMSE* was chosen for the prediction of *PWC* and *EWT*. The *RMSE* was calculated after Siska and Hung (2001):

$$RMSE = \sqrt{\frac{SSE^2}{n}} \tag{4.9}$$

Where *SSE* is the standard sum of errors (measured versus predicted) and *n* is the number of samples.

The performance of the best selected neural network in predicting *PWC* and *EWT* was tested using the independent 30% test dataset.

4.4 Results

4.4.1 Water content and reflectance measurements

Table 4.1 shows the descriptive statistics for *PWC* and *EWT* measurements. *PWC* ranged from 43.29 – 55.17 % with a mean value of 49.33%. *EWT* measurements ranged from 0.04 to 0.15 g cm^{-2} with a mean value of 0.04 g cm^{-2}. Figure 4.3 shows the mean reflectance for the eighty samples with arrows showing the water absorption bands used in the analysis.

Table 4.1 Descriptive statistics for *PWC* and *EWT*.

Samples (n=80)	Unit	Mean	Minimum	Maximum	Range	Standard Deviation
PWC	%	49.33	43.29	55.17	11.88	3.12
EWT	g cm-2	0.08	0.04	0.15	0.11	0.02

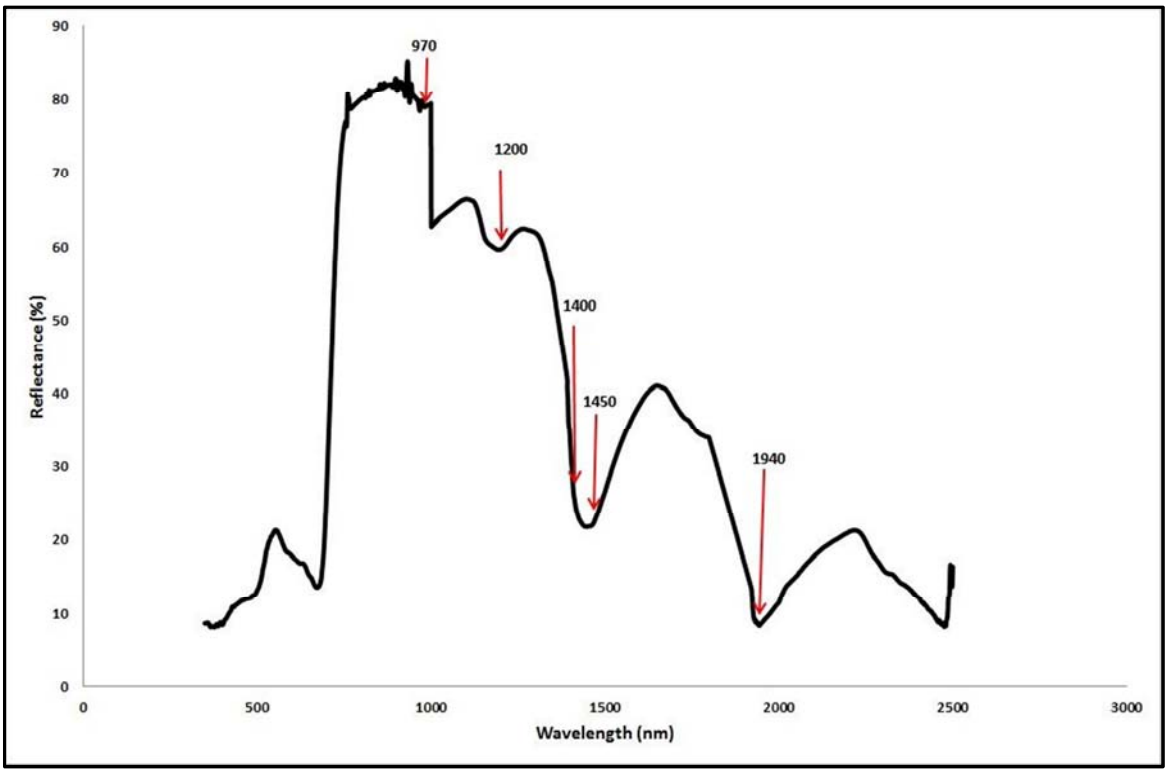

Figure 4.3 Mean spectral reflectance of the 80 samples. Arrows show water absorption bands used in the study.

4.4.2 Parameters of the neural network

The neural network parameters presented in Table 4.2 were used for training the neural network. Figure 4.4 shows the performance of the neural network in predicting *PWC* and *EWT* for the training and test datasets. The neural network algorithm predicted *PWC* and *EWT* with correlation coefficients of 0.90 (*RMSE*=0.18%) and 0.84 (*RMSE*=0.01 g cm^{-2}) on the training dataset. The strength of the prediction was validated using the 30% hold out sample and the neural network algorithm predicted *PWC* and *EWT* with correlation coefficients of 0.88 (*RMSE*=0.32%) and 0.71 (*RMSE*=0.03 g cm^{-2}).

Table 4.2 Parameters of the neural network used for predicting *PWC* and *EWT*.

Parameter	***PWC***	***EWT***
Number of inputs	9	9
Number of outputs	1	1
Number of layers	3	3
Number of hidden nodes	4	8
Neural network type	MLP	MLP

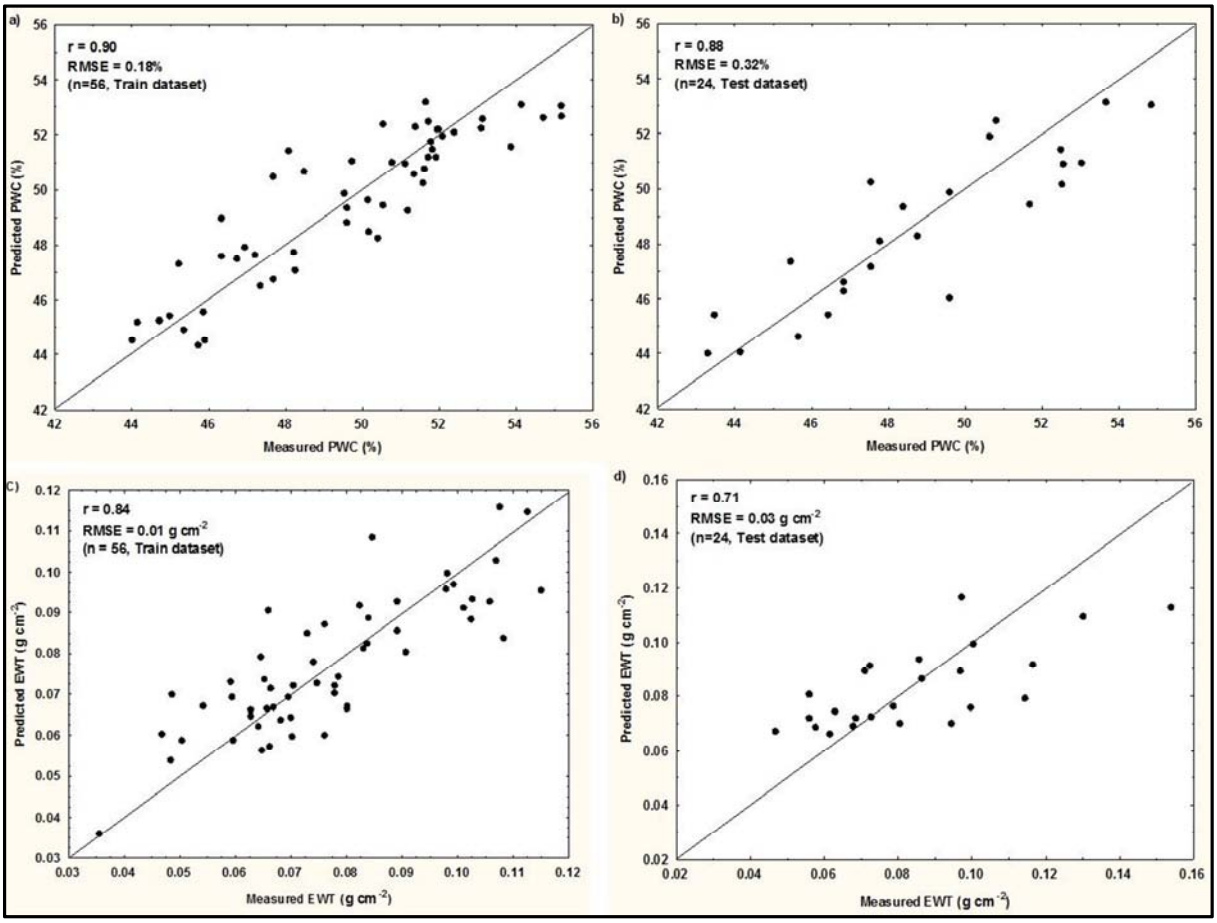

Figure 4.4 Scatterplots showing the relationship between predicted and measured *PWC* and *EWT* for the training and test datasets. (a) *PWC* (Training data), (b) *PWC* (Test data), (c) *EWT* (Training data), (d) *EWT* (Test data)

4.5 Discussion

4.5.1 Predicting water stress induced by T. peregrinus infestation using water absorption bands and spectral indices

Predicting water stress in plantation forests allows for the early identification of strain that is associated with insect infestation or disease. This is of major concern to plantation forest

managers as low levels of water stress are sufficient to reduce tree growth and increase the susceptibility of trees to insect infestation (Eitel et al., 2006). Accurate estimates of plant water content in forest plantations provide a valuable understanding of ecosystem function and plantation health. This is due to the fact that many biochemical processes such as photosynthesis and evapotranspiration are related to the foliar concentration of water (Curran et al., 2001). The ability of field spectrometers and aerial hyperspectral scanners to sample the electromagnetic spectrum in very narrow contiguous bands allows for the application of spectral indices and water absorption bands to assess variations in plant water content (Eitel et al., 2006; Gao, 1996; Penuelas et al., 1993).

The water absorption bands and indices that were input into a neural network algorithm predicted *PWC* and *EWT* with relatively high correlations of 0.88 and 0.71 on the independent test datasets. A sensitivity analysis was carried out on the input variables (water absorption bands and indices) of the neural network in order to identify the most important bands and indices that were used in the prediction. A sensitivity analysis gives insights into the usefulness of individual bands and indices for predicting *PWC* and *EWT* and identifies variables that can be ignored in subsequent analysis. For each variable, the network is executed as if that variable is unavailable in the model. The error obtained when that variable is unavailable is then divided by the error obtained when the variable is available. Important variables have a high ratio, indicating that the performance of the network will deteriorate if that variable is no longer available to the model. Table 4.3 shows the sensitivity of the water absorptions bands and indices in predicting *PWC* and *EWT*.

Table 4.3 Sensitivity analysis of the water absorption bands and indices used in the neural network.

Plant Water Content			**Equivalent Water Thickness**		
Rank	**Variable**	**Ratio**	**Rank**	**Variable**	**Ratio**
1	1450	51.26	1	1450	3.97
2	*NDWI*	29.85	2	1200	3.48
3	*NDII*	18.96	3	*WBI*	3.00
4	1200	18.37	4	1940	2.81
5	*MSI*	8.15	5	1400	2.71
6	970	6.62	6	970	1.84
7	1400	2.35	7	*MSI*	1.41
8	*WBI*	2.03	8	*NDII*	1.17
9	1940	1.30	9	*NDWI*	1.15

The water absorption band at 1450 nm was ranked the most important predictor in estimating both *PWC* and *EWT*. The results are consistent with previous studies which have found the water absorption band at 1450 nm to be strongly related to water content (Danson et al., 1992). More recent results by Mutanga and Ismail (2010) also indicate that the water absorption band at 1450 nm is significantly correlated (r = -0.75) with foliar water content in *Sirex noctilio* infested trees. The *NDWI* was ranked the second most important index in predicting *PWC* followed by the *NDII*. Eitel et al., (2006) showed that the *NDWI* was significantly correlated to relative water content (r = 0.78) and *EWT* (r = 0.75). The 1200 nm water absorption band and the *WBI* index were ranked as second and third most important contributors in the prediction of *EWT*. Similarly, Eitel et al. (2006) showed that the *WBI* is significantly correlated with relative water content (r = 0.90) and *EWT* (r = 0.88). According to Bowyer and Dawson (2004) strong correlations between water content and *WBI* are obtained when there are low water content values. With a decrease in plant water content, there is a decrease in the water absorption bands making it more pronounced and sensitive to changes in water stress (Eitel et al., 2006). The ability to detect water stress associated with early insect infestation provides forests managers with the opportunity to establish control methods before trees reach a point of no recovery. Early stress detection techniques are thus crucial in reducing economic losses in forestry operations. Spectral indices and water absorption bands calculated from high resolution spectral data are therefore essential in assessing water stress associated with insect infestation.

4.6 Conclusion

The aim of this research was to assess the utility of water absorption bands and spectral indices to predict water stress induced by *T. peregrinus* infestations in plantation forests. The following conclusions can be drawn.

1) The integrated approach involving neural networks and field spectral data predicted *PWC* and *EWT* with correlation coefficients of 0.88 and 0.71 with *RMSE* of 0.32% and 0.03 g cm^{-2} on an independent test dataset.
2) The sensitivity analysis ranked the water absorption band at 1450 nm as the most important variable in predicting *PWC* and *EWT* in *T. peregrinus* infested plantations.
3) Water absorption bands and spectral indices calculated from hyperspectral data play a key role in quantifying water stress in insect infested plantations.

Ultimately, the results obtained from this study offer the foundation for the upscaling of these methods to airborne and spaceborne hyperspectral sensors in quantifying water stress associated with early insect infestation. The results from this study are based on the assumption that environmental factors played little or no influence on the variation in plant water content. This is due to the fact that climatic variables were at a norm in the sampled compartment.

4.7 Acknowledgements

We thank Muhammad Sheik Oumar and Romano Lottering for helping with the field work. Funding for this research was provided by the National Research Foundation of South Africa and the University of KwaZulu-Natal.

4.8 Link to next chapter

The preceding chapter indicated the potential of water bands and indices in quantifying water stress in order to identify early, previsual stages of *T. peregrinus* damage. Next, the research is upscaled from field level to spaceborne platforms to test the utility of the new generation WorldView-2 multispectral sensor in predicting and mapping *T. peregrinus* damage levels.

CHAPTER FIVE

5. Predicting *T. peregrinus* damage using the new generation WorldView-2 sensor

This chapter is based on: Oumar, Z., & Mutanga, O. (2013). Using WorldView-2 bands and indices to predict bronze bug (*Thaumastocoris peregrinus*) damage in plantation forests. *International Journal of Remote Sensing*, *34* (6), 2236-2249.

Abstract

T. peregrinus is an insect causing significant damage to *Eucalyptus* plantations internationally. The bug inhibits the photosynthetic ability of the tree resulting in stunted growth and even death of severely infested trees. This study uses high spatial resolution satellite imagery (WorldView-2 sensor data), with unique band settings for the prediction of *T. peregrinus* damage in plantation forests using PLS regression. The PLS models developed from the WorldView-2 sensor bands and indices were inverted to map the severity of damage caused by the pest. The WorldView-2 sensor bands and indices predicted *T. peregrinus* damage with an R^2 value of 0.65 and a *RMSE* of 3.62% on an independent test dataset. The red edge and near-infrared bands of the WorldView-2 sensor and pigment specific indices and red edge indices were identified as significant bands by VIP scores for the prediction of *T. peregrinus* damage. This study demonstrates the potential of WorldView-2 sensor data in successfully predicting *T. peregrinus* damage using PLS regression and identifies important spectral variables for the prediction of forest damage in plantation forests.

Keywords: *T. peregrinus*, WorldView-2 sensor, PLS regression, VIP.

5.1 Introduction

T. peregrinus is a sap sucking insect that causes damage to *Eucalyptus* plantations internationally. *T. peregrinus* originates from Australia but has recently spread to South Africa and Argentina (Jacobs and Neser, 2005). *T. peregrinus* poses a major threat to the commercial forest industry as the bug reduces the photosynthetic ability of the tree resulting in stunted growth and even death of severely infested trees (FAO, 2007). The symptoms of infestation include, reddening of the leaves, dropping of leaves and branch dieback and in severe cases the entire tree may die (Jacobs and Neser, 2005). The monitoring of *T. peregrinus* is essential to ensure forest productivity and future sustainability of forest yields (Oumar and Mutanga, 2011). Current methods used to identify infested trees involve visual assessments by taxonomists and foresters which are time consuming, costly and spatially restrictive. Remote sensing advances in multispectral technology allow for non-destructive and rapid monitoring of forest damage at several landscape levels where ground assessments would be impossible on a regular basis. The ability to detect *T. peregrinus* infestations in plantation forest using remote sensing technology would be beneficial to several aspects of plantation forest management including timber harvest and salvage operations (Coops et al., 2004; Coops et al., 2006; Ismail et al., 2007). The early detection of infested trees using remote sensing technology would provide forest managers with rapid assessments of current damage so that stands of high mortality can be salvaged.

Recent developments in multispectral technology has resulted in high spatial resolution satellite imagery been used as a cost effective method for vegetation mapping. Multispectral systems which commonly collect data in three to six spectral bands within the visible and near-infrared region of the electromagnetic spectrum have been applied to map insect infestation and forest damage over large spatial areas due to the physiological changes present in infested trees (Bentz and Endreson, 2003; Coops et al., 2006; Franklin et al., 1995; White et al., 2005). These studies have focused mainly on mapping advanced stages of forest decline using high resolution imagery (QuickBird, IKONOS, GeoEye) with limited bands in the visible and near-infrared regions of the spectrum (Bentz and Endreson, 2003; Coops et al., 2006; Dennison et al., 2010; Meddens et al., 2011). New improvements in multispectral technology with more strategically placed spectral bands, together with higher spatial resolution imagery are promising for the detection and mapping of forest pests.

In October 2009 a new satellite called WorldView-2 from DigitalGlobe Inc. was launched. WorldView-2 has a spatial resolution of up to 2 meters and has 8 strategically placed spectral bands in the visible to the near-infrared range (DigitalGlobe, 2010). One of the main differences between WorldView-2 and other high resolution satellites such as IKONOS, QuickBird, and GeoEye is that it carries four additional multispectral bands (coastal, yellow, red-edge, and near-infrared2) apart from the conventional four bands (blue, green, red, and near-infrared). With WorldView-2 being a relatively new satellite sensor, few studies have been done to assess its potential in detecting and mapping forest pest such as *T. peregrinus*. It is envisaged that the WorldView-2 sensor will be vital for the prediction of *T. peregrinus* infestations due to its additional bands which are sensitive to changes in plant health and less affected by atmospheric influence (DigitalGlobe, 2010). Furthermore, vegetation indices calculated from these bands which are used for monitoring moisture content (near-infrared1), pigment indices (red and red edge) and vegetation health (red edge, green, yellow) need to be tested to assess its potential in predicting *T. peregrinus* damage using fewer but well positioned bands. However, due to the high inter correlations that exist between remote sensing bands and indices (Arenas-Garci'a and Camps-Valls, 2008), there is a challenge to develop accurate algorithms to identify the most relevant variables from the WorldView-2 sensor for the prediction of forest damage. The inherent high correlations that exist between bands and indices (multicollinearity), image noise and background effects all impede remote sensing analytical techniques resulting in biased over-fitted models (Arenas-Garci'a and Camps-Valls, 2008; Tobias, 1995). Multivariate partial least squares regression overcomes this problem and allows for the modeling of multiple responses while dealing with multicollinearity (Palermo et al., 2009). The PLS algorithm iteratively produces a series of models, to find a few PLS factors (also known as components or latent variables) which explain most of the variation in both the predictor and response variables (Tobias, 1995). The PLS algorithm produces VIP scores which are used to select the relevant predictors in the model according to the magnitude of their values (Chong and Jun, 2005; Palermo et al., 2009). No studies to the best of our knowledge have utilized the VIP scores obtained through PLS regression for the prediction of insect infestation in forest plantations using multispectral data. This study aims to assess the potential of WorldView-2 sensor bands and indices in predicting *T. peregrinus* damage in plantation forests. The second objective of the paper is to map the severity of *T. peregrinus* damage and identify significant bands and indices calculated from the WorldView-2 sensor which are essential in predicting insect infestation using VIP scores.

5.2 Methods

5.2.1 Study Area

The study area (29°48'S 30°13'E) is located in Richmond, KwaZulu-Natal, South Africa (Figure 5.1). Richmond is part of the Bioresource Group (BRG) 5 of KwaZulu-Natal and is known as the Moist Midlands Mistbelt (Camp, 1997; Oumar and Mutanga, 2010). The altitude of Richmond ranges from about 900–1400 m above mean sea level and rainfall ranges from 800 to 1280 mm. Richmond has a mean annual temperature of 17°C. Richmond has large areas of arable land and forestry is ecologically suitable. *Eucalyptus*, *Pinus* and *Acacia* species are planted on deep well drained soils.

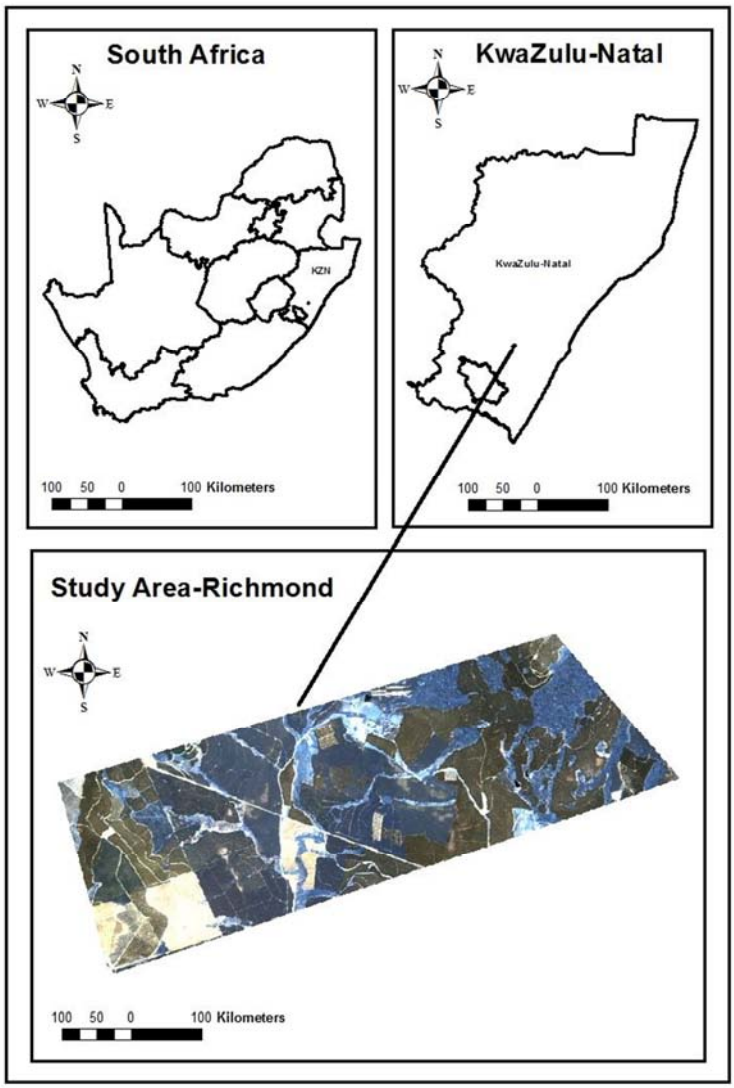

Figure 5.1 Map of study area.

5.2.2 Leaf sampling and visual damage assessment

Three *Eucalyptus smithii* compartments (4-5 years old) that showed varied rates of infestation across the study area were selected for sampling. Systematic sampling was carried out on the 24th and 25th of November 2010, in which transects were arranged across the compartments. The distance between each transect was 5 planted rows of trees (15 meters apart) and every tenth tree in each transect was sampled. This was done in order to cover a wide variation of *T. peregrinus* infestation rates across the compartment. Eighty trees were sampled and Global Positioning Systems (GPS) points were established for each tree using a handheld Trimble, Geo-Explorer unit with submeter accuracy calculated as the average of 50 sequential coordinate readings. Branches were cut down using a pruning saw and fifty leaves were picked from each tree for visual damage assessments.

Each leaf was divided into quadrants and the percentage of necrotic tissue was visually estimated on the fifty mature leaves and then averaged for each sample by a plant pathologist. Visual assessments can be subjective and depend on the skill of the surveyor, therefore the leaves were divided into quadrants and only the percentage of necrotic tissue was estimated in order to reduce subjectivity (Stone and Coops, 2004). A visual assessment was preferred over a computer based approach as it allowed for a larger number of samples to be analysed (Luedeling et al., 2009; Skaloudova et al., 2006).

5.2.3 WorldView-2 imagery

WorldView-2 imagery was acquired on the 1st of December 2010. The WorldView-2 images were orthorectified and georeferenced by the data providers and projected to the UTM Zone 36 S (WGS84) coordinate system. The WorldView-2 sensor captures 0.5 m resolution panchromatic imagery and 2 m resolution multispectral imagery. Table 5.1 shows the spectral range of the WorldView-2 sensor (DigitalGlobe, 2010).

Table 5.1 Spectral range of WorldView-2 bands

WorldView-2 Bands	**Spectral Range (nm)**
Coastal Blue	400-450
Blue	450-510
Green	510-580
Yellow	585-625
Red	630-690
Red Edge	705-745
Near-infrared 1	770-895
Near-infrared 2	860-1040

The WorldView-2 imagery was atmospherically corrected to top-of-atmosphere reflectance using the ENVI software (ENVI, 2006). The GPS points of the individual trees were used to extract the reflectance values from the WorldView-2 multispectral imagery. The individual trees were easily identified on the pan sharpened imagery which fuses a panchromatic and multispectral imagery to create a multispectral image with a spatial resolution of 0.5 m. The reflectance values from the imagery were then put into a PLS regression model.

Seventeen existing vegetation indices (Table 5.2) were also calculated from the reflectance data. These vegetation indices are used for forest health assessments and include pigment specific indices, moisture indices and red edge indices. If the required wavebands were not available to compute the indices, the bands closest to that waveband were selected. The calculated indices were also put into a PLS regression model to assess its capability of predicting *T. peregrinus* damage.

Table 5.2 Vegetation indices used in this study.

Number	Index Name	Abbreviation	Formula	Bands used in this study	Reference
1	Water Band Index	*WBI*	*R900/R970*	*Band 7/Band 8*	(Penuelas et al., 1993)
2	Carter Stress Index	*CSI*	*R695/R760*	*Band 5/Band 7*	(Carter, 1994)
3	Carotenoid Reflectance Index	*CRI*	*(1/R510)-(1/R700)*	(1/*Band3*)-(1/*Band6*)	(Gitelson et al., 2002)
4	Anthocyanin Reflectance Index	*ARI*	*(1/R550)-(1/R700)*	(1/*Band3*)-(1/*Band6*)	(Gitelson et al., 2001)
5	Plant Senescence Reflectance Index	*PSRI*	*(R680-R500)/R750*	(*Band 5-Band 2)/Band 6*	(Merzlyak et al., 1999)
6	Structure Insensitive Pigment Index	*SIPI*	*(R800-R445) /(R800-R680)*	(*Band7-Band1*) /(*Band7-Band5*)	(Penuelas et al., 1995)
7	Photochemical reflectance index	*PRI*	*(R531-R570)/ (R531+R570)*	(*Band2-Band3*)/ (*Band2+Band3*)	(Penuelas et al., 1995)
8	Simple Ratio	*SR*	*Near-infrared/Red*	*Band 8/Band5*	(Rouse et al., 1973)
9	Normalized Difference Vegetation Index	*NDVI*	*(Near-infrared-Red)/(Near-infrared+red)*	*(Band8-Band5)/(Band8+Band5)*	(Rouse et al., 1973)
10	Enhanced Vegetation Index	*EVI*	*2.5(Near-infrared-Red)/(Near-infrared+6Red-7.5Blue+1)*	2.5(*Band8-Band5)/(Band8+6Band5-7.5Band2+1)*	(Huete et al., 1997)
11	Atmospherically Resistance Vegetation Index	*ARVI*	*Near-infrared-(2Red-Blue)/Near-infrared+(2Red-Blue)*	*Band8-(2Band5-Band2)/Band8+(2Band5-Band2)*	(Kaufman and Tanre, 1996)

12	Datt/Maccioni index	*DMI*	*(R780-R710)/ (R780-R680)*	(*Band7-Band6*) /(*Band7-Band5*)	(Barry et al., 2008)
13	Far Red to Red Index	*FFRI*	*R750/R700*	*Band 6/Band5*	(Barry et al., 2008)
14	Lower Red Edge Slope	*LRES*	*(R710-R690)/ (710-690)*	*(Band6-Band5)/(710 -690)*	(Barry et al., 2008)
15	Total Red Edge Slope	*TRES*	*(R740-R690)/ (740-690)*	*(Band6-Band5)/(740 -690)*	(Barry et al., 2008)
16	Red Green Ratio Index	*RGI*	*(R600:700)/(R500:600)*	(*Band5*)/(*Band3*)	(Gamon and Surfus, 1999)
17	Vogelmann Red Edge 1	*VOGRE*	*R740/R720*	*Band 6/Band5*	(Vogelmann et al., 1993)

5.3 Data analysis

5.3.1 Relationship between T. peregrinus damage and WorldView-2 data

The Shapiro-Wilk test was run to test the normality of the data. Pearson correlation coefficient *r* was then calculated for all the WorldView-2 bands and indices. The wavebands and indices of statistically significant correlation ($p < 0.05$) were then evaluated.

5.3.2 Predicting T. peregrinus damage using WorldView-2 bands and indices with PLS regression

PLS regression is a bilinear calibration method which reduces a large number of measured collinear variables to a few non correlated latent variables or factors (Cho et al., 2007; Geladi and Kowlski, 1986). The PLS model finds a few PLS factors that explain a large amount of variation in both the response and predictor variables (Tobias, 1995). The PLS model is formulated as:

$$Y=XB^{'}+E \quad (5.1)$$

Where Y = the matrix containing the response variable (*T. peregrinus* infestations), X = the matrix containing the predictor variables (WorldView-2 bands and indices), B = the matrix containing the regression coefficients and E = the matrix of the residuals (Cho et al., 2007).

The PLS algorithm combines the features of principal components and multiple regression to find a few factors that maximize the covariance between the predictor and the response variables yielding scores that contain most of the information in the observed variables (Cho et al., 2007; Tobias, 1995; Ye et al., 2008). The first few factors normally explain most of the variation in the dataset. However, cross validation is required in order to determine the number of significant components (Oumar et al., 2013). Cross validation is carried out by subsetting a portion of the data to create a prediction model and tests this model against the deleted data (Luedeling et al., 2009). The cross validation estimates the *PRESS* statistic for each factor and selects the models with least error. The cross validation method is performed in a sequential manner, on one component after the other and a component is judged significant if the *PRESS* ratio is smaller than 0.9 for at least one of the Y-variables (Wold et al., 2001). The *PRESS* is calculated for the final model with the estimated number of significant components and is often re-expressed as Q^2 (the cross validated R^2) (Wold et al., 2001). Q^2 is defined as:

$$Q^2 = 1 - P / S \tag{5.2}$$

where P is the predicted residual sum of squares and S is the sum of squares of Y corrected

for the mean.

The Q^2 parameter is used as a measure to identify significant components (Hoskuldsson, 2003; Hoskuldsson, 2008; Wold et al., 2001).

PLS regression was performed on the 8 WorldView-2 sensor bands and the 17 existing vegetation indices. To validate the performance of the PLS models, the dataset was randomly divided into two parts. 70% (n=56) was used for training and the remaining 30% (n=24) was used to test the models. PLS regression was performed on the training dataset and cross validation was used to select the optimal number of components (Q^2) and was carried out ten times (Hoskuldsson, 2003). PLS regression was performed on the WorldView-2 sensor bands, the vegetation indices and the combined dataset. This was done in order to assess the importance of the variables separately and their combined strength in predicting *T. peregrinus* damage.

To evaluate whether the WorldView-2 bands and indices were significant in the model prediction, the recommendation by Wold (1995) was followed whereby an absolute threshold value of 0.8 was recommended for VIP. The variables selected by VIP were then put into a

PLS regression model to assess if it further improves the prediction performance. The PLS regression models were then extrapolated to create prediction maps of *T. peregrinus* infestations. The accuracy of the prediction maps were evaluated using the coefficient of determination (R^2) and the *RMSE* calculated according to Siska and Hung (2001) (equation 5.3) using the independent 30% test dataset.

$$RMSE = \sqrt{\frac{SSE^2}{n}} \tag{5.3}$$

Where *SSE* is the standard sum of errors (observed – predicted) and *n* is the number of samples.

5.4 Results

5.4.1 Visual damage and reflectance

The visual damage assessments ranged from no damage (0%) to 80 %. Table 5.3 shows the descriptive statistics for the *T. peregrinus* visual damage assessments. Figure 5.2 shows the mean reflectance of the WorldView-2 sensor.

Table 5.3 Descriptive statistics for visual damage assessments.

Samples	Unit	Mean	Minimum	Maximum	Range	Standard deviation
80	%	36.13	0	80	0-80	29.51

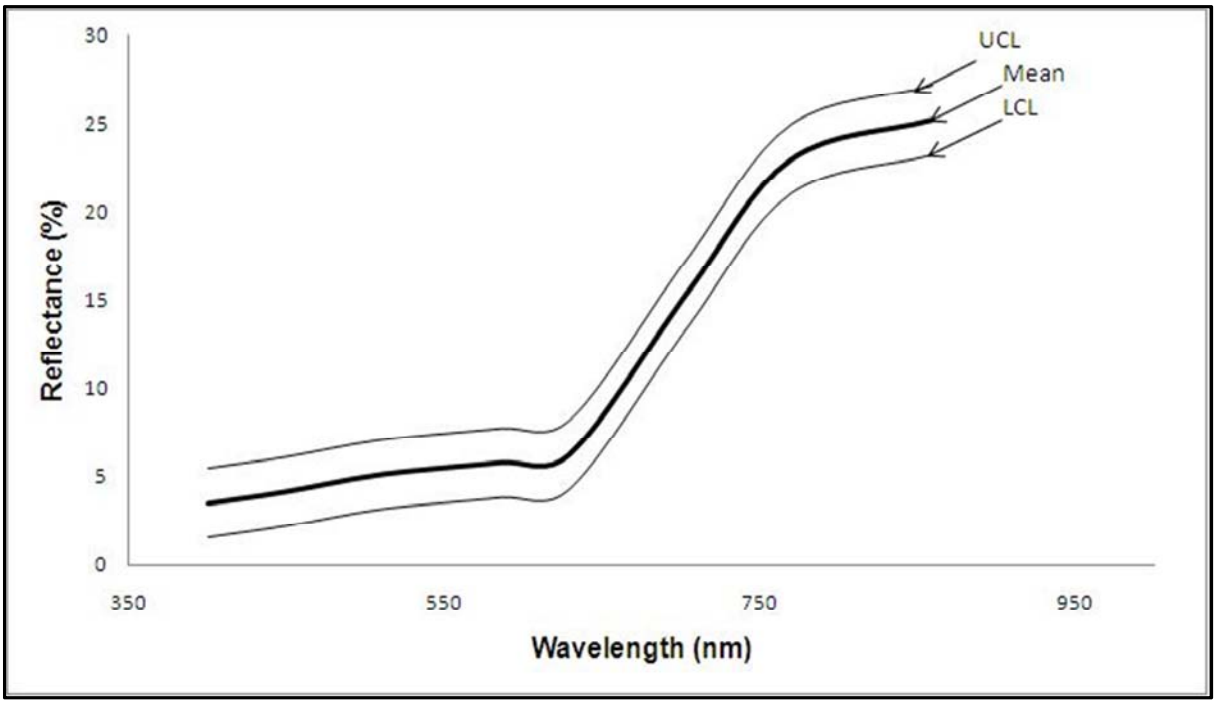

Figure 5.2 Mean reflectance of the WorldView-2 sensor. The mean, upper 95% confidence limit (UCL) and lower 95% confidence limit (LCL) of the reflectance are shown.

5.4.2 Relationship between WorldView-2 bands and indices with visual damage

Pearson correlation coefficient (*r*) was calculated for all bands and indices. Table 5.4 shows the correlation coefficient for the significant ($p < 0.05$) bands and indices. All the WorldView-2 sensor bands were found to be significantly correlated with *T. peregrinus* damage with the red edge and near-infrared wavebands yielding high correlations ranging from 0.60 to 0.74. Seven vegetation indices relating to pigment concentration (chlorophyll, anthocyanin and carotenoid) were significantly correlated with *T. peregrinus* damage, however they yielded poor correlations ranging from -0.22 to 0.35 respectively.

Table 5.4 Statistically significant correlations ($p<0.05$) between WorldView-2 data and *T. peregrinus* damage.

Variable	Correlation Coefficient
Near-infrared 2	-0.74
Near-infrared 1	-0.67
Red Edge	-0.60
Green	-0.40
Coastal Blue	-0.38
Blue	-0.37
CRI	0.35
ARI	0.35
RGI	0.33
Yellow	-0.30
EVI	-0.29
LRES	-0.28
TRES	-0.28
Red	-0.26
DMI	-0.22

5.4.3 Predicting T. peregrinus damage using WorldView-2 bands and indices with PLS regression

Table 5.5 shows the performance of the PLS regression models in predicting *T. peregrinus* damage on the training dataset. The PLS algorithm extracted 3 factors from the WorldView-2 sensor bands and predicted *T. peregrinus* damage with an R^2 value of 0.57. The vegetation indices extracted 2 factors with an R^2 value of 0.42 and the combined dataset extracted 2 factors with an R^2 value of 0.50. Significant variables were identified by VIP scores and were then put into a PLS regression model to establish if it further strengthened the prediction performance. Table 5.6 shows the VIP score of each WorldView-2 sensor band and index selected in the model. The variables selected by VIP scores yielded the best correlation with an R^2 value of 0.58 on the training dataset. The regression models were then extrapolated to map the distribution of *T. peregrinus* damage (Figure 5.3). The performance of the models in the prediction of *T. peregrinus* damage was evaluated using the coefficient of determination (R^2) and the *RMSE* on an independent test dataset (Figure 5.4).

Table 5.5 Performance of PLS regression models in predicting *T. peregrinus* damage on the training dataset.

PLS Models	**Number of PLS factors**	**Training R^2**	**Q^2 (*PRESS*)**
WorldView-2 sensor bands	3	0.57	0.06
Vegetation indices	2	0.42	0.02
Combined dataset	2	0.50	0.08
VIP bands and indices	3	0.58	0.03

Table 5.6 VIP importance of selected WorldView-2 sensor bands and indices.

WorldView-2 Sensor	**VIP Scores**
CRI	1.902
ARI	1.8916
RGI	1.5760
Near-infrared 2	1.3804
Red Edge	1.2213
Near-infrared 1	1.2107
EVI	1.1794
LRES	1.1129
TRES	1.1129
DMI	1.1007
Coastal Blue	0.8383
Blue	0.8167
Green	0.8164

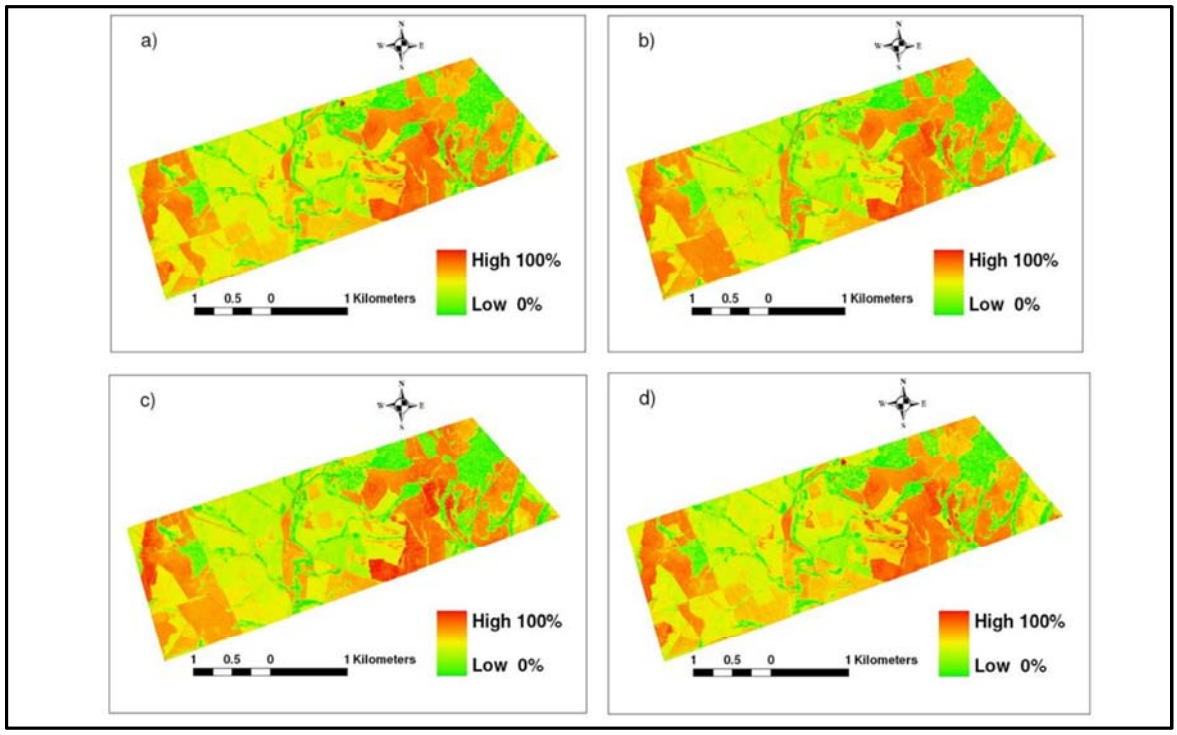

Figure 5.3 Prediction maps created from the PLS regression models. (a) WorldView-2 sensor bands, (b) Vegetation indices, (c) Combined dataset, (d) VIP bands and indices.

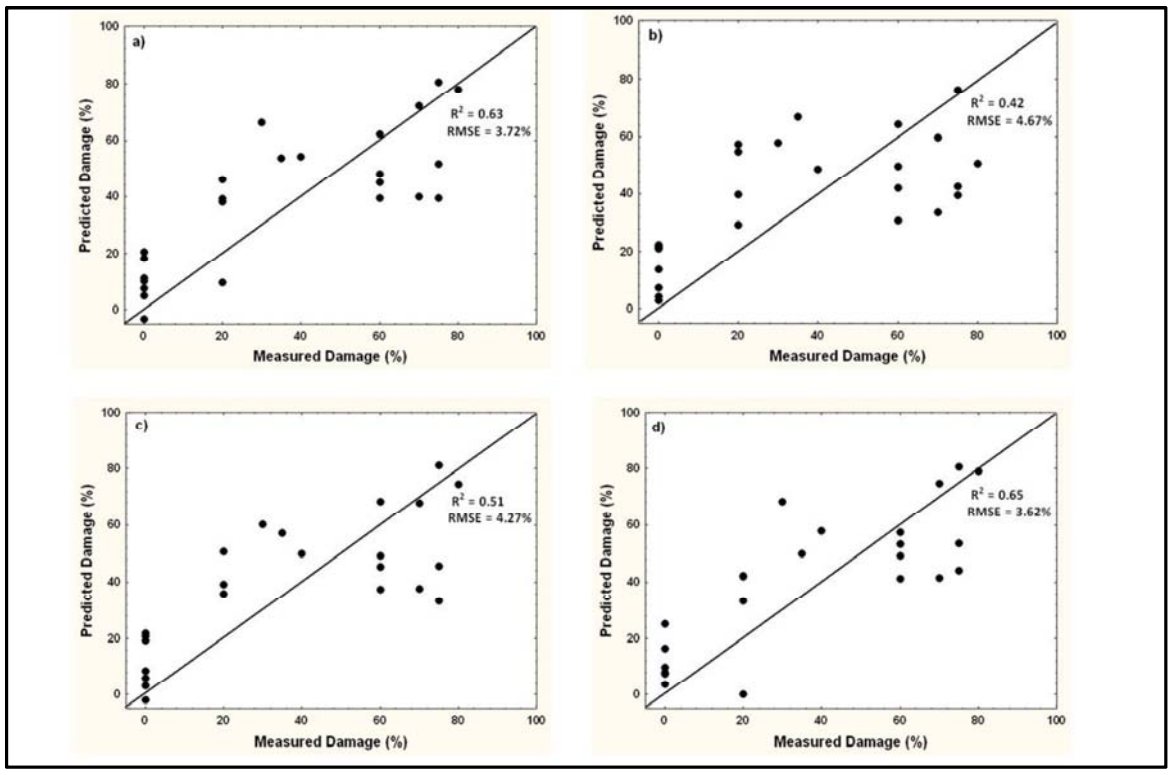

Figure 5.4 Scatterplot showing predicted versus measured *T. peregrinus* damage on an independent test dataset (n=24) using the prediction maps. (a) WorldView-2 sensor bands, (b) Vegetation indices, (c) Combined dataset, (d) VIP bands and indices.

5.5 Discussion

5.5.1 Relationship between WorldView-2 bands and indices with T. peregrinus damage

The relationship between the WorldView-2 sensor bands and indices with *T. peregrinus* damage was evaluated using the Pearson correlation coefficient. From the bands assessed, the red edge and near-infrared bands were highly correlated with *T. peregrinus* damage yielding correlations ranging from 0.60 to 0.74. These wavebands have been recommended in literature for the detection of forest damage as trees that undergo stress result in a reduction in chlorophyll content and thereby change reflectance in these regions (Hoque et al., 1992; Zarco-Tejada et al., 2002). Previous studies have also found the red edge band to be an important band for monitoring trees under stress (Barry et al., 2008; Coops et al., 2004) and damage caused by forest pests in pine plantations (Ismail et al., 2008). Individual indices however, yielded relatively weak correlations with forest damage. The results show that the near- infrared bands of the WorldView-2 sensor which are narrower than other commercially available sensors such as QuickBird and the red edge band are effective in assessing damage caused by *T. peregrinus* infestations in plantation forests.

5.5.2 Predicting T. peregrinus damage using WorldView-2 data

The WorldView-2 sensor bands predicted *T. peregrinus* damage on an independent test dataset with an R^2 value of 0.63 and a *RMSE* of 3.72% performing better than the vegetation indices (R^2 = 0.42, *RMSE* = 4.67%). The combined dataset using both the WorldView-2 sensor bands and indices yielded an R^2 value of 0.51 with a *RMSE* of 4.27%. The bands and indices identified by VIP scores performed the best from all the PLS models yielding the highest R^2 value of 0.65 with the lowest *RMSE* of 3.62% on an independent test dataset. The WorldView-2 bands chosen by VIP scores indicated that 6 bands are important contributors in the model with the near infrared and the red edge bands having high weightings. Seven vegetation indices (*CRI*, *ARI*, *RGI*, *EVI*, *LRES*, *TRES*, *DMI*) were chosen by VIP as important variables for the prediction of *T. peregrinus* damage. Previous studies have shown that these indices are strongly correlated with stressed and damaged leaves (Barry et al., 2008; Coops et al., 2004). The *CRI* was ranked the most important index for the prediction of *T. peregrinus* damage followed by the *ARI* and *RGI*. Barry et al. (2008) also found the *RGI* and *ARI* to be significantly correlated with stressed and damaged eucalypt leaves. The *ARI* is used as a

measure to assess changes to plant foliage. Any increase in anthocyanins indicates changes in foliage due to plant death or growth (Gitelson et al., 2001). The *RGI* index which is used as an indicator for plant stress and to assess redness in plants was also found to be an important variable for the prediction of *T. peregrinus* damage. The red edge, which is the point of maximum slope in vegetation reflectance that occurs between 690-720 nm (Filella and Penuelas, 1994; Horler et al., 1983) is used as an indicator for plant stress and senescence (Dawson and Curran, 1998). The lower red edge slope and total red edge slope were chosen by VIP as key variables for the prediction of *T. peregrinus* damage. Previous studies have found the above spectral indices to be important measures in assessing vegetation health as they have been shown to be strongly correlated with plant physiological properties using hyperspectral data (Barry et al., 2008; Gitelson et al., 2001; Gitelson et al., 2002). However, this research confirms previous efforts, but uses high resolution multispectral data with valuable band settings that are sensitive to vegetation health.

The distribution maps created by the PLS models show the spread of *T. peregrinus* damage across the study area. The map with the highest accuracy (R^2 = 0.65, Figure 3d) shows that high infestation rates are spread across the upper and lower portions of the study area while medium infestation rates are along the centre of the study area. The upper and lower portion of the study area are characterized by steeper slopes and receives lower rainfall than that of the centre of the study area, and hence could be a factor in explaining the higher severity of infestations in these areas due to water stress. Further research is required in order to establish the relationship between environmental factors and climatic data with *T. peregrinus* infestation. Nevertheless, this study has indicated the potential of WorldView-2 imagery in successfully predicting *T. peregrinus* infestations. The ability to create prediction maps with 65% accuracy indicates the potential of WorldView-2 data in mapping damage in forest plantations. The prediction maps can serve as spatial guides for forest managers to improve their detection methods and make cost effective decisions related to forest plantations.

5.6 Conclusion

The aim of this study was to assess the potential of WorldView-2 data in predicting *T. peregrinus* damage. The second objective was to map the severity of infestation and identify significant variables for the prediction of *T. peregrinus* damage. The following conclusions can be drawn:

1) WorldView-2 sensor bands successfully predicted *T. peregrinus* damage with an R^2 value of 0.63 and a *RMSE* value of 3.72% on an independent test dataset.

2) WorldView-2 sensor bands and indices identified by VIP scores yielded the highest R^2 value of 0.65 and the lowest *RMSE* of 3.62%.

3) The red edge and near-infrared bands of the WorldView-2 sensor and pigment specific indices as well as red edge indices were identified as important variables for the prediction of *T. peregrinus* damage.

4) Prediction maps created from WorldView-2 sensor data can serve as spatial guides for forest managers to focus their remediation measures before damage to the trees reaches a point of no recovery.

Although the results are lower in accurate predictions as compared to hyperspectral remote sensing, this study has shown the potential of WorldView-2 sensor data, a relatively cheap satellite with a huge areal coverage, in effectively mapping *T. peregrinus* damage in plantation forests. This effectively shows the applicability of high resolution satellite imagery in plantation forest monitoring.

5.7 Acknowledgements

We thank Muhammad Sheik Oumar and Thato for helping with the field data collection. We are grateful to DigitalGlobe for providing us with the WorldView-2 imagery. Funding for this research was provided by the National Research Foundation and the University of KwaZulu-Natal.

5.8 Link to next chapter

The above chapter showed the potential of the WorldView-2 sensor in predicting and mapping *T. peregrinus* damage using the sensor bands and vegetation indices through regression models. However, some studies have shown migration patterns of the pest following environmental gradients. It is hypothesised that an incorporation of the environmental variables in the prediction model could improve the mapping accuracy of *T. peregrinus* damage in plantation forests. The next chapter therefore attempts to improve the prediction and mapping of *T. peregrinus* damage by incorporating environmental variables in a multiple stepwise regression model.

CHAPTER SIX

6. Improving the prediction of *T. peregrinus* damage using environmental variables and WorldView-2 imagery

This chapter is based on: Oumar, Z. and Mutanga, O., (In review). Integrating environmental variables and WorldView-2 image data to improve the prediction of *Thaumastocoris peregrinus* damage in plantation forests. *ISPRS Journal of Photogrammetry and Remote Sensing*.

Abstract

This study integrated environmental variables together with high spectral resolution WorldView-2 imagery to detect and map *T. peregrinus* damage in plantation forests. The red edge and near-infrared bands of the WorldView-2 sensor were significantly correlated with *T. peregrinus* damage, yielding correlations ranging from -0.60 to -0.74. Temperature and precipitation yielded significant correlations with *T. peregrinus* damage ranging from 0.62 to 0.76. The WorldView-2 bands, 17 spectral vegetation indices and environmental factors were entered into a forward stepwise regression model to predict *T. peregrinus* damage. The regression model was then extrapolated to map the severity of damage and predicted *T. peregrinus* damage with a mean bootstrapped R^2 value of 0.72 and a *RMSE* of 3.21% on an independent test dataset. The results from this study indicate the potential of the new generation WorldView-2 sensor and environmental datasets in improving the mapping and monitoring of insect outbreaks in plantation forests.

Keywords: *T. peregrinus*, environmental variables, vegetation indices, WorldView-2 imagery, pest monitoring.

6.1 Introduction

The ability to detect various stages of *T. peregrinus* infestations in plantation forests is essential for forest management so that stands that are in the early to medium stages of infestation can be felled before they reach a point of no recovery. *T. peregrinus* is a sap sucking insect that has caused significant damage to commercial eucalypt forest plantations internationally as it reduces the photosynthetic ability of the tree resulting in stunted growth and even death of severely infested trees (FAO, 2007; Jacobs and Neser, 2005). Trees that are lightly infested may show little or no sign of damage, trees and leaves that are moderate to heavily infested display a reddening of the leaves and have a 'washed out' appearance while trees that are severely infested result in defoliation and branch die back (Jacobs and Neser, 2005). Table 6.1 depicts the symptoms of *T. peregrinus* infestations. Reducing the impact of *T. peregrinus* infestation is crucial for the future sustainability and productivity of eucalypt plantations internationally.

Table 6.1 Symptoms of *T. peregrinus* infestation.

Stages of infestation	Symptoms
Light Infestation 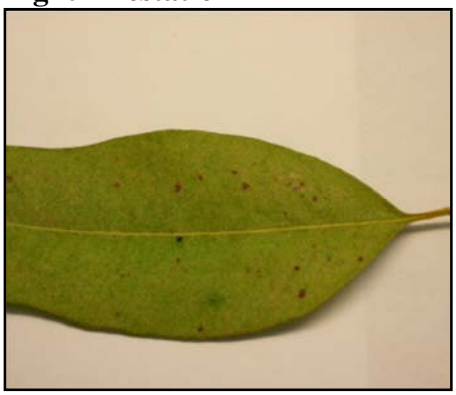 Source: FABI, (2010)	Trees and leaves that are lightly infested may show little or no sign of damage.
Heavy Infestation  Source: (Jacobs and Neser, 2005)	Trees that are heavily infested turn a deep red-brown colour starting at the northern side of the canopy sometimes referred to as 'winter bronzing'. The canopy has a 'washed out' pale appearance when heavily infested (Jacobs and Neser, 2005).
Very Severe Infestation  Source: FABI, (2010)	Trees that are severely infested result in defoliation and die back of branches and in some cases the trees die (Jacobs and Neser, 2005).

The timely collection of information related to the spread and stage of *T. peregrinus* infestation is essential for effective management of forest plantations. *Cleurchoides noackae* has been identified as a biological control agent for *T. peregrinus* (TPCP, 2008b), however the ability to accurately detect *T. peregrinus* infestation is a crucial factor for the deployment of this agent. Research has shown that a combination of high spatial and spectral data can

successfully detect and map multiple stages of tree mortality with relatively high accuracies (Bentz and Endreson, 2003; Coops et al., 2006; Meddens et al., 2011; White et al., 2005; Wulder et al., 2006a). New enhancements in multispectral technology such as that offered by the WorldView-2 sensor may provide an improved opportunity for the detection and mapping of *T. peregrinus* infestation. The WorldView-2 sensor has 8 strategically placed spectral bands with a high spatial resolution of 2 meters which surpasses that of traditional multispectral scanners such as IKONOS, QuickBird and GeoEye. More specifically, the WorldView-2 sensor incorporates four new spectral bands with high spectral dependency that include the red edge (705-745 nm), coastal (400-450 nm), yellow (585-625 nm) and near-infrared 2 (860-1040 nm) which are sensitive to changes in plant health and could enhance the prediction of *T. peregrinus* damage. Vegetation indices calculated from these fewer but well positioned bands which contain high spectral fidelity and are used for forest health monitoring (red edge, green, yellow), moisture stress assessments (near-infrared 1) and pigment stress concentration (red edge, yellow) could result in an improved prediction of *T. peregrinus* damage in forest plantations.

Apart from high spatial and spectral resolution imagery, multisource information containing environmental datasets which include climate and topography are imperative for the monitoring of forest damage (Li et al., 2010; Olthof et al., 2004; Wang et al., 2010). Topographic features such as slope and elevation play a considerable role in the ignition of pest outbreaks because local climate variables such as air temperature, solar radiation, humidity and host species distribution are based on topography, resulting in spatial patterns of insect induced tree mortality (Kharuk et al., 2007). Furthermore climatic factors which include temperature and precipitation have a strong influence on the survival, development, reproduction and distribution of forest pests and the damage they cause by altering tree physiology and tree defence mechanisms (FAO, 2007; Menéndez, 2007). *T. peregrinus* which is characterized by shorter generation times, high mobility and high reproductive rates are likely to respond to climatic and topographic changes. Accordingly, the ability to predict *T. peregrinus* infestations in plantation forests using climatic and topographic datasets together with multispectral data containing unique band settings might be further augmented. It is against this background that this study aims to assess the potential of the new generation WorldView-2 sensor in conjunction with climatic and topographic datasets for predicting and mapping the severity of *T. peregrinus* damage in plantation forests. This will help facilitate a

better understanding of whether environmental factors explain variation in infestation at different locations.

6.2 Methods

6.2.1 The study area

The study area (29°48'S 30°13'E) is situated in Richmond, KwaZulu-Natal South Africa and covers an area of 875 hectares. Richmond has large areas of arable land with timber and sugar cane been the main resource planted on deep well drained soils. Richmond receives an annual rainfall ranging from 800-1280 mm with a mean annual temperature of 17°C. Richmond is situated at an altitude of about 900-1400 m above mean sea level with *Eucalyptus, Pinus* and *Acacia* planted across the study area. Figure 6.1 shows a map of the study area.

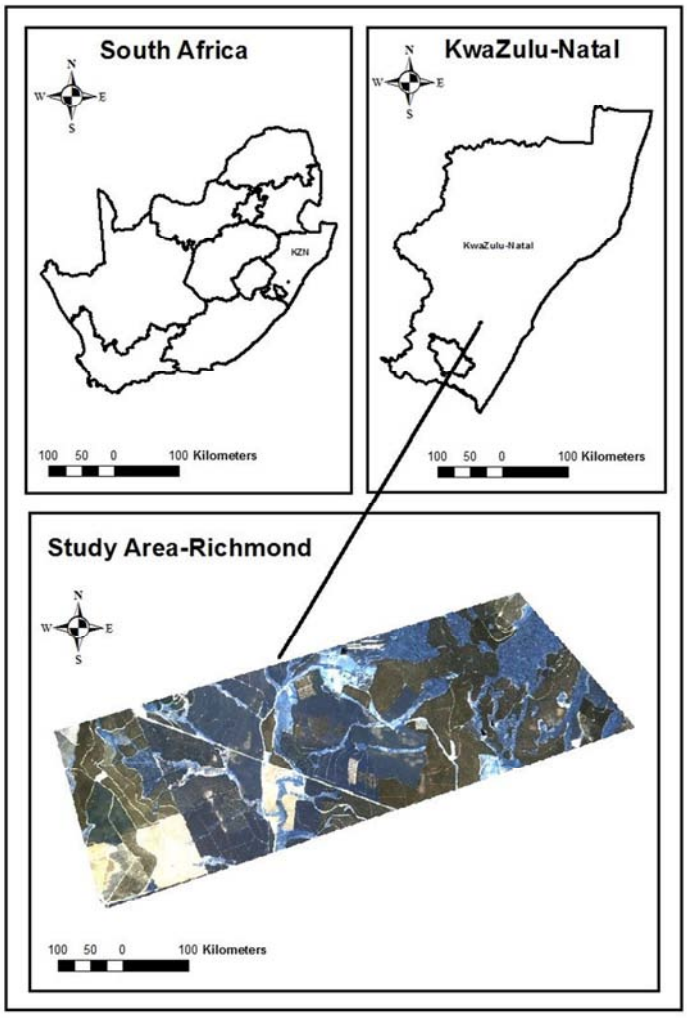

Figure 6.1 Map of the Study area

6.2.2 Leaf sampling and T. peregrinus damage

Three *Eucalyptus smithii* compartments (4-5 years old) that showed different rates of infestation across the study area were sampled. The compartments were 3 km apart and showed variability in damage levels. Systematic sampling was done on the 24th and 25th of November 2010, in which 15 transects were arranged across the compartments. The distance between transects was 5 planted rows of trees (15 meters apart) and every tenth tree in each transect was sampled. This was done so a wide variation of *T. peregrinus* infestation rates across the compartments could be captured. Eighty trees were sampled and Global Positioning Systems (GPS) points were recorded for each tree using a handheld Trimble, Geo-Explorer unit with submeter accuracy. Branches were cut down using a pruning saw and fifty leaves were picked from each tree for visual damage assessments. Each leaf was divided into quadrants and the percentage of necrotic tissue was visually estimated on the fifty mature leaves and then averaged for each sample by a plant pathologist. A visual assessment was preferred over a computer based approach as it allowed for a larger number of samples to be analysed (Luedeling et al., 2009; Skaloudova et al., 2006).

6.2.3 WorldView-2 Image data

WorldView-2 imagery was acquired on the 1st of December 2010. The WorldView-2 sensor captures 0.5 m resolution panchromatic and 2 m resolution multispectral imagery. The multispectral imagery comprises of eight spectral bands in the spectral range of 400-450nm (coastal blue), 450-510nm (blue), 510-580nm (green), 585-625nm (yellow), 630-690nm (red), 705-745nm (red edge), 770-895nm (near infrared 1) and 860-1040nm (near infrared 2). The WorldView-2 images were orthorectified and georeferenced by the data providers and projected to the UTM Zone 36 S (WGS84) coordinate system. The images were atmospherically corrected to top of atmosphere reflectance using the quick atmospheric correction model (QUAC). QUAC determines atmospheric compensation parameters directly from the information contained within the scene and thus allows for the retrieval of reasonably accurate reflectance spectra (ENVI, 2006). GPS points of individual trees were used to extract the reflectance values from the WorldView-2 multispectral imagery. Additionally seventeen existing vegetation indices (Table 6.2) that are used for forest health assessments were calculated from the WorldView-2 imagery to evaluate its potential in predicting and mapping *T. peregrinus* infestations.

Table 6.2 Vegetation indices used in this study.

Number	Index Name	Abbreviation	Formula	Bands used in this study	Reference
1	Water Band Index	*WBI*	*R900/R970*	*Band 7/Band 8*	(Penuelas et al., 1993)
2	Carter Stress Index	*CSI*	*R695/R760*	*Band 5/Band 7*	(Carter, 1994)
3	Carotenoid Reflectance Index	*CRI*	*(1/R510)-(1/R700)*	(1/*Band3*)-(1/*Band6*)	(Gitelson et al., 2002)
4	Anthocyanin Reflectance Index	*ARI*	*(1/R550)-(1/R700)*	(1/*Band3*)-(1/*Band6*)	(Gitelson et al., 2001)
5	Plant Senescence Reflectance Index	*PSRI*	*(R680-R500)/R750*	(*Band 5-Band 2)/ Band 6*	(Merzlyak et al., 1999)
6	Structure Insensitive Pigment Index	*SIPI*	*(R800-R445) /(R800-R680)*	(*Band7-Band1*) /(*Band7-Band5*)	(Penuelas et al., 1995)
7	Photochemical reflectance index	*PRI*	*(R531-R570)/ (R531+R570)*	(*Band2-Band3*)/ (*Band2+Band3*)	(Penuelas et al., 1995)
8	Simple Ratio	*SR*	*Near-infrared/Red*	*Band 8/Band5*	(Rouse et al., 1973)
9	Normalized Difference Vegetation Index	*NDVI*	*(Near-infrared-Red)/(Near-infrared+red)*	*(Band8-Band5)/(Band8+Band5)*	(Rouse et al., 1973)
10	Enhanced Vegetation Index	*EVI*	*2.5(Near-infrared-Red)/(Near-infrared+6Red-7.5Blue+1)*	2.5(*Band8-Band5)/(Band8+6Band5-7.5Band2+1)*	(Huete et al., 1997)
11	Atmospherically Resistance Vegetation Index	*ARVI*	*Near-infrared-(2Red-Blue)/Near-infrared+(2Red-Blue)*	*Band8-(2Band5-Band2)/Band8+(2Band5-Band2)*	(Kaufman and Tanre, 1996)

12	Datt/Maccioni index	*DMI*	*(R780-R710)/ (R780-R680)*	(*Band7-Band6*) /(*Band7-Band5*)	(Barry et al., 2008)
13	Far Red to Red Index	*FFRI*	*R750/R700*	*Band 6/Band5*	(Barry et al., 2008)
14	Lower Red Edge Slope	*LRES*	*(R710-R690)/ (710-690)*	*(Band6-Band5)/(710-690)*	(Barry et al., 2008)
15	Total Red Edge Slope	*TRES*	*(R740-R690)/ (740-690)*	*(Band6-Band5)/(740-690)*	(Barry et al., 2008)
16	Red Green Ratio Index	*RGI*	*(R600:700)/(R500:600)*	(*Band5*)/(*Band3*)	(Gamon and Surfus, 1999)
17	Vogelmann Red Edge 1	*VOGRE*	*R740/R720*	*Band 6/Band5*	(Vogelmann et al., 1993)

6.2.4 Environmental datasets

The environmental datasets consisted of climate and topographic data that showed variation across the three sampled compartments. The climate dataset was obtained from the South African atlas of climatology and agrohydrology (Schulze et al., 1997). These datasets were derived from 1000 meteorological stations across South Africa from 1990 to 1997 and a description of the methodology is provided by Schulze et al. (1997). The climatic variables include mean annual precipitation and mean annual temperature. The precipitation dataset is made up of 1.7 km grids that cover the whole of South Africa. Rainfall coverage for the three sampled compartments was extracted from the precipitation dataset. The temperature dataset is a map of South Africa which integrates monthly and seasonal patterns of maximum and minimum temperatures (Schulze et al., 1997). Temperature readings were extracted for the three sampled compartments from the temperature dataset. The topographic variables include slope and aspect which was derived from a 20 m digital elevation model (DEM) obtained from the KwaZulu-Natal Department of Agriculture dataset. Data from the topographic datasets were extracted for the three compartments.

6.3 Data Analysis

6.3.1 Relationship between visual damage with WorldView-2 bands, vegetation indices and environmental factors

The data was tested for normality using the Shapiro-Wilk test. The relationship between *T. peregrinus* damage and the WorldView-2 bands, vegetation indices and environmental factors was assessed using the Pearson correlation coefficient (r). The statistically significant correlations at the 95% confidence interval were then assessed.

6.3.2 Predicting and mapping T. peregrinus damage using WorldView-2 bands, vegetation indices and environmental factors

The WorldView-2 bands, vegetation indices and environmental factors were entered into a forward stepwise regression model for the prediction of *T. peregrinus* damage. The dataset was randomly divided into 70% training data (n=56) and 30% test data (n=24), which was used for validating the performance of the model. This proportion of 70/30 training and test datasets is recommended in literature as it gives more weight to model building (Mutanga and Rugege, 2006). The regression model from the training dataset was then inverted to map the distribution of *T. peregrinus* damage. The predictive accuracy of the modeled map was assessed using the correlation coefficient (R^2) and the *RMSE* on the independent 30% test dataset.

Additionally, bootstrapping correlations was performed on the predicted versus measured test dataset in order to increase the statistical confidence of the results (Efron, 1982). A total of 200 iterations were executed for each pair.

6.4 Results

6.4.1 Relationship between visual damage with WorldView-2 imagery, vegetation indices and environmental factors

The visual damage measurements ranged from 0% to 80% across the study area with a mean value of 36%. The bar graph in Figure 6.2 shows the relationship between *T. peregrinus* damage with the WorldView-2 bands, vegetation indices and the environmental factors. The red edge, near infrared 1 and near-infrared 2 of the WorldView-2 sensor yielded high and significant correlations with *T. peregrinus* damage ranging from -0.60 to -0.74. From the vegetation indices computed, the anthocyanin, carotenoid and red green index yielded low

but significant correlations with *T. peregrinus* damage ranging from 0.33 to 0.35. Environmental factors such as rainfall and temperature yielded high and significant correlations with *T. peregrinus* damage ranging from 0.62 (rainfall) to 0.76 (temperature).

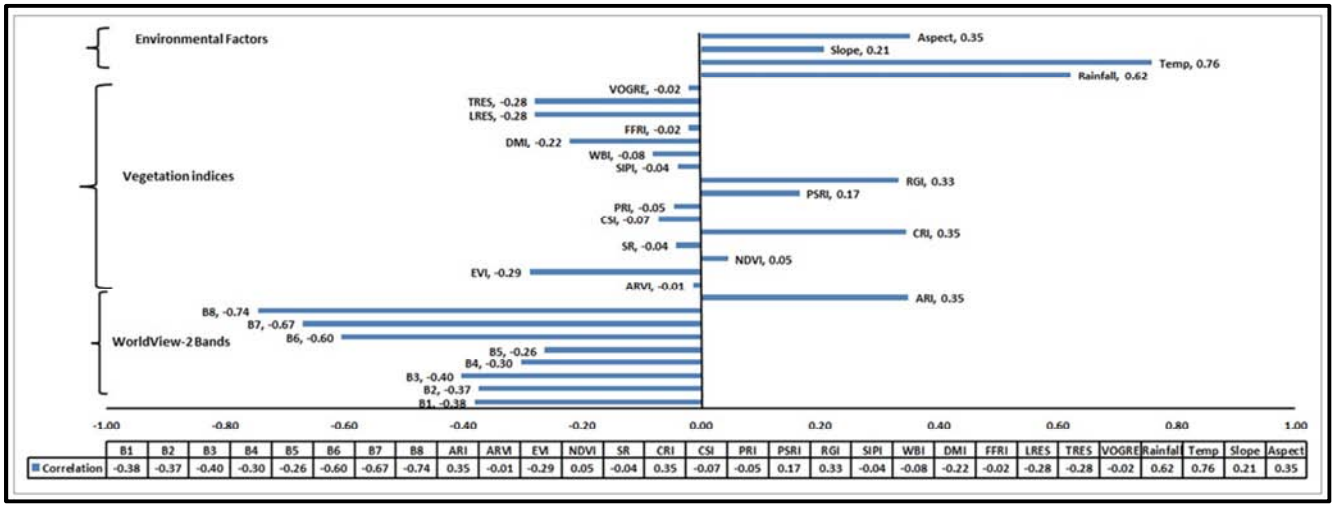

Figure 6.2 Bar graph showing the relationship between *T. peregrinus* damage with WorldView-2 bands, vegetation indices and environmental datasets.

6.4.2 Predicting and mapping T. peregrinus damage using WorldView-2 imagery, vegetation indices and environmental factors

The forward stepwise regression model selected two variables from the 29 predictors for the prediction of *T. peregrinus* damage. Temperature and the near-infrared band 8 of the WorldView-2 sensor predicted *T. peregrinus* damage with an R^2 value of 0.65 and a *RMSE* of 2.29% on the training dataset (Figure 6.3). The strong correlation between the predicted and observed damage can be attributed to the model predicting several trees with 0 % damage. This is due to the fact that we sampled trees with various levels of damage and some trees had no damage. By including these trees in the model, there is increased variability in the dataset thereby strengthening the relationship with the vegeation indices and environmnetal factors. The regression model was then inverted to map the distribution of *T. peregrinus* damage as illustrated in Figure 6.4. The accuracy of the prediction model was assessd using the 30% independent test dataset. The regression model predicted *T. peregrinus* damage with a mean bootstrapped R^2 value of 0.72 and a *RMSE* of 3.21 % on the independent test dataset. Figure 6.5 shows the correlation between the predicted verses measured damage on the independent test dataset.

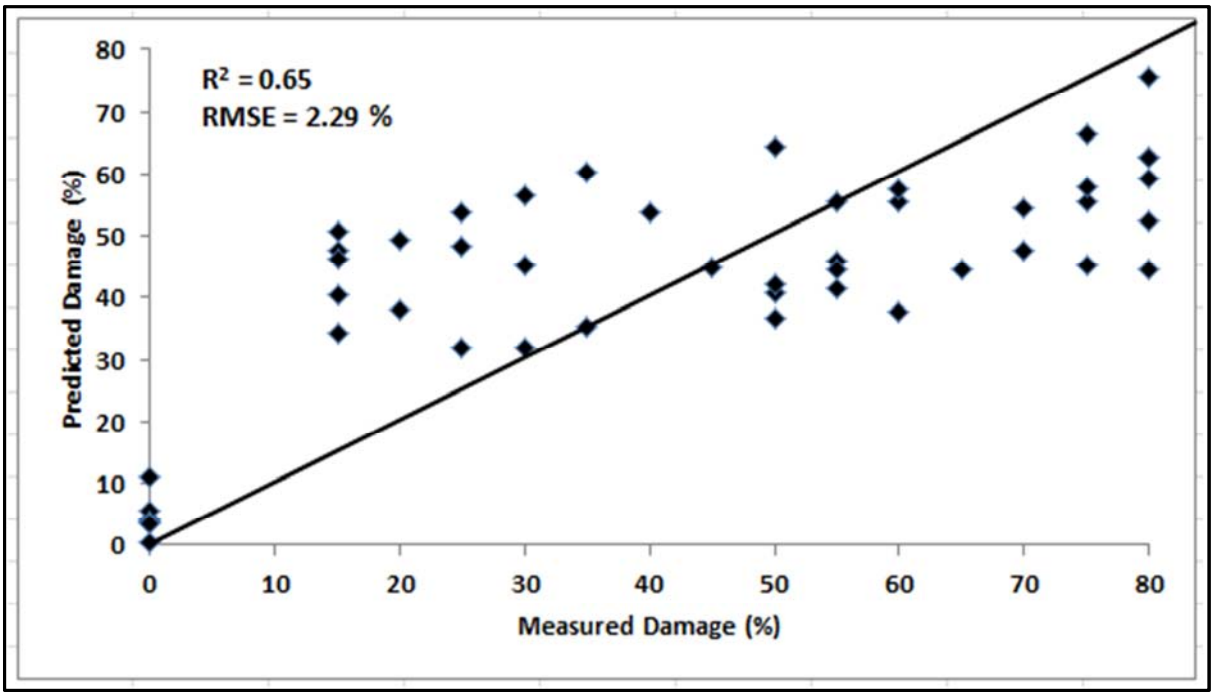

Figure 6.3 Forward stepwise regression model using the training dataset (n=56).

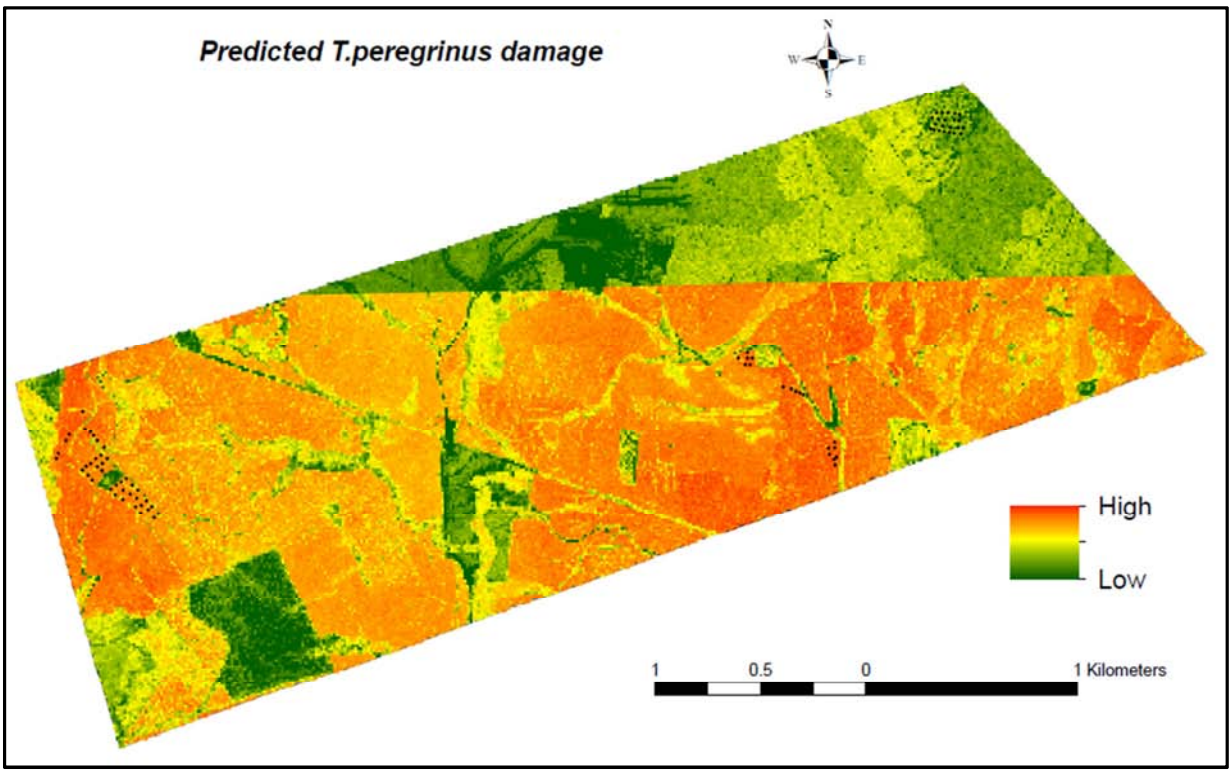

Figure 6.4 Predicted *T. peregrinus* damage map.

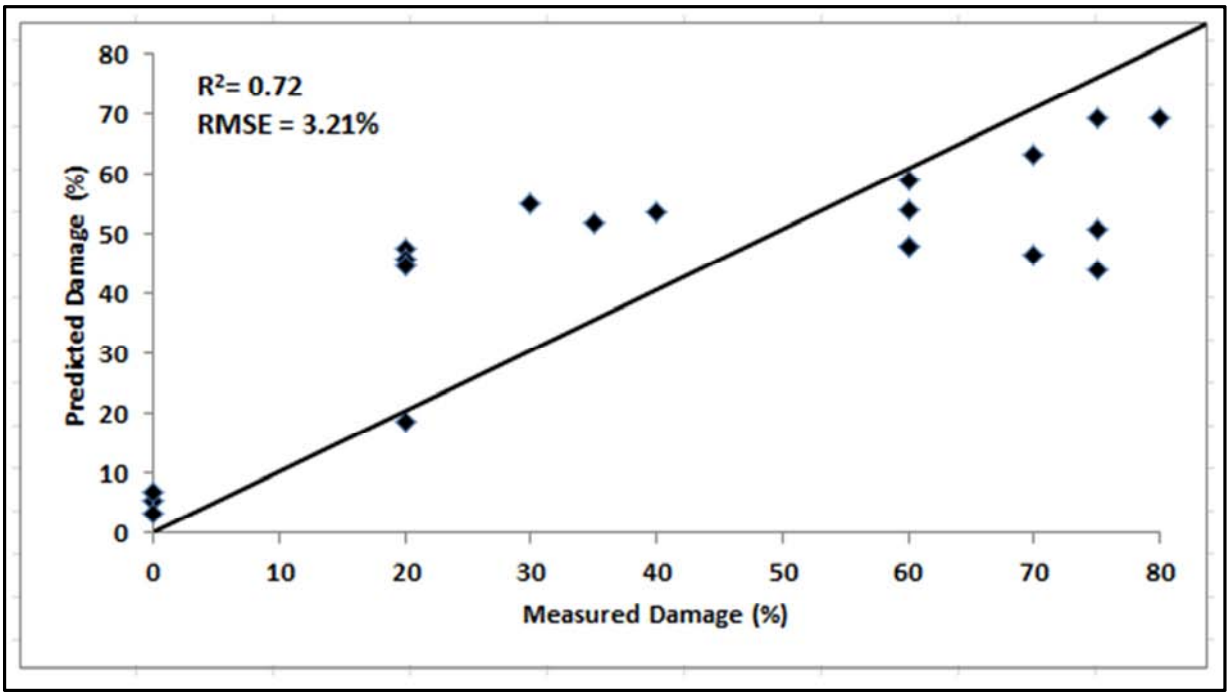

Figure 6.5 Regression model using the independent test dataset (n= 24).

6.5 Discussion

6.5.1 Relationship between T. peregrinus damage with WorldView-2 imagery and environmental factors

Correlations between WorldView-2 data and *T. peregrinus* damage show that the coastal blue, blue and green bands of the WorldView-2 sensor yield statistically significant but low correlations with *T. peregrinus* damage ranging from -0.38 to -0.40 (Figure 6.2). The red edge and near infrared bands of the WorldView-2 sensor were strongly correlated with *T. peregrinus* damage. Findings by Carter and Miller (1994) indicate that the ratio of the red edge (690-700 nm) to the near-infrared (760 nm) allows for early detection of stress induced chlorosis. This ratio of the red edge to the near-infrared responds to plant physiological measures of fluorescence and plant water status making it a good indicator for measuring plants under stress (Barry et al., 2008; Eitel et al., 2011). Other plant physiological changes due to insect infestation include damage to the waxy cuticle, decrease in chlorophyll content and destruction of cell walls (Stone et al., 2001) thereby resulting in reflectance changes in the near-infrared and red edge reflectance. From the vegetation indices tested, the anthocyanin, carotenoid and red green index yielded low but significant correlations ranging from 0.33 to 0.35. The anthocyanin concentration in plants is used to assess changes in plant foliage as a result of plant growth or death (Gitelson et al., 2001). Barry et al. (2008) also

reported the anthocyanin reflectance index and the red green index to be important predictors for assessing stress in damaged eucalypt leaves. Most of the aforementioned studies were based on hyperspectral field and lab data (Barry et al., 2008; Carter and Knapp, 2001; Carter and Miller, 1994; Colombo et al., 2008; Gitelson et al., 2002). However, this study makes use of an improved multispectral sensor and corroborates previous results that have been reported using narrowband hyperspectral reflectance. From the environmental datasets assessed, rainfall and temperature yielded significant and high correlations with *T. peregrinus* damage ranging from 0.62 to 0.76 while aspect yielded a low but significant correlation of 0.35. The utility of the environmental factors in predicting *T. peregrinus* damage was also assessed separately from the other datasets. The environmental factors predicted damage with an R^2 value of 0.61 on an independent dataset with temperature been a significant factor . This further illustatres the importance of linking the spread of pest damage to certain environmental factors. Dunn and Crutchfield (2008) report that the two dominant environmental factors that influence insect infestation are temperature and moisture. Moisture availability and variability are major determinants of insect habitation while increase in temperatures result in higher rates of pest outbreaks (Dunn and Crutchfield, 2008). Lombardero et al. (2000) reports that shortened winters and increased summer temperatures result in increased insect feeding, faster growth rates and rapid insect reproduction. These factors contribute to the spread and intensity of damage in forest plantations. The three step methodology of collaborating satellite spectral data, vegetation indices and environmental factors facilitates a better understanding and identification of important factors that affect *T. peregrinus* infestations in plantation forests.

6.5.2 Predicting and mapping T. peregrinus damage

This study has shown the utility of the WorldView-2 sensor in combination with environmental datasets for the prediction and mapping of *T. peregrinus* damage in plantation forests. The results are comparable to that of Li (2010) who used high resolution QuickBird imagery and environmental variables to classify pine wilt disease in China. Li (2010) created distribution maps of pine wilt disease using slope and *NDVI* values generated from QuickBird imagery. This study has indicated that temperature and the near-infrared band 8 of the WorldView-2 sensor are vital parameters for assessing *T. peregrinus* damage levels. Temperature yielded the highest correlation with *T. peregrinus* damage (r = 0.76) and is a crucial factor for the prediction of *T. peregrinus* damage. Numerous climate and forest

experts have observed that outbreaks in insect infestation are a consequence of a climatic shift to warmer temperatures (Dunn and Crutchfield, 2008; Menéndez, 2007). The predicted damage map confirms this with high damage levels observed towards the centre of the study area, which is characterized by slightly higher temperatures as compared to the upper portion of the study area which is lower in temperature. The near-infrared band 8 (860-1040 nm) yielded the second highest correlation with *T. peregrinus* damage (r = -0.74) and is a band that is less influenced by atmospheric conditions and is often used to measure change in vegetation phenology (Carter, 1994; Carter and Knapp, 2001; DigitalGlobe, 2010; Oumar et al., 2013). Prediction maps serve as spatial guides for forest managers to enhance their detection methods and make cost effective decisions related to plantation forest management (Oumar and Mutanga, 2012).

6.6 Conclusion

The aim of this study was to assess the potential of the new generation WorldView-2 sensor in conjunction with environmental datasets for predicting and mapping the severity of *T. peregrinus* damage in plantation forests. The following conclusions can be reached:

1) The red edge and near-infrared bands of the WorldView-2 sensor are strongly correlated with *T. peregrinus* damage yielding correlations ranging from -0.60 to -0.74.
2) Temperature and precipitation are important indicators for monitoring *T. peregrinus* damage yielding correlations of 0.76 and 0.62 respectively.
3) Temperature and the near-infrared-2 of the WorldView-2 sensor predicted *T. peregrinus* damage with a mean bootstrapped R^2 value of 0.72 on an independent test dataset and a *RMSE* of 3.21%.
4) Prediction maps can be used by forest managers in salvage operations before trees reach a point of no recovery.

Overall, this study indicates the potential of an integrated approach for mapping and monitoring pest damage in plantation forest using an improved multispectral sensor which contains key vegetation wavelengths.

6.7 Acknowledgements

We thank Muhammad Sheik Oumar and Thato for helping with the field data collection. We are grateful to DigitalGlobe for providing us with the WorldView-2 imagery. Funding for this research was provided by the National Research Foundation and the University of KwaZulu-Natal.

CHAPTER SEVEN

7. A synthesis

7.1 Introduction

Why do we need to use remote sensing technologies to detect and map *T. peregrinus* damage in plantation forests? *T. peregrinus* has caused extensive damage to eucalypt plantations internationally. There is an imperative need to identify stands that are infested so proper remediation methods can be implemented before trees reach a point of no recovery. Remote sensing technology has the ability to spatially quantify the extent and severity of damage over large areas thereby aiding in salvage operations and strengthening forest health monitoring programmes. This study aimed to assess the potential of remote sensing techniques to accurately detect and map *T. peregrinus* damage in plantation forests. The specific objectives of the thesis were: (1) to extensively review literature on the applicability of remote sensing technology in mapping *T. peregrinus* damage, (2) to assess the utility of hyperspectral narrow band data in predicting the physiological stages of *T. peregrinus* damage, and (3) to predict and map *T. peregrinus* damage with the new generation WorldView-2 sensor using remote sensing techniques. The results pertaining to the objectives of the thesis are discussed in the subsequent sections.

7.2 To extensively review literature on the applicability of remote sensing technology in mapping *T. peregrinus* damage

Chapter two showed how developments in multispectral and hyperspectral technology can be used to detect the various stages of *T. peregrinus* damage. The chapter illustrated how improvements in multispectral sensor characteristics can be used to detect and map medium to advanced stages of *T. peregrinus* damage. The applicability of hyperspectral platforms in assessing early or previsual stages of *T. peregrinus* infestation is also discussed. It was concluded that vegetation indices calculated from hyperspectral data needed to be developed and tested to predict the physiological stages of *T. peregrinus* damage. It was further established that remote sensing techniques which make use of improvements in sensor characteristics need to be tested in mapping *T. peregrinus* damage. Once these techniques have been tested and developed they can be used operationally as an effective method to quantify, detect and monitor *T. peregrinus* damage in plantation forests.

7.3 Predicting *T. peregrinus* damage using narrowband normalized indices and hyperspectral indices with PLS regression

In order to assess the potential of narrowband data in predicting *T. peregrinus* damage, normalized indices based on *NDVI* ratios were calculated from field spectra resampled to the Hyperion sensor. Spectral indices used for assessing stress in vegetation were also calculated from the resampled hyperspectral data. Both these datasets were tested in predicting *T. peregrinus* damage using PLS regression. Table 7.1 shows the performance of the PLS regression models in predicting *T. peregrinus* damage. The backward variable selection model performed the best and predicted *T. peregrinus* damage with an R^2 value of 0.74 and the lowest *RMSE* of 1.30%. The indices selected by the backward variable selection model include the anthocyanin reflectance index, the carotenoid reflectance index and the 864.4 and 8847 nm index. The result indicates the potential of hyperspectral indices and spectral indices in predicting *T. peregrinus* damage in plantation forests and offers the foundation for the upscaling of the methods to operational hyperspectral sensors such as Hyperion. However, the strength of any forest health monitoring programme is dependent on the ability to quantify early physiological stages of damage. The next section tested the ability of field spectroscopy in predicting water stress induced by *T. peregrinus* infestations.

Table 7.1 Performance of PLS regression models in predicting damage on an independent test dataset.

PLS Models	Mean R^2	*RMSE* (%)	Standard error	95% Confidence limit
Top 20 normalized indices (n=20)	0.63	1.57	0.07	0.01
Twenty three spectral indices (n = 23)	0.59	1.67	0.07	0.01
Combined dataset (n = 43)	0.65	1.49	0.06	0.01
Indices based on VIP scores (n = 23)	0.71	1.35	0.07	0.01
Indices based on backward variable selection model (n = 3)	0.74	1.30	0.06	0.01

7.4 Predicting plant water content in *T. peregrinus* infested plantations with field spectroscopy and neural networks

The ability to predict plant water stress induced by *T. peregrinus* infestations allows for the early detection, often previsual strain that is associated with insect damage and gives weight to many forest health monitoring programmes. Water absorption bands and indices calculated from field hyperspectral reflectance were input into a neural network algorithm to predict plant water content and equivalent water thickness in *T. peregrinus* infested plantations. The neural network algorithm predicted *PWC* and *EWT* with correlation coefficients of 0.88 and 0.71 on independent test datasets. Figure 7.1 shows the predictive performance of these models on both the training and tests datasets. The results indicate the importance of water absorption bands and indices calculated from hyperspectral data in quantifying the severity of water stress in *T. peregrinus* infested plantations. The result is significant for assessing early physiological stages of *T. peregrinus* damage. The next objective of this thesis was to test the utility of the new generation WorldView-2 sensor in predicting and mapping *T. peregrinus* damage.

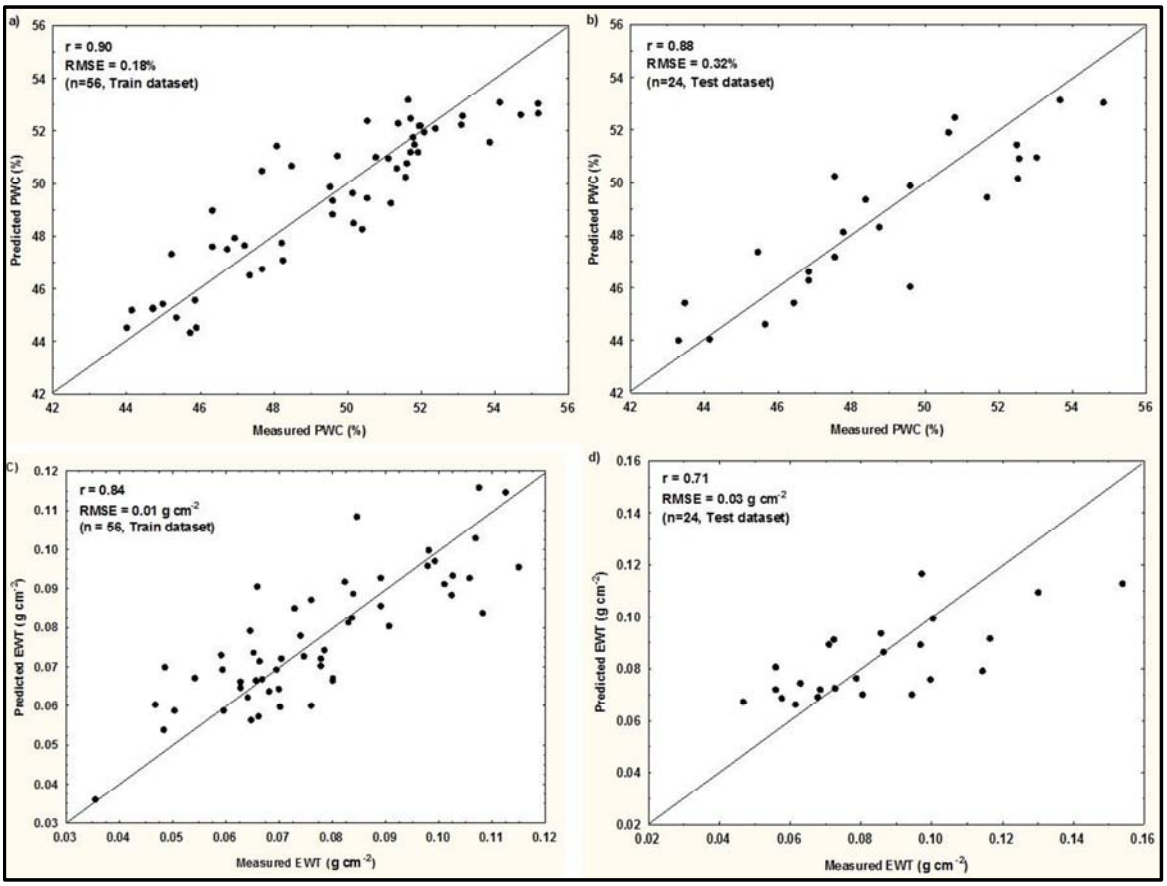

Figure 7.1 Performance of the neural network algorithm in predicting *PWC* and *EWT* on train and test datasets.

7.5 Predicting and mapping *T. peregrinus* damage using WorldView-2 bands and indices

The new and improved WorldView-2 sensor which contains key vegetation wavelengths was tested in mapping *T. peregrinus* damage using PLS regression. The WorldView-2 bands and indices were input into PLS regression models to predict *T. peregrinus* damage. The regression models were then extrapolated to map the distribution of damage in plantation forests. WorldView-2 bands and indices chosen by VIP scores performed the best and predicted *T. peregrinus* damage with an R^2 value of 0.65 on an independent test dataset. Figure 7.2 and Figure 7.3 show the predicted maps and the performance of the PLS regression models in predicting damage on independent test datasets. The red edge and near-infrared bands of the WorldView-2 sensor and pigment specific indices as well as red edge indices were identified as important spectral variables for the prediction of damage. The results show the capability of the new generation WorldView-2 sensor in mapping *T. peregrinus* damage. The next paper focused on incorporating environmental variables with WorldView-2 imagery to improve the prediction and mapping of *T. peregrinus* damage. Environmental factors such as climate and topography have a strong influence on the buildup and decline of pest outbreaks in plantation forests. It was envisaged that environmental factors together with the new generation WorldView-2 sensor bands will further strengthen the prediction and mapping of *T. peregrinus* damage.

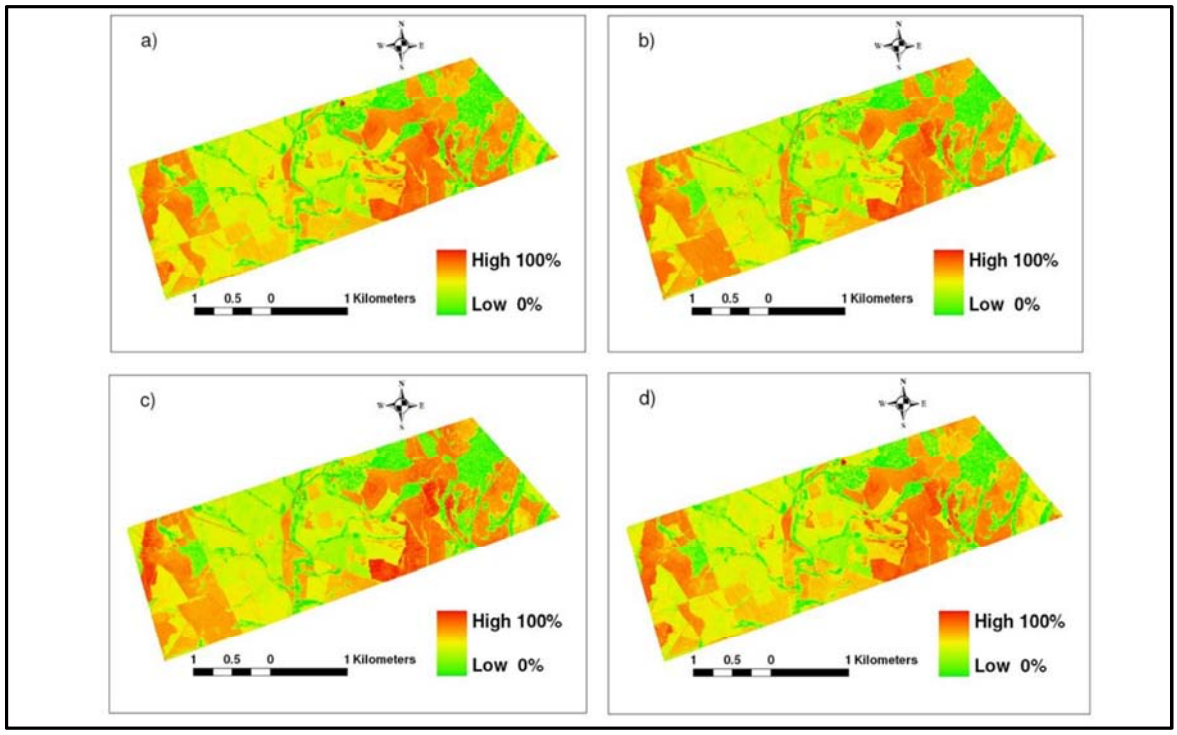

Figure 7.2 Prediction maps created from the PLS regression models. (a) WorldView-2 sensor bands, (b) Vegetation indices, (c) Combined dataset, (d) VIP bands and indices.

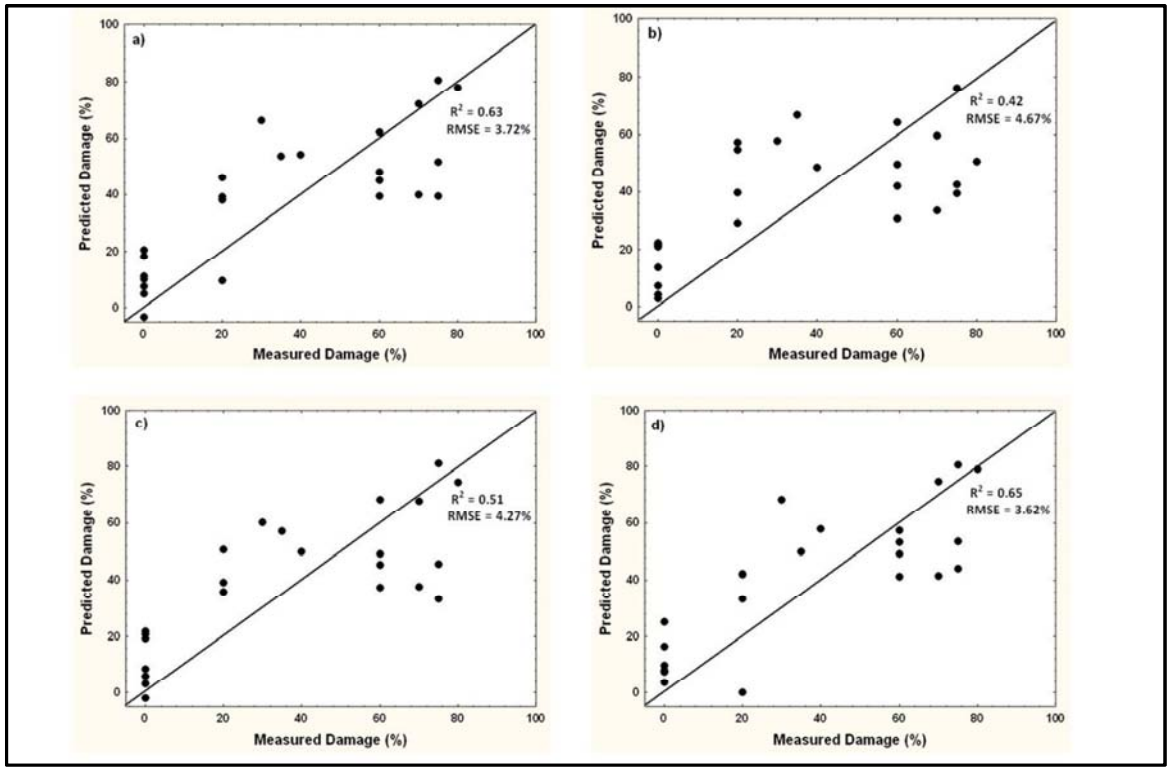

Figure 7.3 Predicted versus measured *T. peregrinus* damage on an independent test dataset (n=24) using the prediction maps. (a) WorldView-2 sensor bands, (b) Vegetation indices, (c) Combined dataset, (d) VIP bands and indices.

7.6 Improving the prediction and mapping of *T. peregrinus* damage using environmental datasets and WorldView-2 imagery

The integrated approach involving environmental variables, vegetation indices and WorldView-2 imagery successfully predicted *T. peregrinus* damage with an R^2 value of 0.72 on an independent test dataset. The near-infrared band 8 of the WorldView-2 sensor and the temperature dataset were identified as significant variables for the prediction of damage. The regression model was then inverted to map the distribution of damage as illustrated in Figure 7.4. This study built on the previous chapter and showed the importance of an integrated approach which helps us better understand the factors that influence *T. peregrinus* infestations in plantation forests.

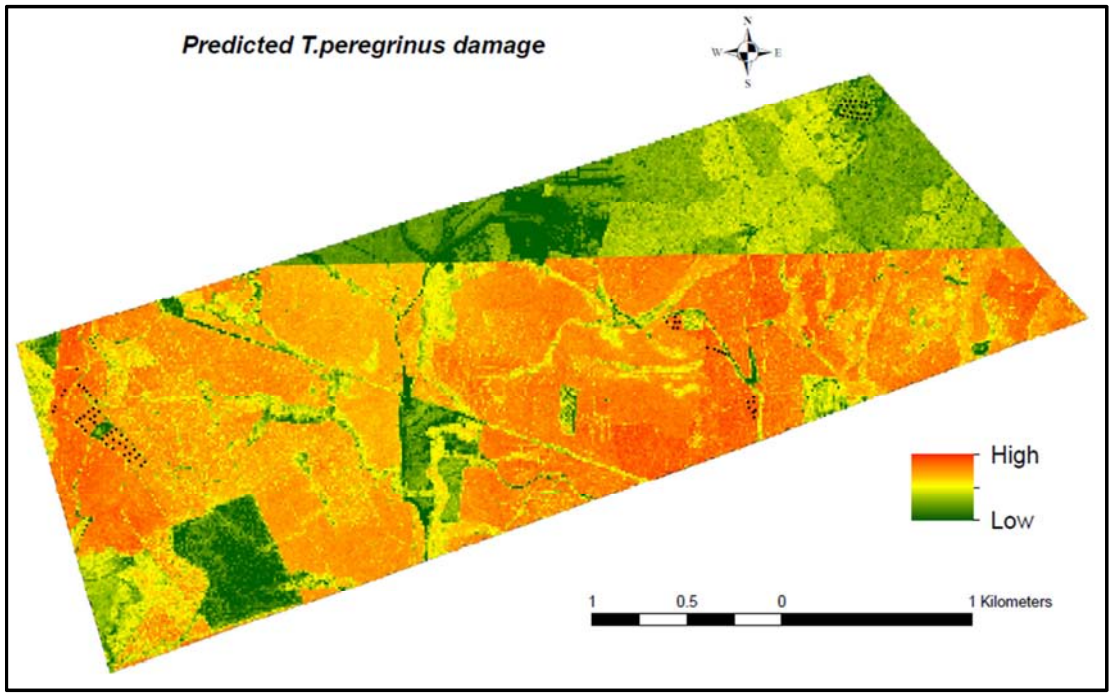

Figure 7.4 Predicted *T. peregrinus* damage map.

7.7 Conclusion

The aim of this research was to assess the potential of remote sensing techniques to accurately detect and map *T. peregrinus* damage in plantation forests. Based on the results carried out in this research the following conclusions can be drawn:

- Improvements in multispectral and hyperspectral platforms make it possible to detect and map the different stages of *T. peregrinus* damage in plantation forests.

- Narrowband normalized indices and spectral indices calculated from field hyperspectral data can successfully predict various stages of *T. peregrinus* damage.
- Field spectroscopy can be used to assess early physiological stages of damage by predicting water stress in *T. peregrinus* infested plantations.
- The new generation WorldView-2 sensor is able to predict and map various stages of *T. peregrinus* damage with relatively high accuracies.
- The red edge and near-infrared bands of the WorldView-2 sensor are highly correlated with *T. peregrinus* damage.
- Integrating environmental variables, vegetation indices and WorldView-2 imagery improves the overall mapping accuracy of *T. peregrinus* damage.

7.8 The future

The results from this study indicate the potential of remote sensing technology in successfully detecting and mapping *T. peregrinus* damage in forest plantations. This research highlights the importance of the new generation WorldView-2 sensor, in mapping early to advanced stages of *T. peregrinus* damage. The result is significant for forest health monitoring in South Africa using a relatively cheap satellite with huge areal coverage. This will effectively strengthen pest management programmes.

The research demonstrates the ability of spaceborne multispectral sensors and field hyperspectral sensors in detecting and mapping varied rates of *T. peregrinus* damage. One future challenge would be to upscale the results from this study to assess early physiological stages of damage using hyperspectral airborne or spaceborne sensors. Often the exorbitant cost of data from these sensors limits their use in forest health assessments. However, it is envisaged that with the launch of the ZA-ARMC 1 in South Africa imminent, the remote sensing of early physiological stress associated with *T. peregrinus* damage can be upscaled.

Finally, the successful use of PLS regression and neural networks in identifying important spectral variables for the prediction and mapping of *T. peregrinus* damage, shows the importance of these statistical techniques in reducing the multicollinearity problem which is often associated with remote sensing data. Opportunities exist to explore these techniques using airborne or spaceborne hyperspectral sensors to improve the mapping of *T. peregrinus* damage in plantation forests.

References

Analytical Spectral Devices, 2002. FieldSpec Pro Users guide, Boulder, Colorado.

Arenas-Garci'a, J. and Camps-Valls, G., 2008. Efficient kernel orthonormalized PLS for remote sensing applications. IEEE Transactions on Geoscience and Remote Sensing, 46(10): 2872-2881.

Barry, K.M., Stone, C. and Mohammed, C.L., 2008. Crown-scale evaluation of spectral indices for defoliated and discoloured eucalypts. International Journal of Remote Sensing, 29(1): 47-69.

Bentz, B.J. and Endreson, D., 2003. Evaluating Satellite Imagery for estimating Mountain Pine Beetle-Caused Lodgepole Pine Mortality: Current Status, *Proceedings of the Mountain Pine Beetle Symposium: Challenges and Solutions*, Kelowna, British Columbia.

Blackburn, G.A., 2007. Hyperspectral remote sensing of plant pigments. Journal of Experimental Botany, 58(4): 855-867.

Bonneau, L.R., Shields, K.S. and Civco, D.L., 1999. A technique to identify changes in hemlock forest health over space and time using satellite image data. Biological Invasions, 1: 269-279.

Bowyer, P. and Danson, F.M., 2004. Sensitivity of spectral reflectance to variation in fuel moisture content at leaf and canopy level. Remote Sensing of Environment, 92: 297-308.

Button, G., 2007. *Thaumastocoris peregrinus*, *Forestry Facts*. NCT Forestry.

Camp, K.G., 1997. The Bioresource Groups of KwaZulu-Natal. Cedara, South Africa.

Campbell, P.K.E., Rock, B.N., Martin, M.E., Neefus, C.D., Irons, J.R., Middleton, E.M. and Albrechtova, J., 2004. Detection of initial damage in Norway spruce canopies using hyperspectral airborne data. International Journal of Remote Sensing, 25(24): 5557-5583.

Carpintero, D.L. and Dellape, P.M., 2006. A new species of *Thaumastocoris* Kirkaldy from Argentina (Heteroptera: Thaumastocoridae: Thaumastocorinae). Zootaxa, 1228: 61-68.

Carter, G., 1994. Ratios of leaf reflectances in narrow wavebands as indicators of plant stress. International Journal of Remote Sensing, 15(3): 697-703.

Carter, G.A., 1991. Primary and secondary effects of water content on the spectral reflectance of leaves. American Journal of Botany, 78(7): 916-924.

Carter, G.A., 1993. Responses of leaf spectral reflectance to plant stress. American Journal of Botany, 80(3): 239-243.

Carter, G.A. and Knapp, A.K., 2001. Leaf optical properties in higher plants: linking spectral characteristics to stress and chlorophyll concentration. American Journal of Botany, 88: 667-684.

Carter, G.A. and Miller, R.L., 1994. Early detection of plant stress by digital imaging within narrow stress-sensitive wavebands. Remote Sensing of Environment, 50(3): 295-302.

Ceccato, P., Flasse, S., Tarantola, S., Jacquemoud, S. and Gregoire, J., 2001. Detecting vegetation leaf water content using reflectance in the optical domain. Remote Sensing of Environment, 77: 22-33.

Chittineni, S. and Bhogapathi, R.B., 2012. A study of the behaviour of a neural network for grouping the data. International Journal of Computer Science Issues, 9(1): 228-234.

Cho, M.A., Skidmore, A., Corsi, F., van Wieren, S.E. and Sobhan, I., 2007. Estimation of green grass/herb biomass from airborne hyperspectral imagery using spectral indices and partial least squares regression. International Journal of Applied Earth Observation and Geoinformation, 9(4): 414-424.

Cho, M.A. and Skidmore, A.K., 2006. A new technique for extracting the red edge position from hyperspectral data: The linear extrapolation method. Remote Sensing of Environment 101: 181-193.

Chong, I. and Jun, C., 2005. Performance of some variable selection methods when multicollinearity is present. Chemometrics and Intelligent Laboratory Systems, 78: 103-112.

Ciesla, W.M., 2000. Remote sensing in forest health protection. United States Department of Agriculture.

Colombo, R., Meroni, M., Marchesi, A., Busseto, L., Rossini, M., Giardino, C. and Panigada, C., 2008. Estimation of leaf and canopy water content in poplar plantations by means of hyperspectral indices and inverse modeling. Remote Sensing of Environment, 112: 1820-1834.

Coops, N., Stanford, M., Old, K., Dudzinski, M., Culvenor, D. and Stone, C., 2003. Assessment of Dothistroma Needle Blight of *Pinus radiata* Using Airborne Hyperspectral Imagery. Phytopathology, 93(12): 1524-1532.

Coops, N.C., Johnson, M., Wulder, M.A. and White, J.C., 2006. Assessment of Quickbird high spatial resolution imagery to detect red attack damage due to mountain pine beetle infestation. Remote Sensing of Environment, 103: 67-80.

Coops, N.C., Stone, C., Culvenor, D.S. and Chisholm, L., 2004. Assessment of Crown Condition in Eucalypt Vegetation by Remotely Sensed Optical Indices. Journal of Environmental Quality, 33: 956-964.

Curran, P.J., 1989. Remote sensing of foliar chemistry. Remote Sensing of Environment, 30(3): 271-278.

Curran, P.J., Dungan, J.L. and Peterson, D.L., 2001. Estimating the foliar biochemical concentration levels with reflectance spectrometry. Remote Sensing of Environment, 76: 349-359.

Danson, F.M., Steven, M.D., Malthus, T.J. and Clark, J.A., 1992. High-spectral resolution data for determining leaf water content. International Journal of Remote Sensing, 13(3): 461-470.

Datt, B., 1999. Remote sensing of water content in *Eucalyptus* leaves. Australian Journal of Botany, 47: 909-923.

Daughtry, C.S.T., Walthall, C.L., Kim, M.S., Brown De Colstoun, E. and Mcmurtrey III, J.E., 2000. Estimating corn leaf chlorophyll concentration from leaf and canopy reflectance. Remote Sensing of Environment, 74: 229-239.

Dawson, T.P. and Curran, P.J., 1998. A new technique for interpolating the reflectance red edge position. International Journal of Remote Sensing, 19(11): 2133-2139.

Dennison, P.E., Brunelle, A.R. and Carter, V.A., 2010. Assessing canopy mortality during a mountain pine beetle outbreak using GeoEye-1 high spatial resolution satellite data. Remote Sensing of Environment.

DigitalGlobe, 2010. The Benefits of the 8 Spectral Bands of WorldView-2, White Paper. DigitalGlobe^{R} USA.

Dunn, D. and Crutchfield, J.P., 2008. Entomogenic Climate Change. q-bio.PE - Populations and Evolution (arXiv:0805.3851v1).

Dye, M., Mutanga, O. and Ismail, R., 2008. Detecting the severity of *Sirex noctilio* (woodwasp) infestation in a pine plantation in KwaZulu-Natal, South Africa using texture measures calculated from high spatial resolution imagery. African Entomology.

Efron, B., 1982. The jacknife, the bootstrap, and other resampling plans. Society of industrial and applied mathematics, Philadelphia.

Eitel, J.U.H., Gessler, P.E., Smith, A.M.S. and Robberecht, R., 2006. Suitability of existing and novel spectral indices to remotely detect water stress in Populus spp. Forest Ecology and Management, 229: 170-182.

Eitel, J.U.H., Vierling, L.A., Litvak, M.E., Long, D.S., Schulthess, U., Ager, A.A., Krofcheck, D.J. and Stoscheck, L., 2011. Broadband, red-edge information from satellites improves early stress detection in a New Mexico conifer woodland. Remote Sensing of Environment, 115: 3640-3646.

Ekstrand, S., 1994. Assessment of Forest Damage with Landsat TM: Correction for Varying Forest Stand Characteristics. Remote Sensing of Environment, 47: 291-302.

Entcheva Campbell, P.K., Rock, B.N. and Martin, M.E., 2004. Detection of initial damage in Norway spruce canopies using hyperspectral airborne data. International Journal of Remote Sensing, 25(24): 5557-5583.

ENVI, 2006. Environment for Visualising Images. Release 4.3. ITT industries, Inc, Boulder, USA.

FAO, 2007. Overview of Forest Pests, Food and Agriculture Organization of the United Nations.

Feilhauer, H., Asner, G.P., Martin, R.E. and Schmidtlein, S., 2010. Brightness-normalized Partial Least Squares Regression for hyperspectral data. Journal of Quantitative Spectroscopy and Radiative Transfer, 111: 1947-1957.

Filella, I. and Penuelas, J., 1994. The red edge position and shape as indicators of plant chlorophyll content, biomass and hydric status. International Journal of Remote Sensing, 15(7): 1459-1470.

Frank, I. and Friedman, J., 1993. A statistical view of some chemometrics regression tools. Technometrics, 35: 109-135.

Franklin, S.E., Waringg, R.H., McCreight, R.W., Cohen, W.B. and Fiorella, M., 1995. Aerial and satellite sensor detection and classification of western spruce budworm defoliation in a subalpine forest. Canadian Journal of Remote Sensing, 21(3): 299-308.

Fraser, R.H. and Lativofic, R., 2005. Mapping insect-induced tree defoliation and mortality using coarse spatial resolution satellite imagery. International Journal of Remote Sensing, 26(1): 193-200.

Gamon, J.A. and Surfus, J.S., 1999. Assessing leaf pigment content and activity with a reflectometer. New Phytologist, 143: 105-117.

Gao, B.C., 1996. NDWI-a normalized difference water index for remote sensing of vegetation liquid water from space. Remote Sensing of Environment, 58: 257-266.

Gates, D.M., Keagan, H.J., Schleter, J.C. and Weidner, V.R., 1965. Spectral properties of plants. Applied Optics, 4: 11-20.

Geladi, P. and Kowlski, B., 1986. Partial least-squares regression: A tutorial. Analytica Chimica Acta, 185: 1-17.

Genc, H., Genc, L., Turhan, H., Smith, S.E. and Nation, J.L., 2008. Vegetation indices as indicators of damage by the sunnpest (Hemiptera: Scutelleridae) to field grown wheat. African Journal of Biotechnology, 7(2): 173-180.

Gitelson, A. and Merzlyak, M., 1994. Spectral reflectance changes associated with autumn senescence of Aesculus hippocastanum L. and Acer platanoides L. leaves. Spectral features and relation to chlorophyll estimation. Journal of Plant Physiology, 143(3): 286-292.

Gitelson, A., Merzlyak, M. and Chivkunova, O., 2001. Optical Properties and Nondestructive Estimation of Anthocyanin Content in Plant Leaves. Photochemistry and Photobiology, 74(1): 38-45.

Gitelson, A., Zur, Y., Chivkunova, O. and Merzlyak, M., 2002. Assessing Carotenoid Content in Plant Leaves with Reflectance Spectroscopy. Photochemistry and Photobiology, 75(3): 272-281.

Guyot, G. and Barett, F., 1988. Utilisation de la haute resolution pour suivre l'etat des couverts vegetaux, Proceedings of the Fourth International colloquium on Physical Measurements and Signatures in Remote Sensing. European Space Agency, Noordwijk, pp. 279-286.

Hardisky, M.A., Klemas, V. and Smart, R.M., 1983. The influences of Soil Salinity, Growth Form, and Leaf Moisture on the Spectral Reflectance of Spartina Alterniflora Canopies. Photogrammetric Engineering and Remote Sensing, 49: 77-83.

Hoque, E., Hutzler, P.J.S. and Hiendl, H., 1992. Reflectance, colour, and histological features as parameters for the early assessment of forest damages. Canadian Journal of Remote Sensing, 18: 104-110.

Horler, D.N.H., Dockray, M. and Barber, J., 1983. The red edge of plant leaf reflectance. International Journal of Remote Sensing, 4(2): 273-288.

Hoskuldsson, A., 2003. Analysis of latent structures in linear models. Journal of Chemometrics, 17: 630-645.

Hoskuldsson, A., 2008. H-methods in applied sciences. Journal of Chemometrics, 22: 150-177.

Huete, A.R., Liu, H., Batchily, K. and van Leeuwen, W., 1997. A Comparison of Vegetation Indices Over a Global Set of TM Images for EOS-MODIS. Remote Sensing of Environment, 59(3): 440-451.

Hunt, E.R. and Rock, B.N., 1989. Detection of changes in leaf water content using near-and middle-infrared reflectances. Remote Sensing of Environment, 30: 43-54.

Ismail, R., 2009. *Remote sensing of forest health: The detection and mapping of Pinus patula trees infested by Sirex noctilio.* Dissertation Thesis, University of KwaZulu-Natal, Pietermaritzburg, 175 pp.

Ismail, R., Mutanga, O. and Ahmed, F., 2008. Discriminating Sirex noctilio attack in pine forest plantations in South Africa using high spectral resolution data. In: M. Kalacska and A.E. Sanchez-Azofeifa (Editors), Hyperspectral Remote Sensing of Tropical and Sub-Tropical Forests. Taylor and Francis: CRC Press.

Ismail, R., Mutanga, O. and Bob, U., 2007. Forest health and vitality: The detection and monitoring of *Pinus patula* trees infected by *Sirex noctilio* using digital multispectral imagery (DMSI). Southern Hemisphere Forestry Journal, 69(1): 39-47.

Jacobs, D.H. and Neser, S., 2005. *Thaumastocoris australicus* Kirkaldy (Heteroptera: Thaumastocoridae): a new insect arrival in South Africa, damaging to *Eucalyptus* trees. South African Journal of Science, 101: 233-236.

Kaufman, Y. and Tanre, D., 1996. Strategy for Direct and Indirect Methods for Correcting the Aerosol Effect on Remote Sensing: from AVHRR to EOS-MODIS. Remote Sensing of Environment, 55: 65-79.

Kharuk, V.I., Ranson, K.J. and Fedotova, E., 2007. Spatial pattern of Siberian silkmoth outbreak and taiga mortality. Scandinavian Journal of Forest Research, 22: 531-536.

Landgrebe, D., 1999. Some fundamentals and methods for hyperspectral image data analysis. In: G. Cohn and J.C. Owicki (Editors), Systems and Technologies for Clinical Diagnostics and Drug Discovery II (Proceedings Volume), San Jose CA, pp. 104-113.

Lawrence, R. and Labus, M., 2003. Early Detection of Douglas-Fir Beetle Infestation with Subcanopy Resolution Hyperspectral Imagery. WJAF, 18(3): 1-5.

Li, M., Liu, M., Liu, M. and Ju, Y., 2010. Monitoring Exotic Forest Pest Based on High-resolution Remote Sensing Image and CART Model, 3rd International Congress on Image and Signal Processing. IEEE, Yantai, pp. 2203-2206.

Liu, L., Wang, J., Huang, W., Zhao, C., Zhang, B. and Tong, Q., 2004. Estimating winter wheat plant water content using red edge parameters. International Journal of Remote Sensing, 25: 3331-3342.

Lombardero, M.J., Ayres, M.P., Ayres, B.D. and Reeve, J.D., 2000. Cold Tolerance of Four Species of Bark Beetle (Coleoptera:Scolytidae) in North America. Environmental Entomology, 29(3): 421-432.

Luedeling, E., Hale, A., Zhang, M., Bentley, W.J. and Dharmasri, L.C., 2009. Remote Sensing of spider mite damage in California peach orchards. International Journal of Applied Earth Observation and Geoinformation, 11: 244-255.

Maccioni, A., Agati, G. and Mazzinghi, P., 2001. New vegetation indices for remote sensing of chlorophylls based on leaf directional reflectance spectra. Journal of Photochemistry and Photobiology B: Biology, 61: 52-61.

Macomber, S.A. and Woodcock, C.E., 1994. Mapping and Monitoring Conifer Mortality Using Remote Sensing in the Lake Tahoe Basin. Remote Sensing of Environment, 50: 255-256.

Meddens, A.J.H., Hicke, J.A. and Vierling, L.A., 2011. Evaluating the potential of multispectral imagery to map multiple stages of tree mortality. Remote Sensing of Environment, 115: 1632-1642.

Menéndez, R., 2007. How are insects responding to global warming? Tijdschrift voor Entomologie, 150: 355-365.

Merzlyak, M., Gitelson, A., Chivkunova, O. and Rakitin, V., 1999. Non-destructive optical detection of pigment changes during leaf senescence and fruit ripening. Physiologia plantarum, 106(1): 135-141.

Milton, E.J., Schaepman, M.E., Anderson, K., Kneubuhler, K. and Fox, N., 2009. Progress in field spectroscopy. Remote Sensing of Environment, 113: 92-109.

Mutanga, O., 2004. Hyperspectral remote sensing of tropical grass quality and quantity. Wageningen University, Netherlands.

Mutanga, O. and Ismail, R., 2010. Variation in foliar water content and hyperspectral reflectance of *Sirex noctilio* infested *Pinus patula* trees. Southern Forests, 72(1): 1-7.

Mutanga, O. and Kumar, L., 2007. Estimating and mapping grass phosphorous concentration in an African savanna using hyperspectral image data. International Journal of Remote Sensing, 28: 1-15.

Mutanga, O. and Rugege, D., 2006. Integrating remote sensing and spatial statistics to model herbaceous biomass distribution in a tropical savanna. International Journal of Remote Sensing, 27: 3499-3514.

Mutanga, O., Skidmore, A. and Prins, H.H.T., 2004. Predicting in situ pasture quality in the Kruger National Park, South Africa, using continuum-removed absorption features. Remote Sensing of Environment, 89(3): 393-408.

Mutanga, O. and Skidmore, A.K., 2004a. Integrating imaging spectrometry and neural networks to map grass quality in the Kruger National Park, South Africa. Remote Sensing of Environment, 90: 104-115.

Mutanga, O. and Skidmore, A.K., 2004b. Narrow band vegetation indices overcome the saturation problem in biomass estimation. International Journal of Remote Sensing, 25: 1-16.

Nadel, R.L., 2007. *Thaumastocoris:* The solution. Wood Southern Africa and Timber Times: 10-11.

Nadel, R.L. and Noack, A.E., 2012. Current understanding of the biology of T*haumastocoris peregrinus* in the quest for a management strategy. International Journal of Pest Management, 58(3): 257-266.

Nadel, R.L., Slippers, B., Scholes, M.C. and Wingfield, M.J., 2007. Distribution and population structure of the Bronze bug, *Thaumastocoris peregrinus* in South African *Eucalyptus* plantations., Eucalypts and diversity: Balancing productivity and sustainability-IUFRO 2007, Durban.

Olthof, I., King, D.J. and Lautenschlager, R.A., 2004. Mapping deciduous forest ice storm damage using Landsat and environmental data. Remote Sensing of Environment, 89: 484-496.

Oumar, Z. and Mutanga, O., 2010. Predicting plant water content in *Eucalyptus grandis* forest stands in KwaZulu-Natal, South Africa using field spectra resampled to the Sumbandila Satellite Sensor. International Journal of Applied Earth Observation and Geoinformation, 12: 158-164.

Oumar, Z. and Mutanga, O., 2011. The potential of remote sensing technology for the detection and mapping of *Thaumastocoris peregrinus* in plantation forests. Southern Forests: A Journal of Forest Science, 73(1): 23-31.

Oumar, Z. and Mutanga, O., 2013. Using WorldView-2 bands and indices to predict bronze bug (*Thaumastocoris peregrinus*) damage in plantation forests. International Journal of Remote Sensing, 34(6): 2236-2249.

Oumar, Z., Mutanga, O. and Ismail, R., 2013. Predicting *Thaumastocoris peregrinus* damage using narrow band normalized indices and hyperspectral indices using field spectra resampled to the Hyperion sensor. International Journal of Applied Earth Observation and Geoinformation, 21: 113-121.

Palermo, G., Piraino, P. and Zucht, H., 2009. Performance of PLS regression coefficients in selecting variables for each response of a multivariate PLS for omics-type data. Advances and Applications in Bioinformatics and Chemistry, 2: 57-70.

Penuelas, J., Baret, F. and Filella, I., 1995. Semi-empirical indices to assess carotenoids/chlorophyll a ratio from leaf spectral reflectance. Photosynthetica, 31(2): 221-230.

Penuelas, J., Filella, I., Biel, C., Serrano, L. and Save, R., 1993. The reflectance at 950-970 as an indicator of plant water status. International Journal of Remote Sensing, 14(10): 1887-1905.

Penuelas, J. and Filella, L., 1998. Visible and near-infrared reflectance techniques for diagnosing plant physiological status. Trends in plant science, 3(4): 151-156.

Pontius, J., Martin, M., Plourde, L. and Hallet, R., 2008. Using Hyperspectral Technologies to Map Hemlock Decline: Pre-Visual Decline Assessment for Early Infestation Detection, *Third Symposium on Hemlock Woolly Adelgid*.

Pu, R., Kelly, M., Anderson, G.L. and Gong, P., 2008. Using CASI Hyperspectral Imagery to Detect Mortality and Vegetation Stress Associated with a New Hardwood Forest Disease. Photogrammetric Engineering and Remote Sensing, 74(1): 65-75.

Radeloff, V.C., Mladenoff, D.J. and Boyce, M.S., 1999. Detecting Jack Pine Budworm Defoliation Using Spectral Mixture Analysis: Separating Effects from Determinants. Remote Sensing of Environment, 69: 156-169.

Ripple, W.J., 1986. Spectral reflectance relationships to leaf water stress. Photogrammetric Engineering and Remote Sensing, 52: 1669-1675.

Rouse, J.W., Haas, R.H., Schell, J.A. and Deering, D.W., 1973. Monitoring Vegetation Systems in the Great Plains with ERTS., Third ERTS Symposium. NASA, Washington, DC, pp. 309-317.

Schmidt, K., 2003. Hyperspectral remote sensing of vegetation species distribution in a saltmarsh. Wageningen University, Netherlands.

Scholes, B. and Annamalai, L., 2006. CSIR imaging expertise propels SA to a science high, *Aerospace Science Scope*, pp. 19-21.

Schulze, R.E., Maharaj, M., Lynch, S.D., Howe, B.J. and Melvil-Thomson, B., 1997. South African atlas of agrohydrology and climatology. Water Research Commission Report, TT82/96.

Sims, D. and Gamon, J., 2002. Relationships between leaf pigment content and spectral reflectance across a wide range of species, leaf structures and developmental stages. Remote Sensing of Environment, 81(23): 337-354.

Siska, P.P. and Hung, I.H., 2001. Assessment of kriging accuracy in the GIS environment, The 21st Annual ESRI International User Conference., San Diego, CA.

Skaloudova, B., Krivan, V. and Zemek, R., 2006. Computer-assisted estimation of leaf damage caused by spider mites. Computers and Electronics in Agriculture, 53: 81-91.

Skidmore, A.K., Turner, B.J., Brinkhof, W. and Knowles, E., 1997. Performance of a neural network: Mapping forest using GIS and remotely sensed data. Photogrammetric Engineering and Remote Sensing, 63: 501-514.

Somers, B., Verbesellt, J., Ampe, E.M., Sims, N., Verstraeten, W.W. and Coppin, P., 2010. Spectral mixture analysis to monitor defoliation in mixed-aged *Eucalyptus globulus* Labill plantations in southern Australia using Landsat 5-TM and EO-1 Hyperion data. International Journal of Applied Earth Observation and Geoinformation, 12: 270-277.

StatSoft, I., 2002. STATISTICA for Windows [Computer program manual]. StatSoft, Inc, Tulsa, OK.

Stimson, H.C., Breshears, D.D., Ustin, S.L. and Kefauver, S.C., 2005. Spectral sensing of foliar water conditions in two co-occurring conifer species: *Pinus edulis* and *Juniperus monosperma*. Remote Sensing of Environment, 96: 108-118.

Stone, C., Chisholm, L. and Coops, N., 2001. Spectral reflectance characteristics of eucalypt foliage damaged by insects. Australian Journal of Botany, 49: 687-698.

Stone, C. and Coops, N., 2004. Assessment and monitoring of damage from insects in Australian eucalypt forests and commercial plantations. Australian Journal of Entomology, 43: 283-292.

Sunar Erbek, F., Ozkan, C. and Taberner, M., 2004. Comparison of maximimum likelihood classification method with supervised artificial neural network algorithms for land use activities. International Journal of Remote Sensing, 25: 1733-1748.

Tobias, R.D., 1995. An Introduction to Partial Least Squares Regression, Proceedings of the Twentieth Annual SAS Users Group International Conference SAS Institute Inc Cary,NC.

Toomey, M. and Vierling, L.A., 2005. Multispectral remote sensing of landscape level foliar moisture: techniques and applications for forest ecosystem monitoring. Canadian Journal of Forest Research, 35: 1087-1097.

TPCP, 2007a. Monitoring the Bronze Bug, *Thaumastocoris peregrinus* in South Africa. Tree Protection News, 14: 7-8.

TPCP, 2007b. An update on *Thaumastocoris* research in South Africa. Tree Protection News, 13: 6-7.

TPCP, 2008a. *Thaumastocoris peregrinus* (TPCP) monitoring trial. Tree Protection News, 15: 13-14.

TPCP, 2008b. Towards understanding and controlling *Thaumastocoris peregrinus*. Tree protection News, 16: 16-17.

Treitz, P.M. and Howarth, P.H., 1999. Hyperspectral remote sensing for estimating biophysical parameters of forest ecosystems. Progress in Physical Geography, 23: 359-390.

Trombetti, M., Riano, D., Rubio, M.A., Cheng, Y.B. and Ustin, S.L., 2008. Multi-temporal vegetation canopy water content retrieval and interpretation using artificial neural networks for the continental USA. Remote Sensing of Environment 112: 203-215.

Tucker, C.J., 1979. Red and Photographic Infrared Linear Combinations for Monitoring Vegetation. Remote Sensing of Environment, 8: 127-150.

Turnbull, J.W., 1999. Eucalypt plantations. New Forests, 17: 37-52.

Vogelmann, J.E., Rock, B.N. and Moss, D.M., 1993. Red Edge Spectral Measurements from Sugar Maple Leaves. International Journal of Remote Sensing, 14: 1563-1575.

Wang, L., Huang, H. and Luo, Y., 2010. Remote sensing of insect pests in larch forest based on physical model, Geoscience and Remote Sensing Symposium (IGARSS). IEEE, Honolulu, HI, pp. 3299-3302.

White, J.C., Wulder, M.A., Brooks, D., Reich, R. and Wheate, R.D., 2005. Detection of red attack stage mountain pine beetle infestation with high spatial resolution satellite imagery. Remote Sensing of Environment, 96: 340-351.

Wingfield, M.J., Slippers, B., Hurley, B.P., Coutinho, T.A., Wingfield, B.D. and Roux, J., 2008. Eucalypt pests and diseases: growing threats to plantation productivity. South Forests, 70(2): 139-144.

Wold, S., 1995. PLS for multivariate linear modeling. In: H.v.d. Waterbeemd (Editor), Chemometric methods in molecular design: Methods and principles in medicinal chemistry, Weinheim, Germany: Verlag-Chemie.

Wold, S., Sjostrom, M. and Eriksson, L., 2001. PLS-regression: a basic tool of chemometrics. Chemometrics and Intelligent Laboratory Systems, 58: 109-130.

Wulder, M.A., White, J.C., Bentz, B., Alvarez, M.F. and Coops, N.C., 2006a. Estimating the probability of mountain pine beetle red-attack damage. Remote Sensing of Environment, 101: 150-166.

Wulder, M.A., White, J.C. and Bentz, B.J., 2006b. Detection and mapping of mountain pine beetle red attack: matching information needs with appropriate remotely sensed data.

Ye, X., Sakai, K., Sasao, A. and Asada, S., 2008. Potential of airbornre hyperspectral imagery to estimate fruit yield in citrus. Chemometrics and Intelligent Laboratory Systems, 90: 132-144.

Zarco-Tejada, P.J., Miller, J.R., Mohammed, G.H., Noland, T.L. and Sampson, P.H., 2002. Vegetation Stress Detection through Chlorophyll $a + b$ Estimation and Fluorescence Effects on Hyperspectral Imagery. Journal of Environmental Quality, 31: 1433-1441.

Zhang, Y., Pullianen, J., Koponen, S. and Hallikainen, M., 2002. Application of an empirical neural network to surface water quality estimation in the gulf of Finland using combined optical data and microwave data. Remote Sensing of Environment, 81: 327-336.